Chemical Vapor Deposition of Carbon Nanotubes

Yan Li　李 彦　yanli@pku.edu.cn

College of Chemistry, Peking University

Department of Mechanical Engineering, The University of Tokyo

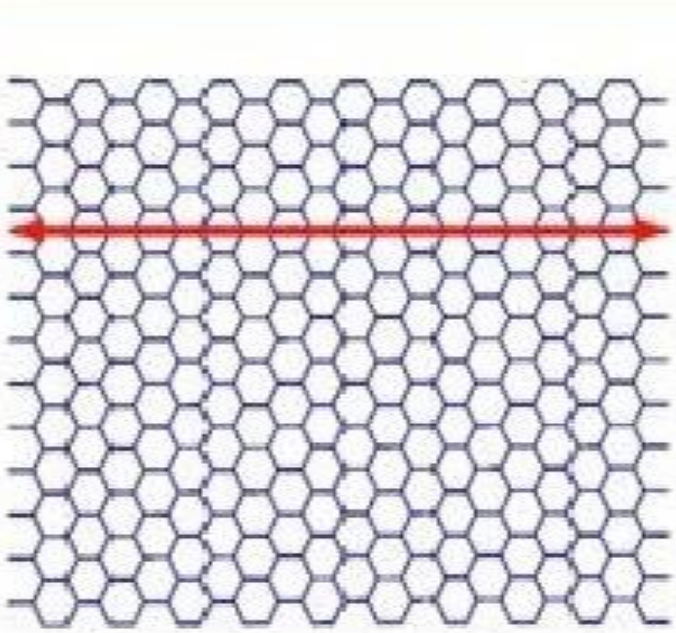

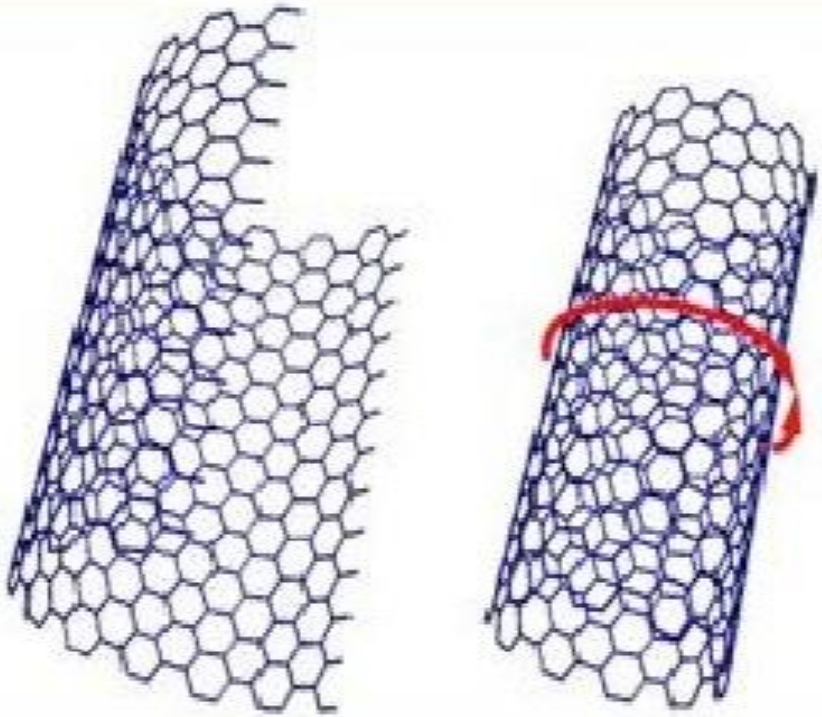

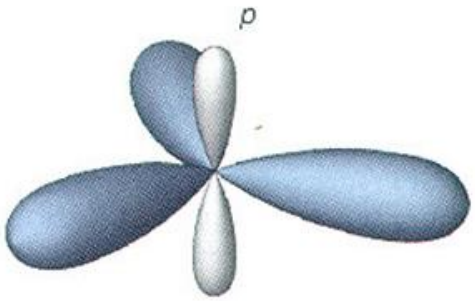
p

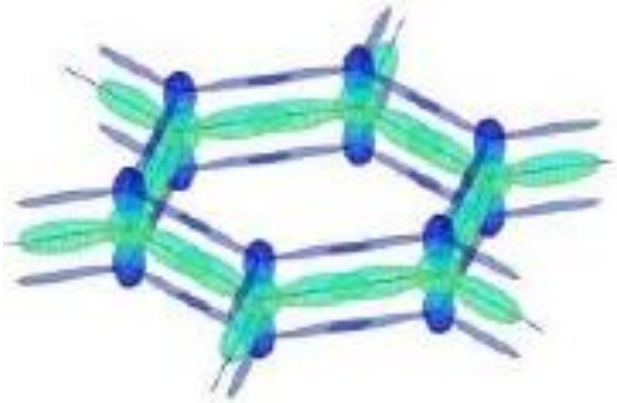

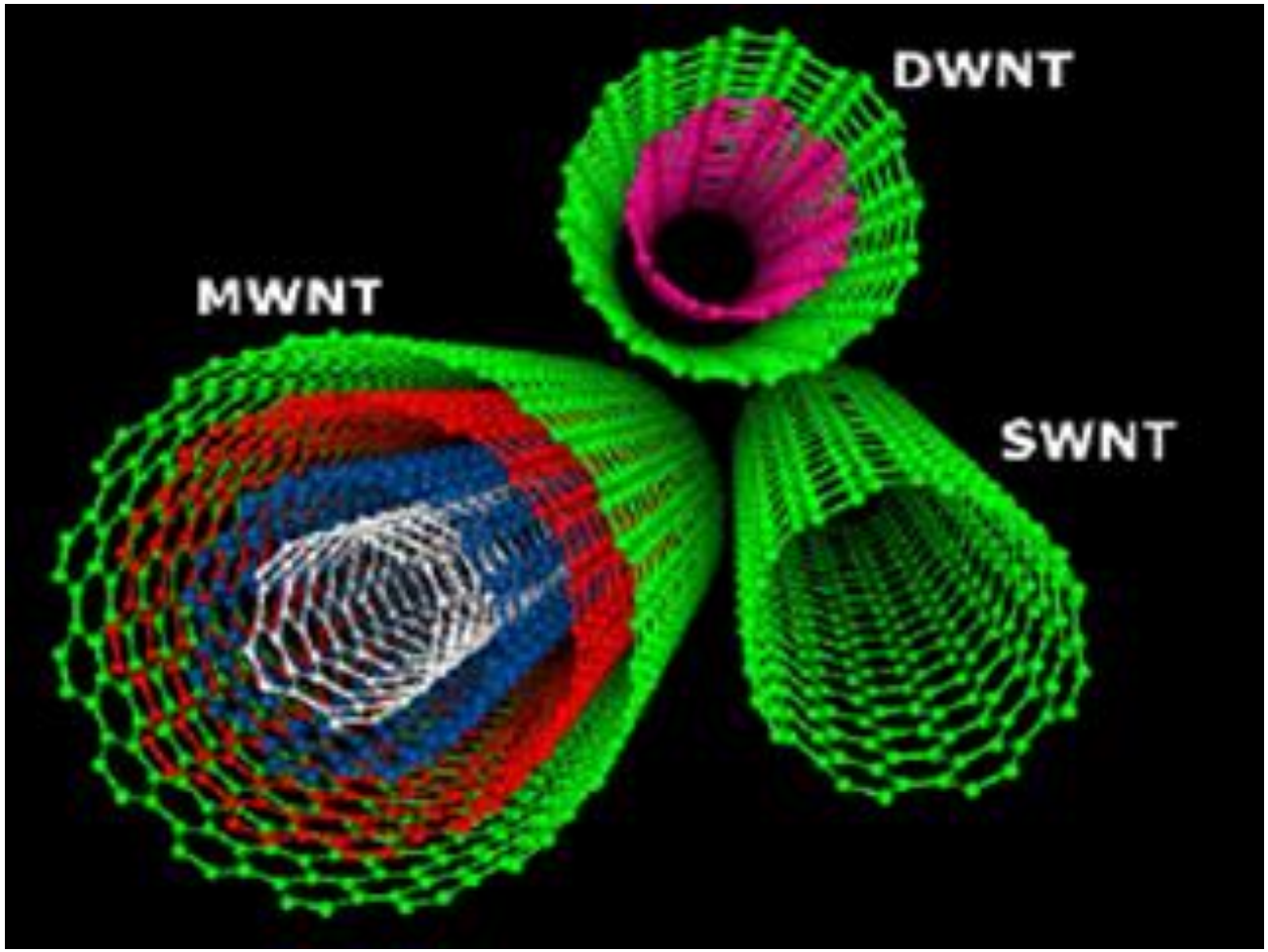
DWNT
MWNT
SWNT

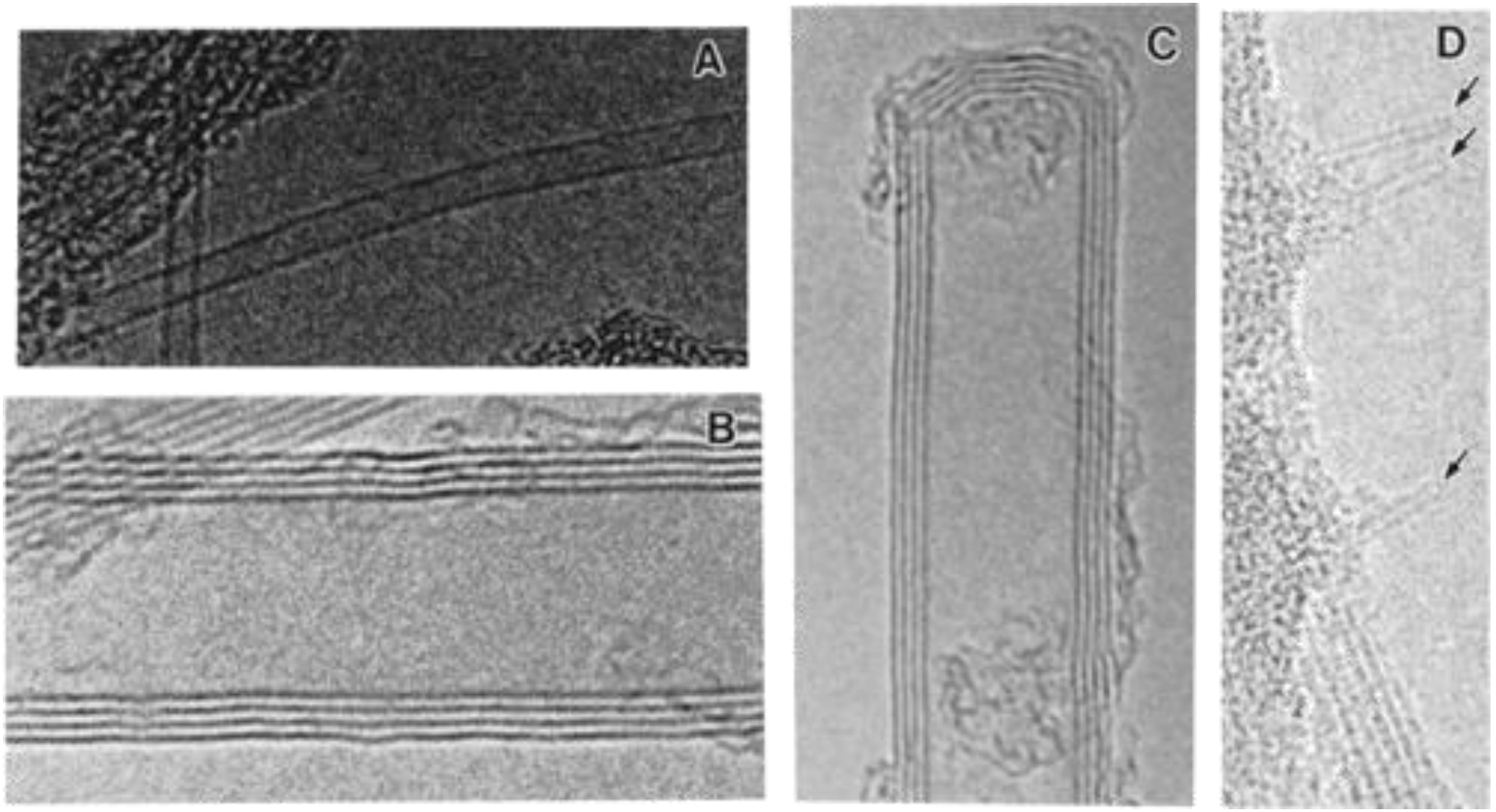

HRTEM images of carbon nanotubes

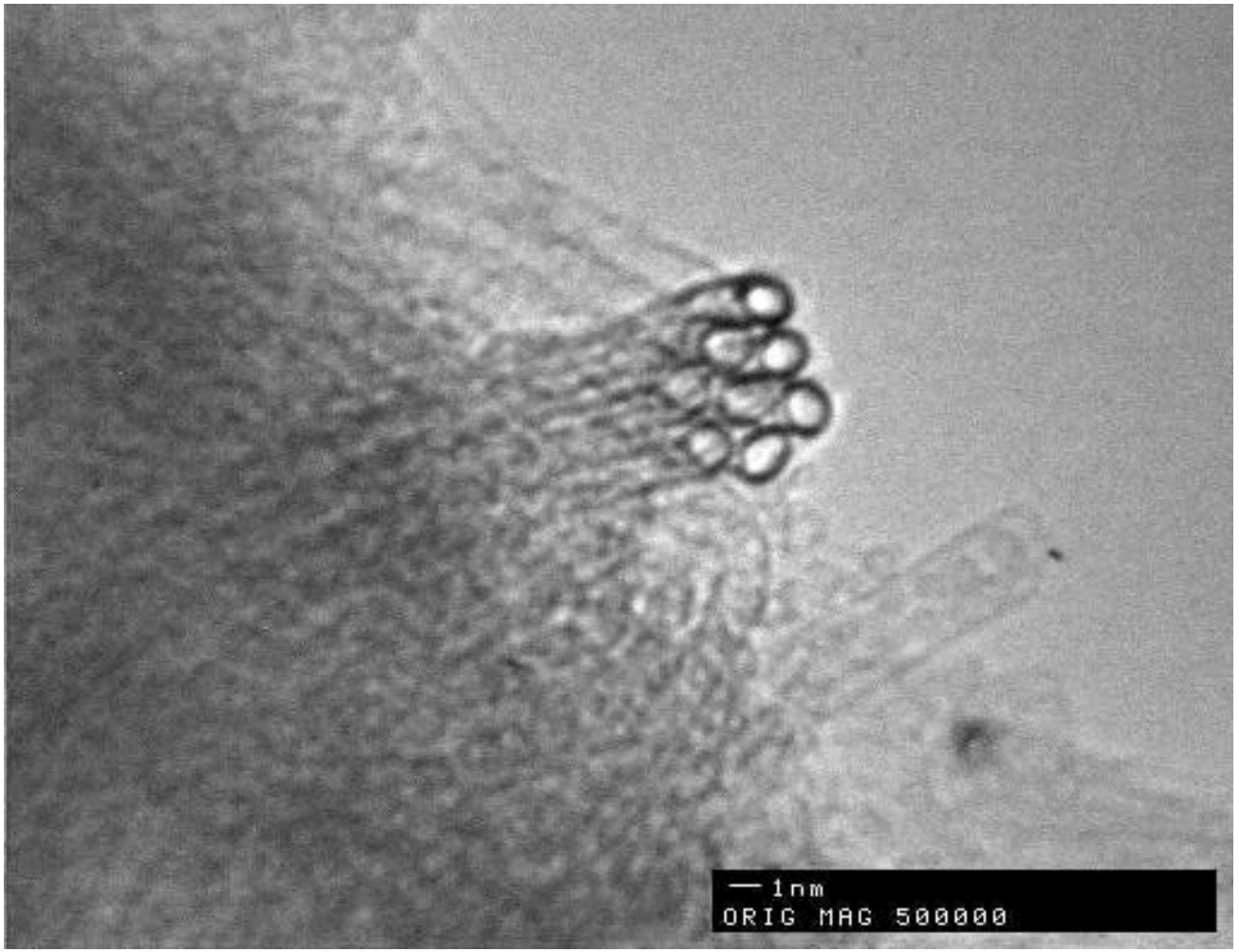
1nm
ORIG MAG 500000

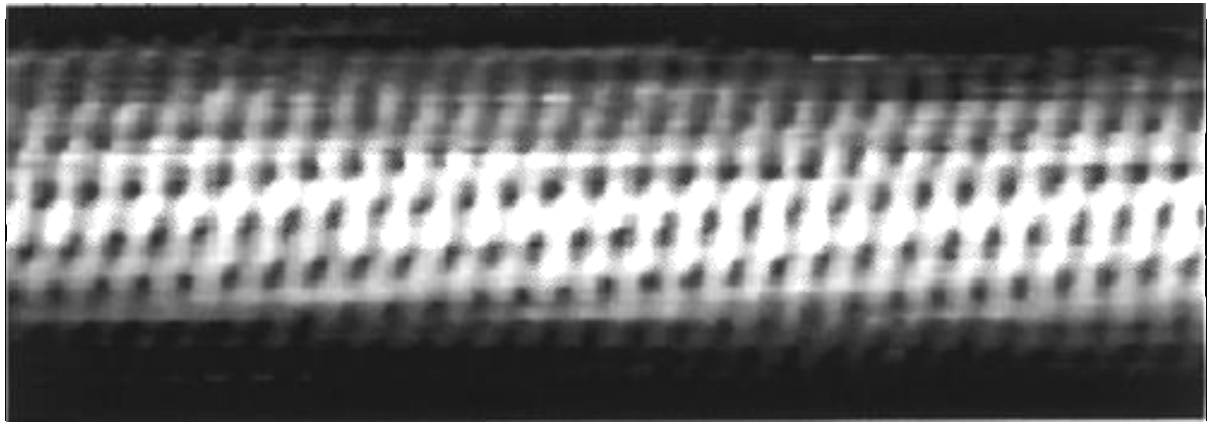

STM image of a single-walled carbon nanotube

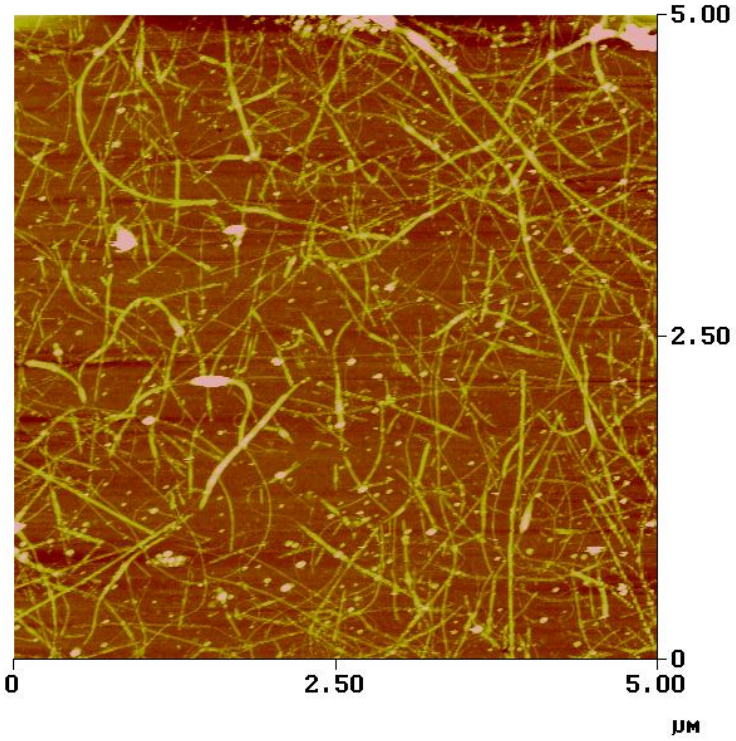

AFM image of SWNTs and SWNT bundles

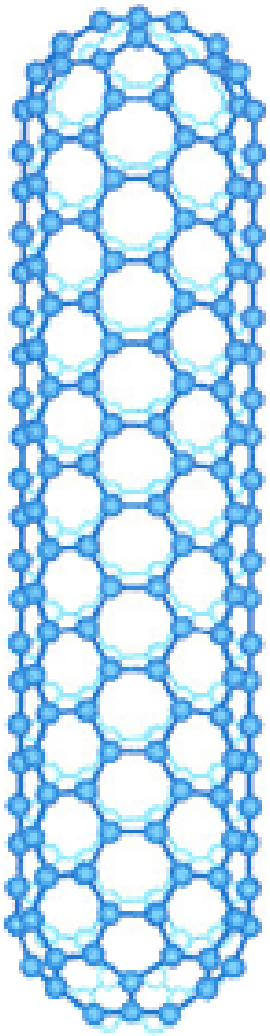

No dangling bonds

Clean interface

Properties of Single Walled Carbon Nanotubes

	SWNT	By comparison
Size	0.4 to 4 nm in diameter	E-beam lithography can create lines 50 nm in wide, a few nm thick
Density	1.33 to 1.40 g/cm^3	Al: 2.7 g/cm^3
Tensile Strength	45 billion pascals	High-strength steel alloys break at 2 billion Pa
Resilience	Can be bent at large angels and restraightened without damage	Metals and carbon fibres fracture at grain boundaries
Current Carrying Capacity	Estimated at 1 billion amps per square centimeter	Copper wires burn out at about 1 milion A/cm^2
Field Emission	Can activate phosphors at 1-3 V if electrodes are spaced 1µm apart	Mo tips require fields of 50-100 V/pm and have limited lifetimes
Heat Transmission	Predicted to be as high as 6,000 W/m•K	Nearly pure diamond transmits 3,320 W/m•K
Temperature Stability	Stable up to 2,800ºC in vacume, 750 ºC in air	Metal wires in microchips melt at 600 to 1,000 ºC

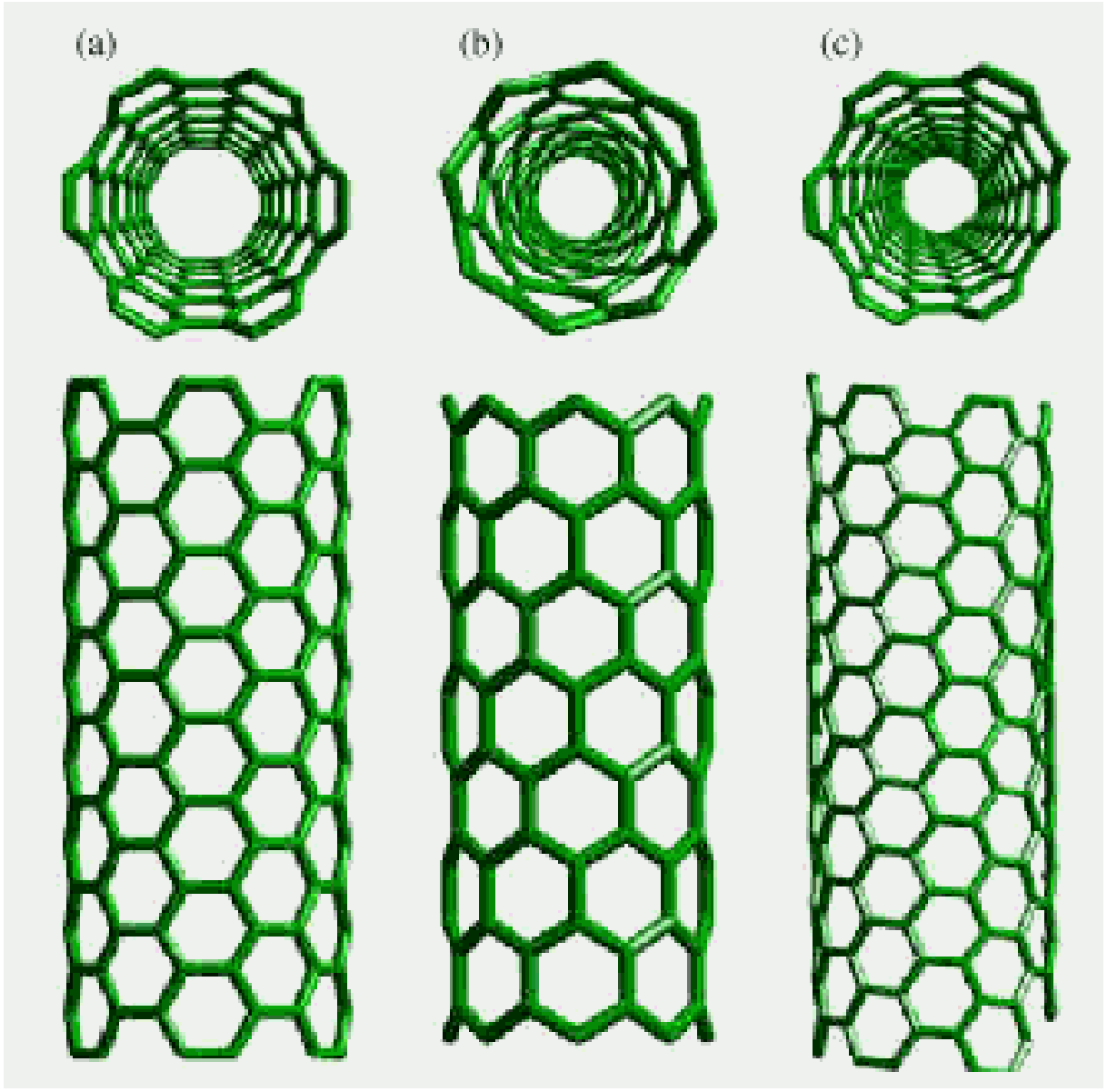
(a)
(b)
(c)

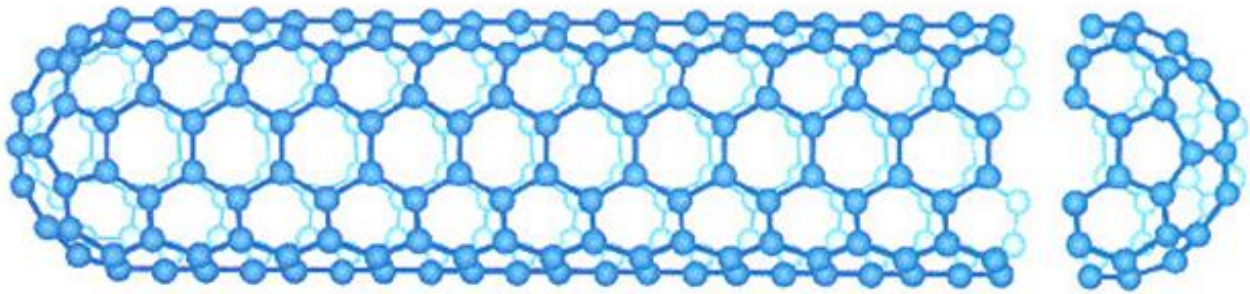

(n,m) = (5,5)

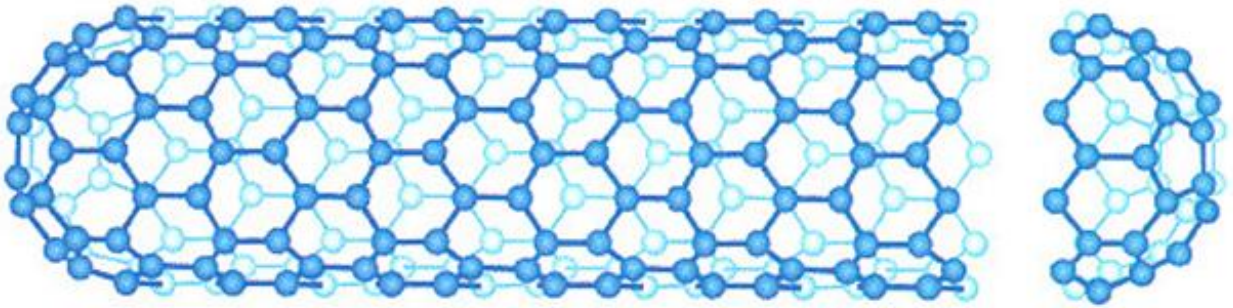

(n,m) = (9,0)

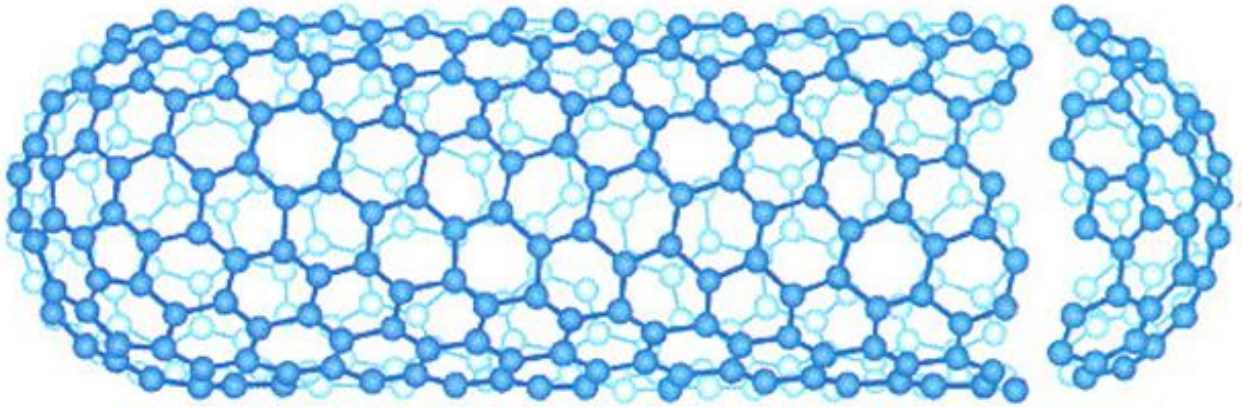

(n,m) = (10,5)

Structure-Determined Bandgap of SWNTs

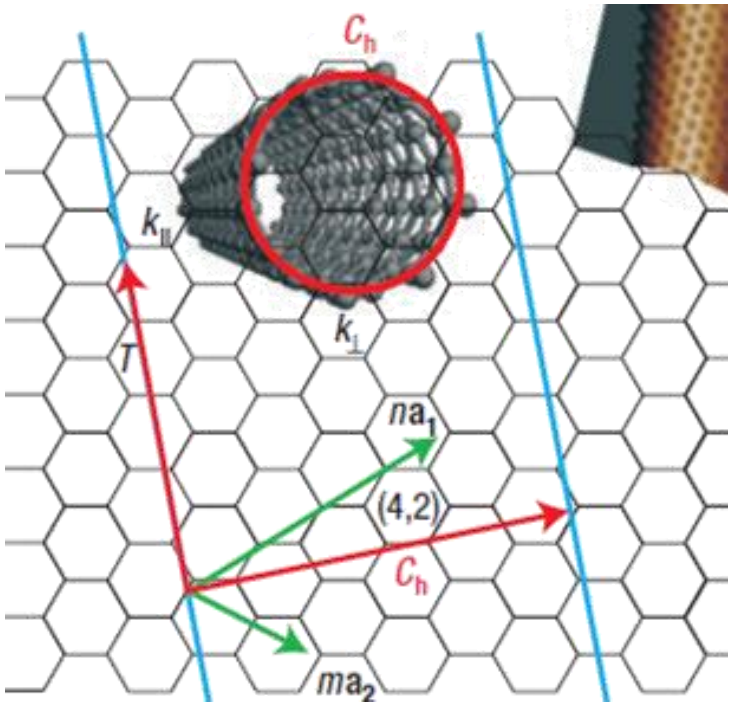

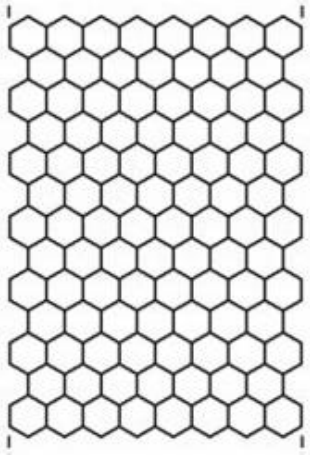

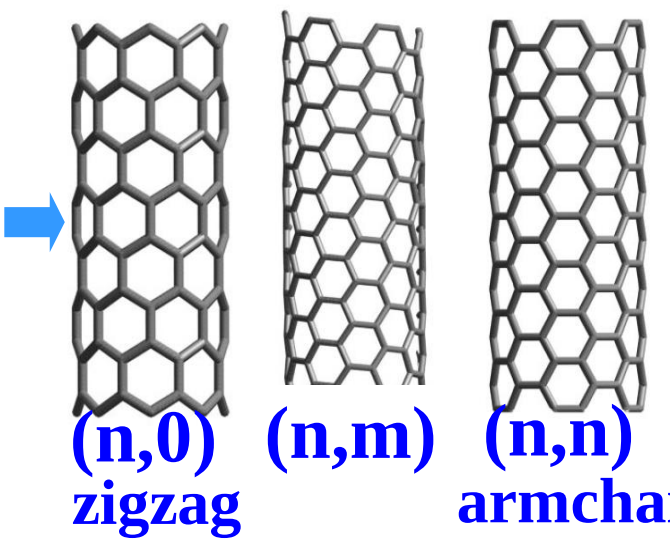

(n,0) **(n,m)** **(n,n)**

zigzag **armchair**

$$d_t = |C_h| / \pi = \frac{a}{\pi}\sqrt{n^2 + nm + m^2}$$

Band structure of SWNTs

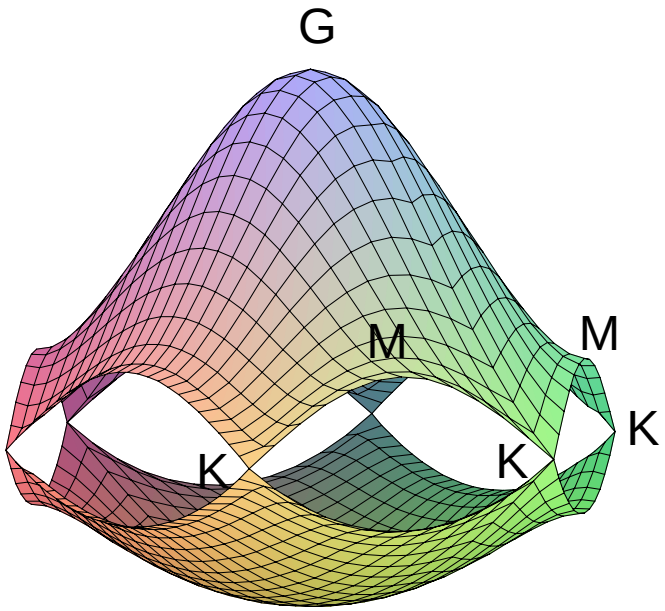

Band structure of Graphene

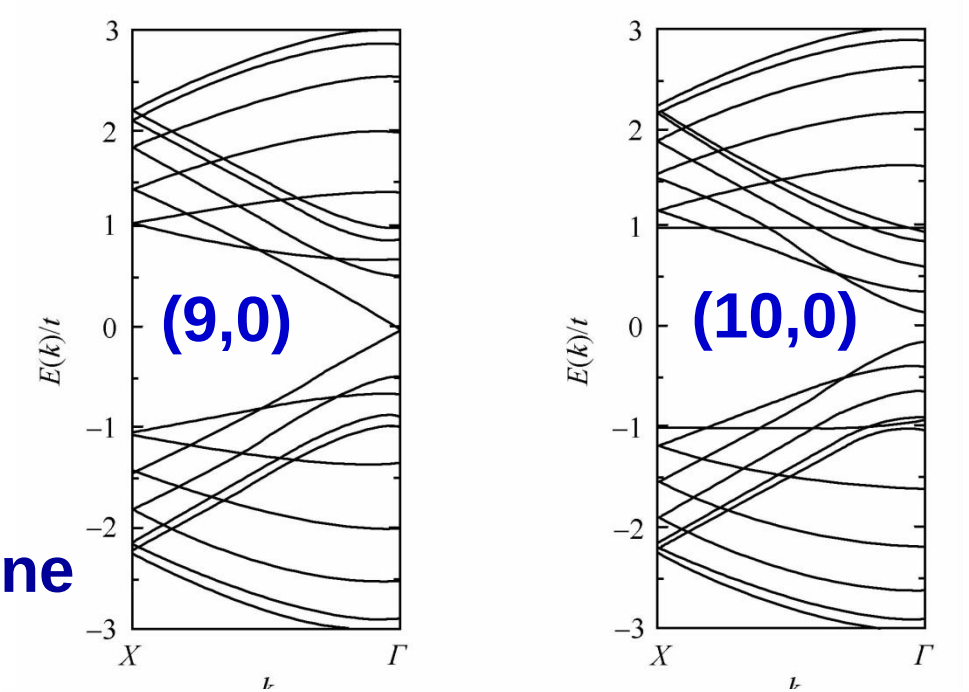

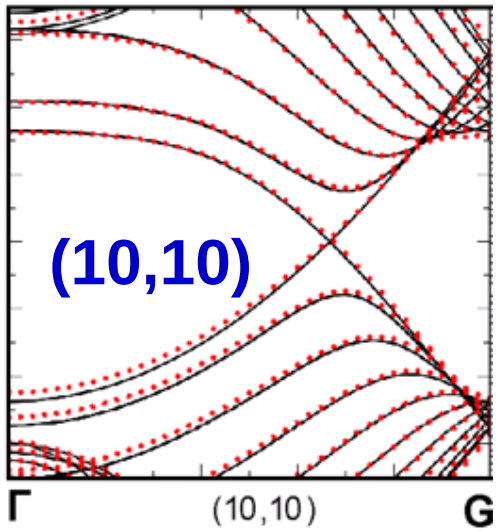

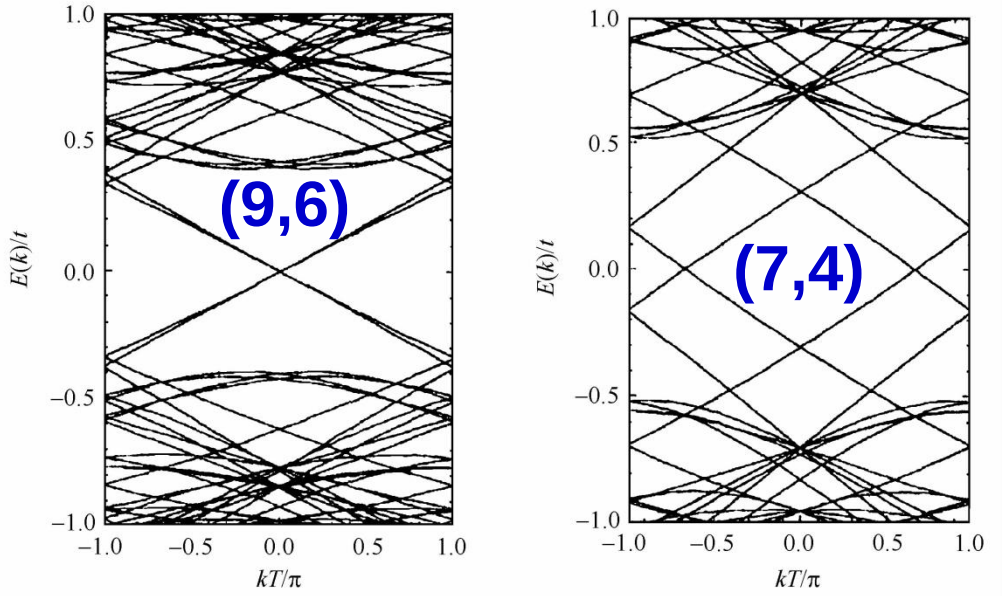

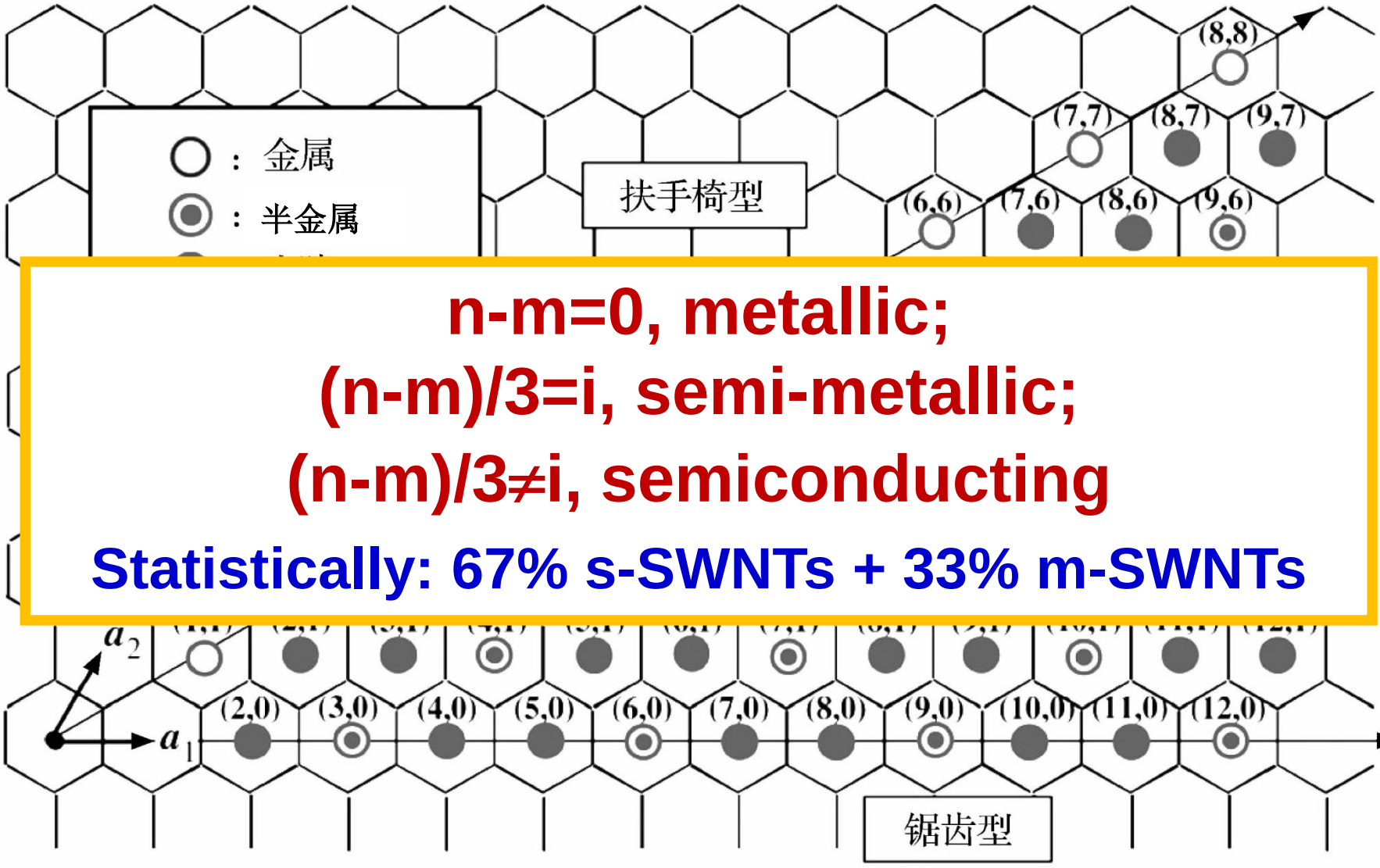

n-m=0, metallic;

(n-m)/3=i, semi-metallic;

(n-m)/3≠i, semiconducting

Statistically: 67% s-SWNTs + 33% m-SWNTs

Methods for Preparation of SWNTs

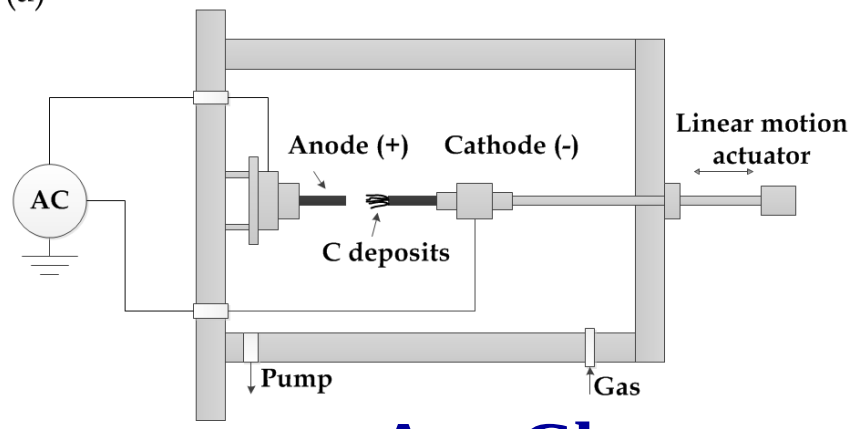

Arc-Charge

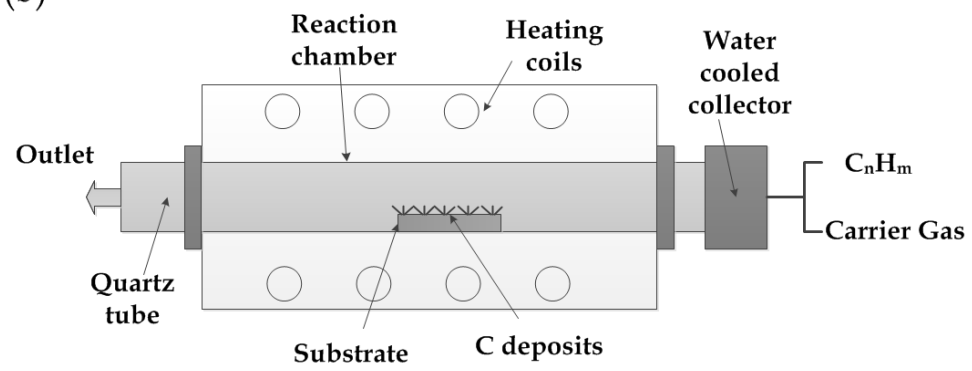

Chemical Vapor Deposition

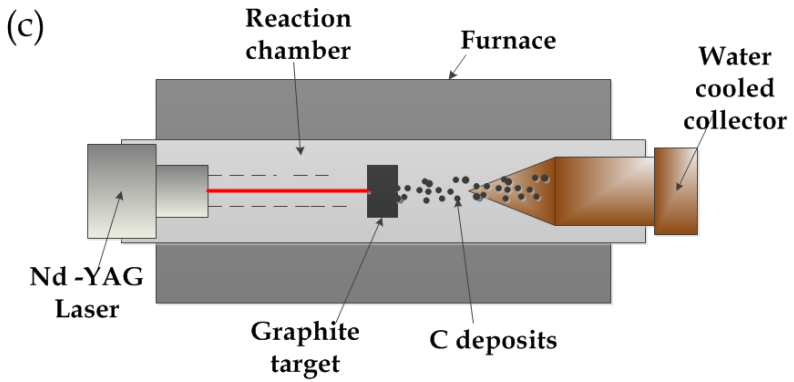

Laser Ablation

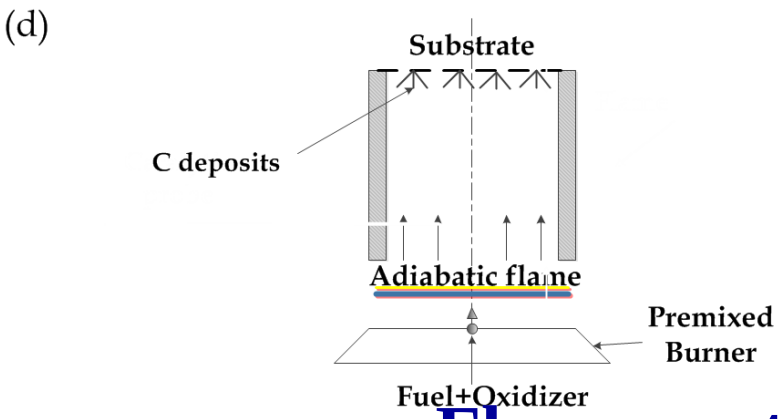

Flame synthesis

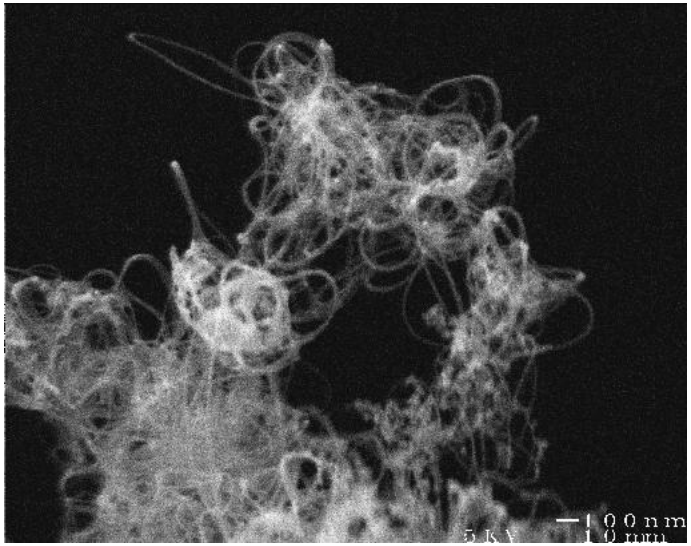

Laser Method

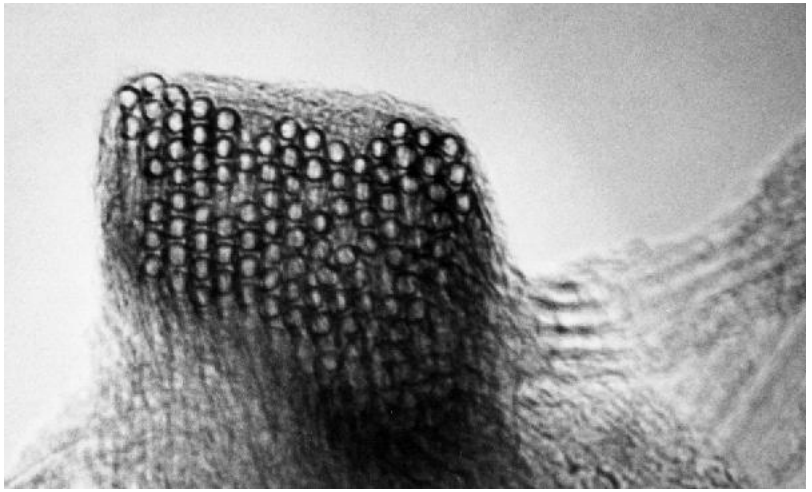

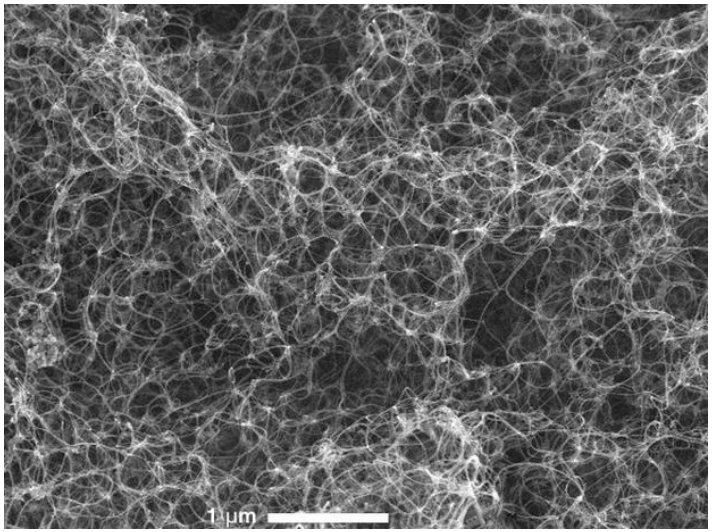

Arc Method

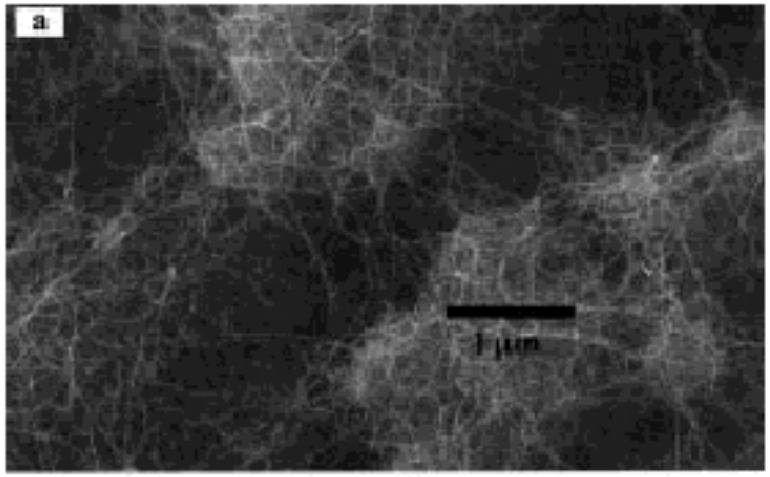

CVD Method

Arc-Charge

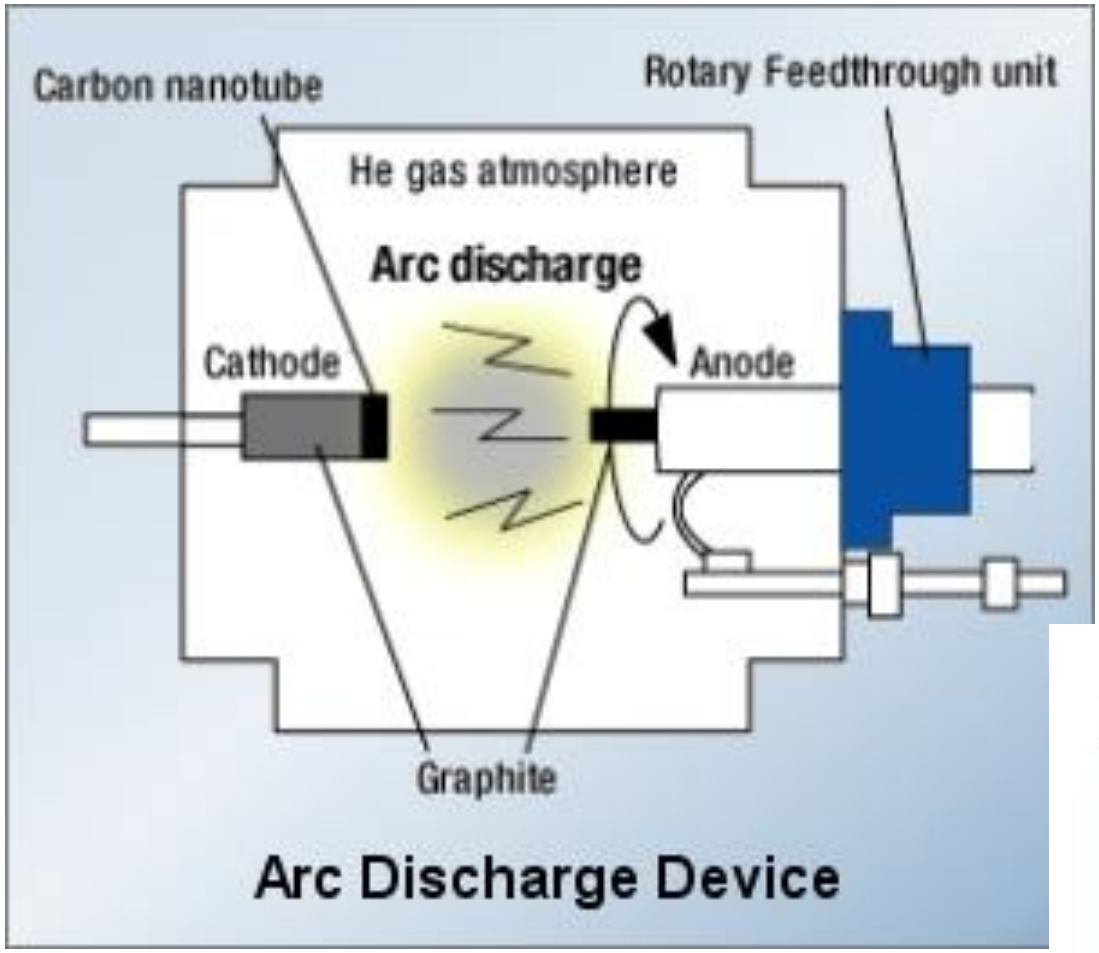
Carbon nanotube
Rotary Feedthrough unit
He gas atmosphere
Arc discharge
Cathode
Anode
Graphite
Arc Discharge Device

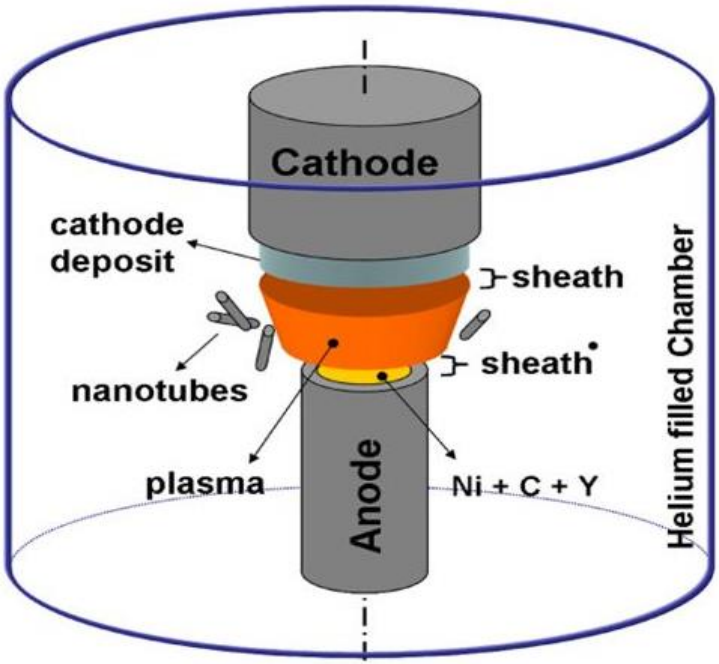
Cathode
cathode deposit
sheath
sheath
nanotubes
plasma
Ni + C + Y
Anode
Helium filled Chamber

Laser Ablation

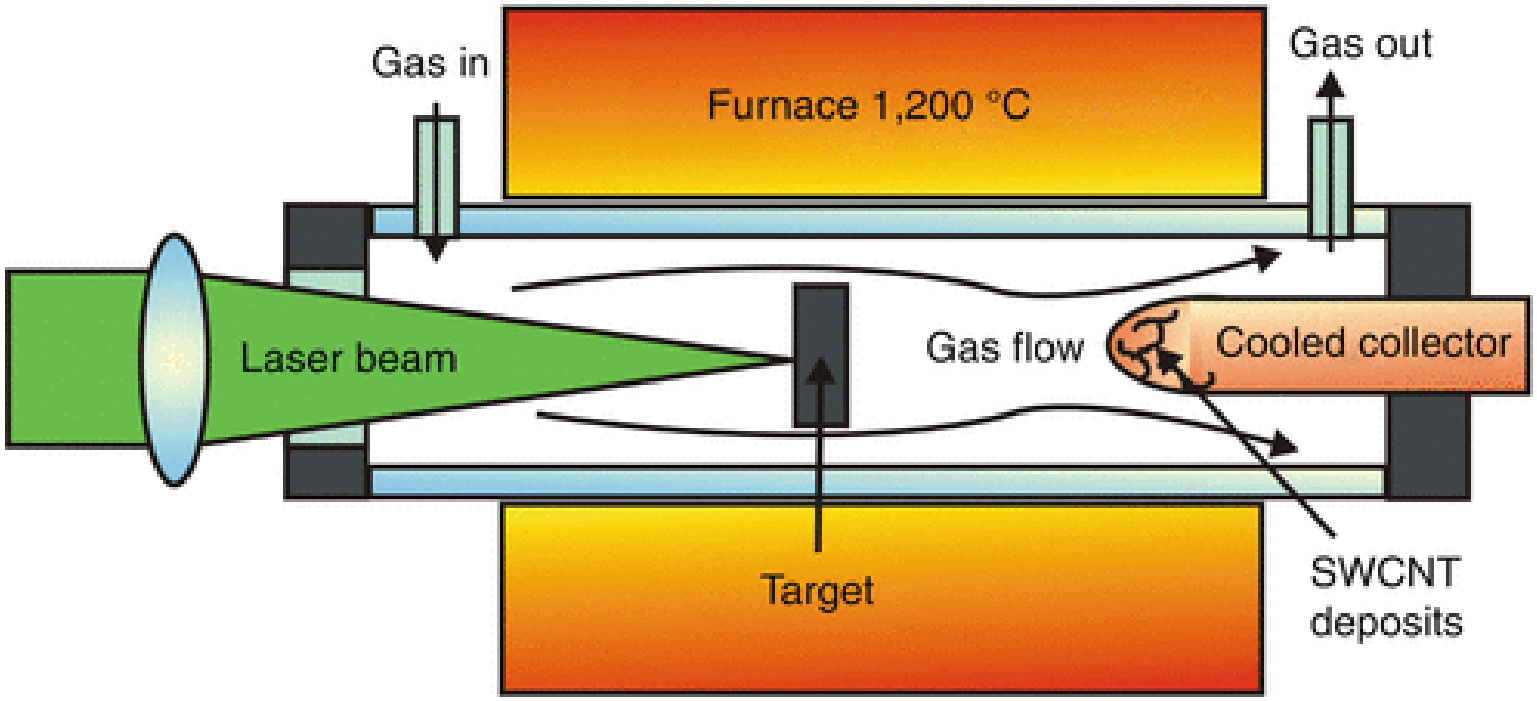

C target (2% Ni:Co)

Chemical Vapor Deposition (CVD)

Precursor gases (often diluted in carrier gases) are delivered into the reaction chamber at approximately ambient temperatures. As they pass over or come into contact with a heated substrate (with catalysts), they react or decompose to form solid phase products.

Some reactions used in CVD process

$$CH_4 \xrightarrow{600\text{-}1000^oC} C + H_2$$

$$SiH_4 \xrightarrow{600\text{-}800^oC} Si + H_2$$

$$Ni(CO)_4 \xrightarrow{140\text{-}240^oC} Ni + CO$$

$$3SiH_4 + 4NH_3 \xrightarrow{750^oC} Si_3N_4 + 12H_2$$

$$CH_4 \xrightarrow[800\text{-}1000^oC]{\textbf{Plasma}} C\ (diamand) + H_2$$

CVD processes such as:

Atmospheric Pressure Chemical Vapour Deposition (APCVD)

Low Pressure Chemical Vapour Deposition (LPCVD)

Metal-Organic Chemical Vapour Deposition (MOCVD)

Plasma Assisted Chemical Vapour Deposition (PACVD) or Plasma Enhanced Chemical Vapour Deposition (PECVD)

Laser Induced Chemical Vapour Deposition (LCVD)

Photochemical Vapour Deposition (PCVD)

Vapor-Liquid-Solid Growth of 1D materials

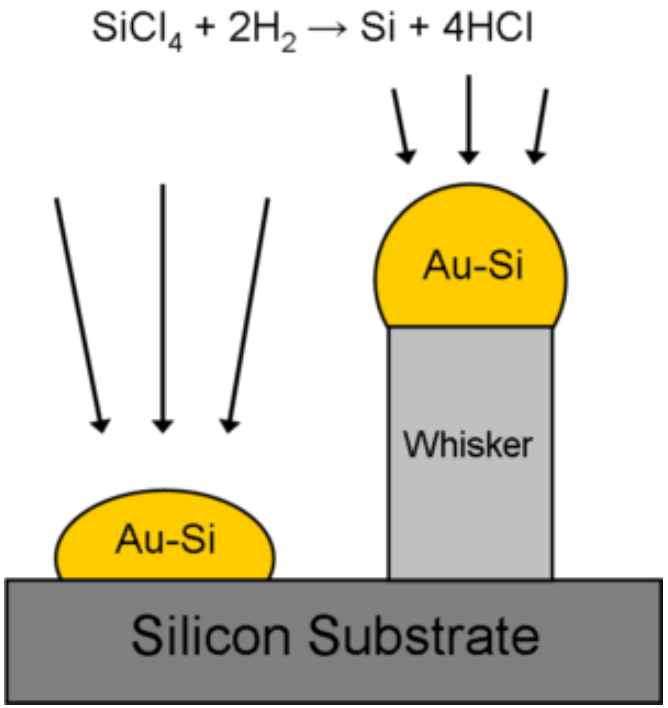

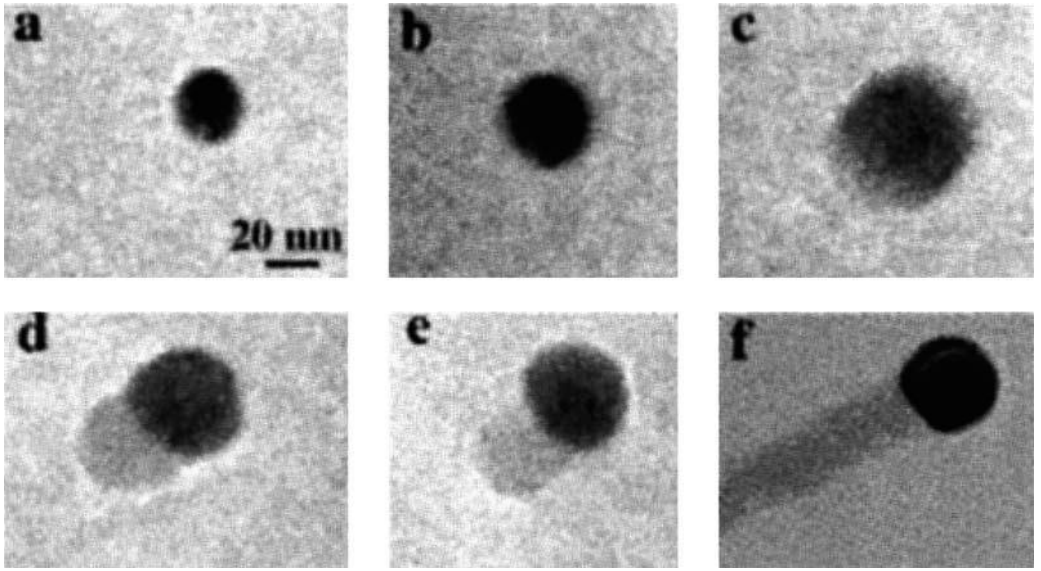

The growth of Ge nanowires catalyzed gold nanoparticle *(in situ* TEM

Chem. Mater., 16 (12), 2449 -2456, 2004.

Chemical Vapor Deposition

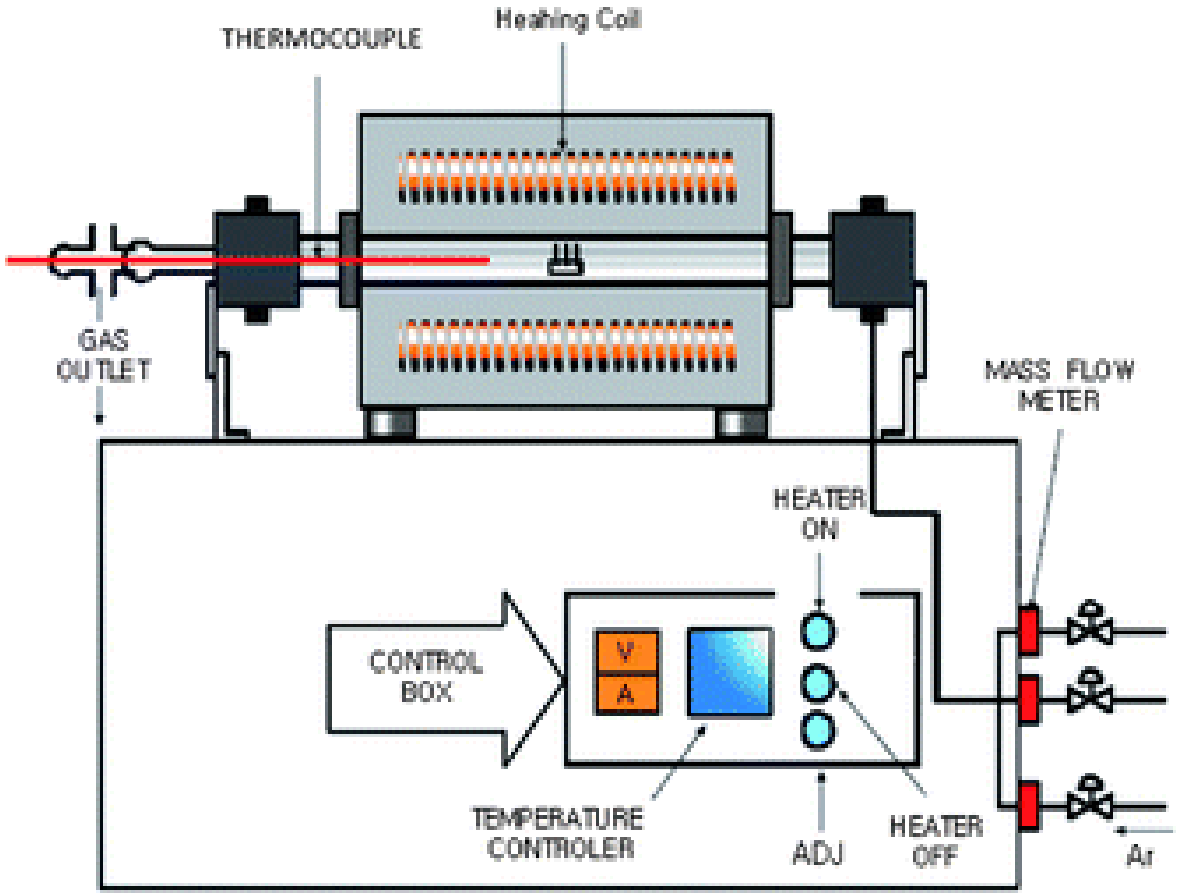

FeedStock Gas: CO, CH_4, C_2H_5OH etc.

Catalyst: Fe, Mo, Ni, Co, Cu etc.

Temperature: 700 – 1100 °C


AALBORG
MASS FLOW CONTROLLER GFC
AALBORG
AALBORG
CAUTION
ATTENTION
PRECAUTION

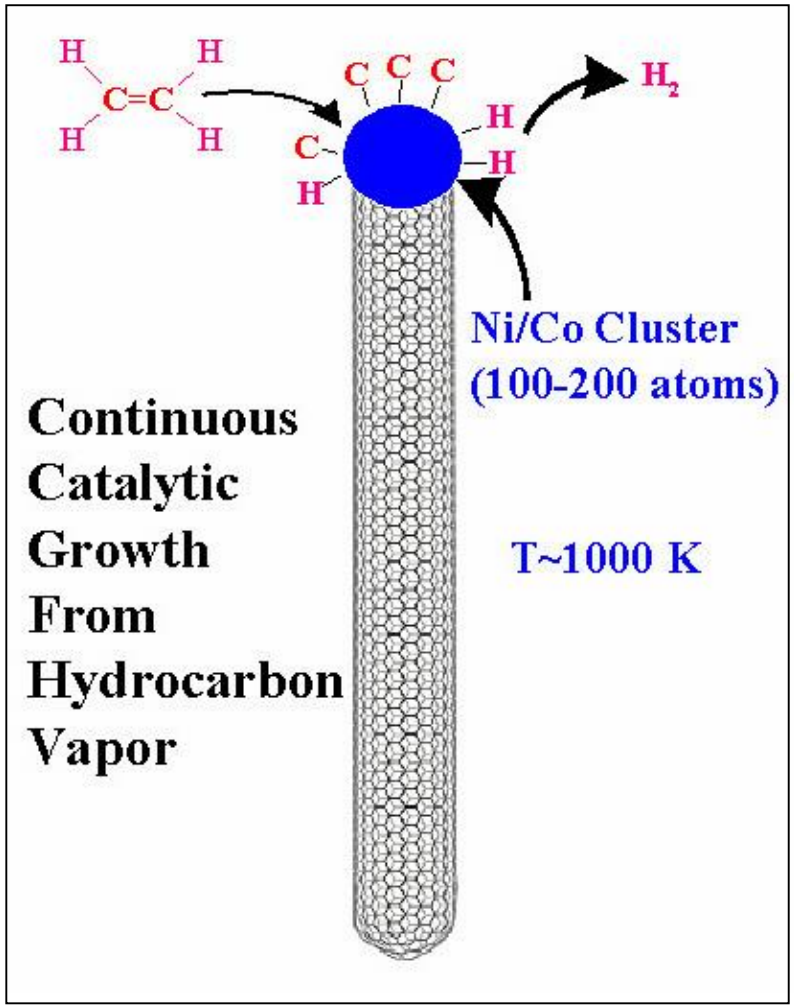

Top-growth

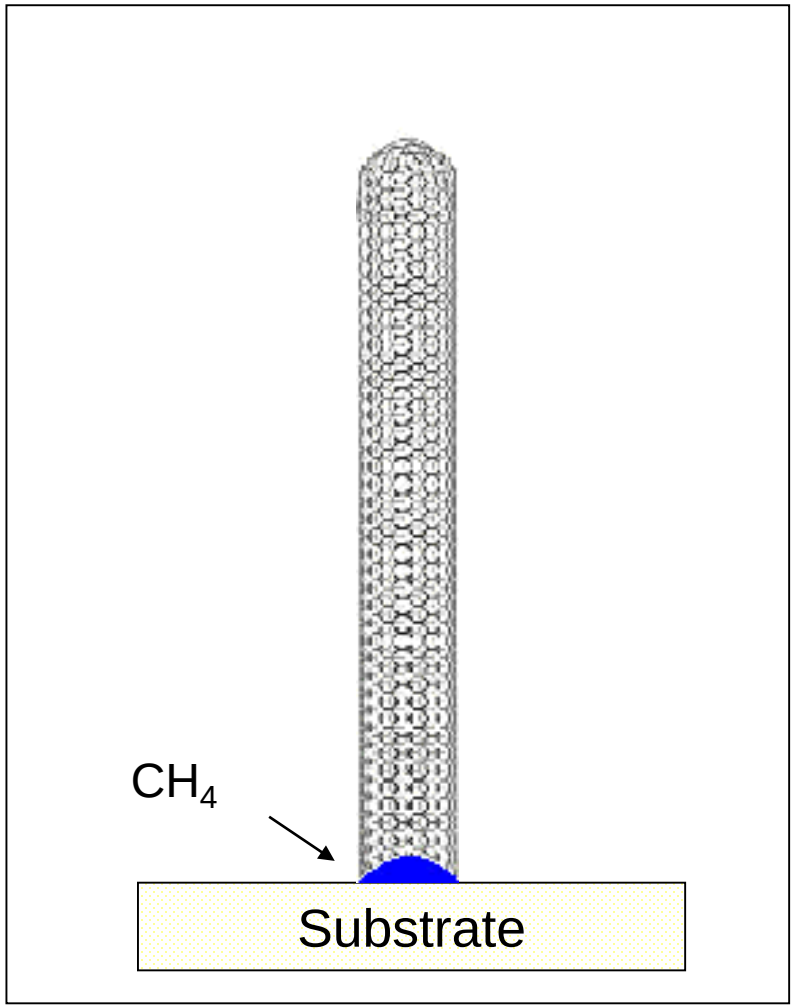

Base-growth

- Advantage:
  - Easier to scale-up;
  - More parameters to control;
  - Suitable for both bulk synthesis and surface-growth

1) $CH_4(g) \rightarrow 2H_2(g) + C$ (nanotube)

$\Delta_r H_m^\theta = 74.81\ kJ\cdot mol^{-1}$

$\Delta_r S_m^\theta = 0.077\ kJ\cdot mol^{-1}\cdot K^{-1}$

$\Delta_r G_T^\theta = \Delta_r H_m^\theta - T\Delta_r S_m^\theta < 0$

$T_{转} = \Delta_r H_m^\theta / \Delta_r S_m^\theta = 971K$ $T>971K,\ \Delta_r G_T^\theta < 0$

2) $2CO(g) \rightarrow CO_2(g) + C$ (nanotube)

$\Delta_r H_m^\theta = -172.5\ kJ\cdot mol^{-1}$

$\Delta_r S_m^\theta = -0.176\ kJ\cdot mol^{-1}\cdot K^{-1}$

$\Delta_r G_T^\theta = \Delta_r H_m^\theta - T\Delta_r S_m^\theta < 0$

$T_{转} = \Delta_r H_m^\theta / \Delta_r S_m^\theta = 980K$ $T<980K,\ \Delta_r G_T^\theta < 0$

HiPco — High Pressure CO CVD

Developed in Rice

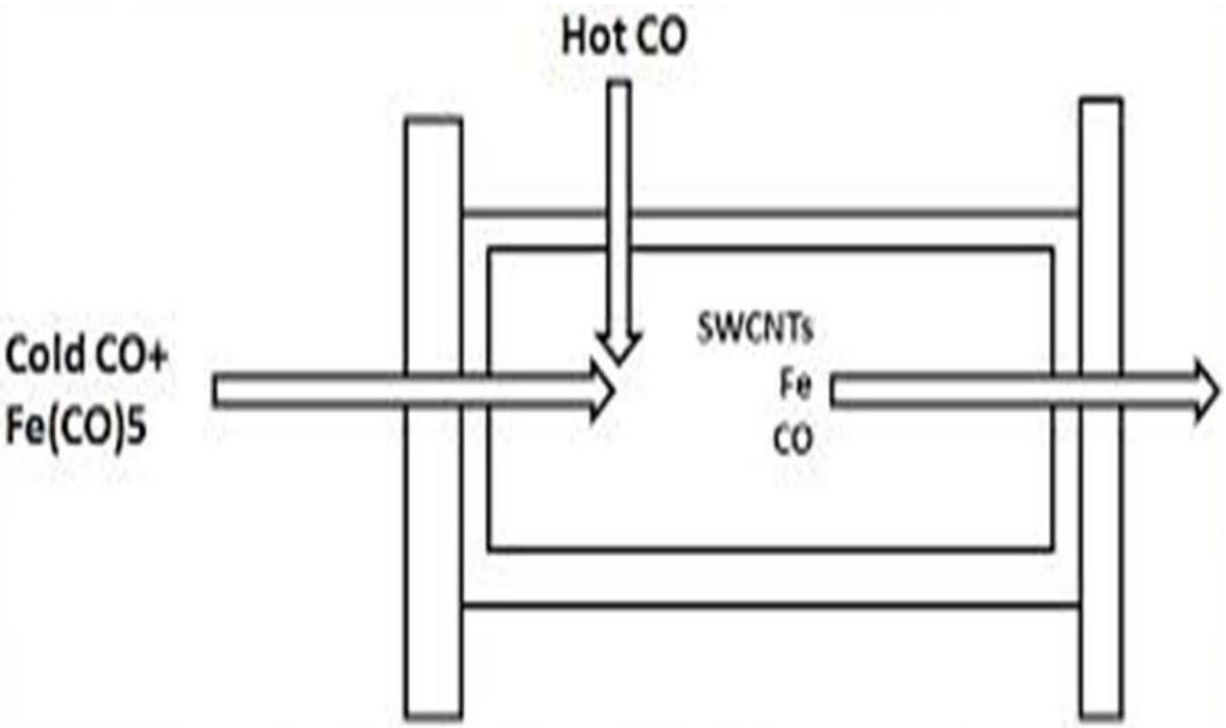


NANOELECTRONICS
HIPCO SWCNT
Acc.V Spot Magn Det WD 1 µm
30.0 kV 3.0 25000x SE 11.1

VLS growth of SWNTs catalyzed by metallic nanoparticles

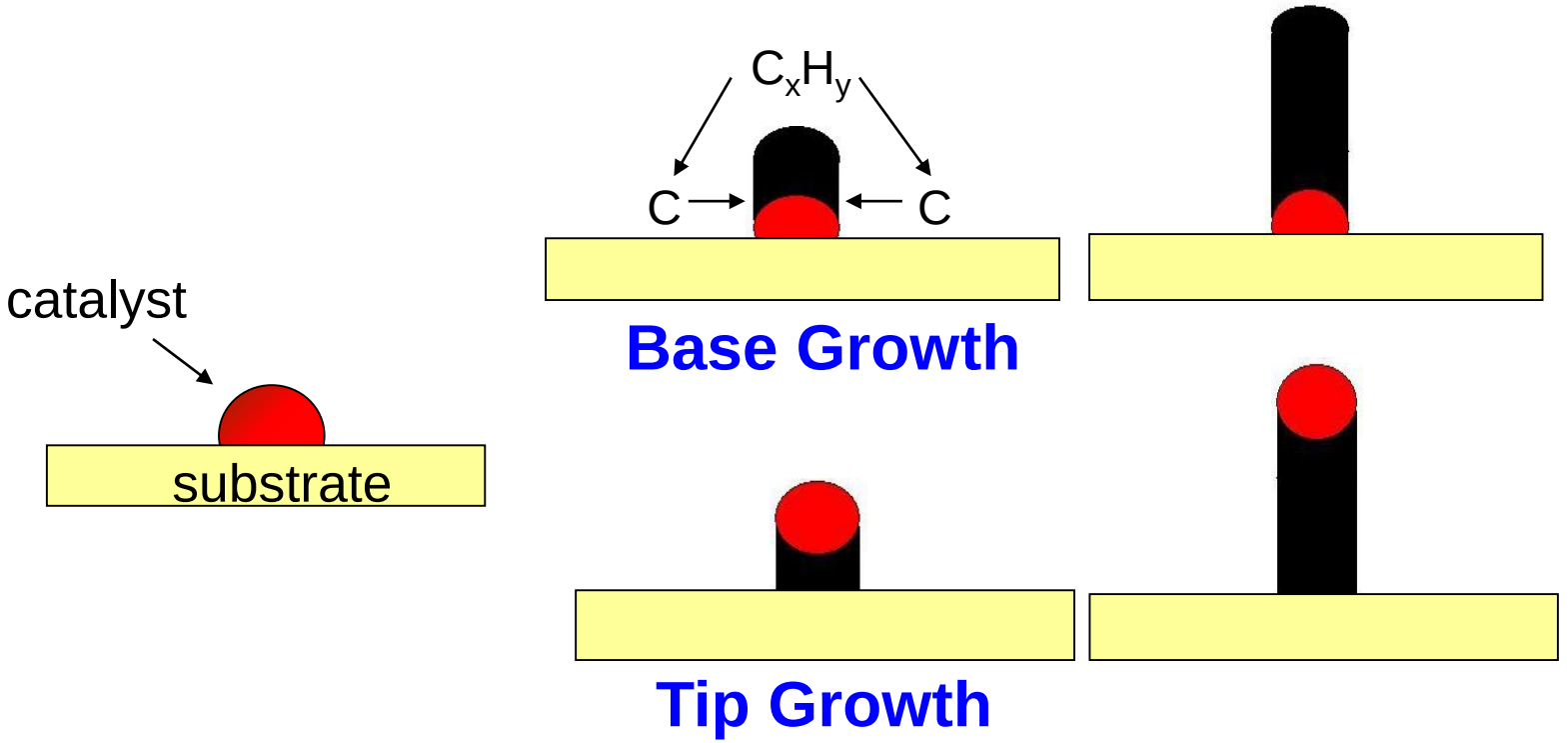

Roles of the catalysts:

- to catalyze the decomposition of carbon feeding stocks
- to initiate the nucleation and growth of nanotubes

Base-Growth of SWNTs

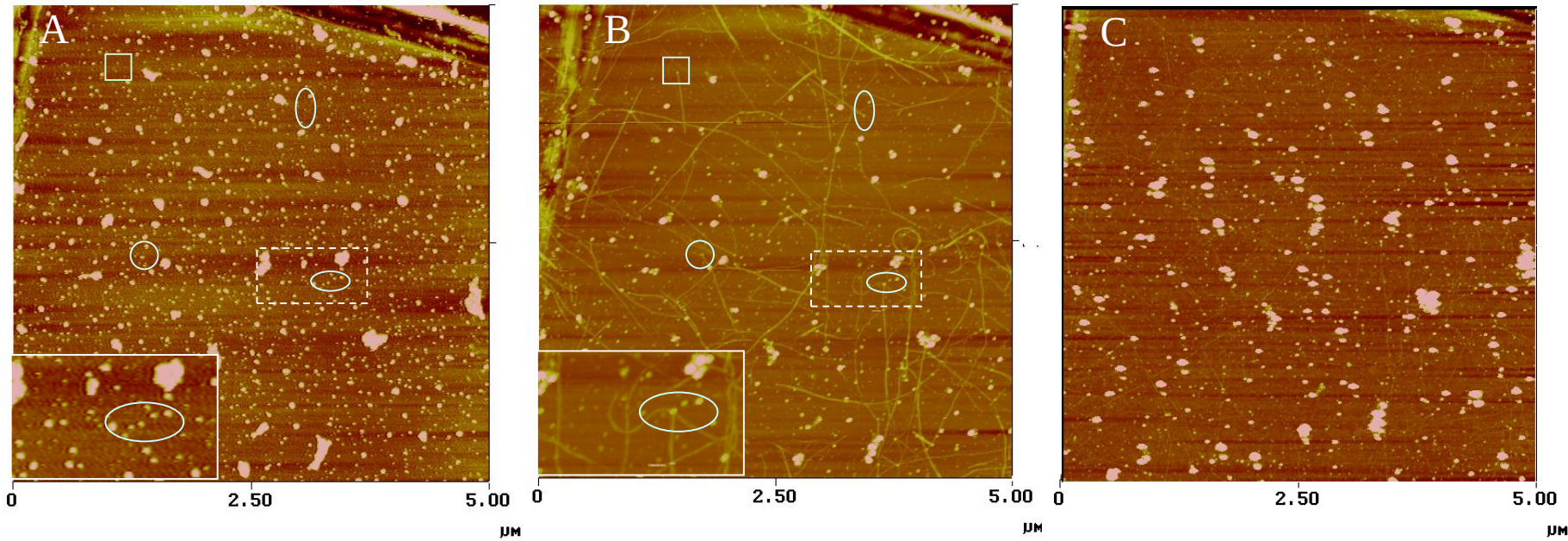

On Silicon Surface

A) original nanoparticles B) after CVD C) after heated in air

Unpublished results

Base-Growth of SWNTs

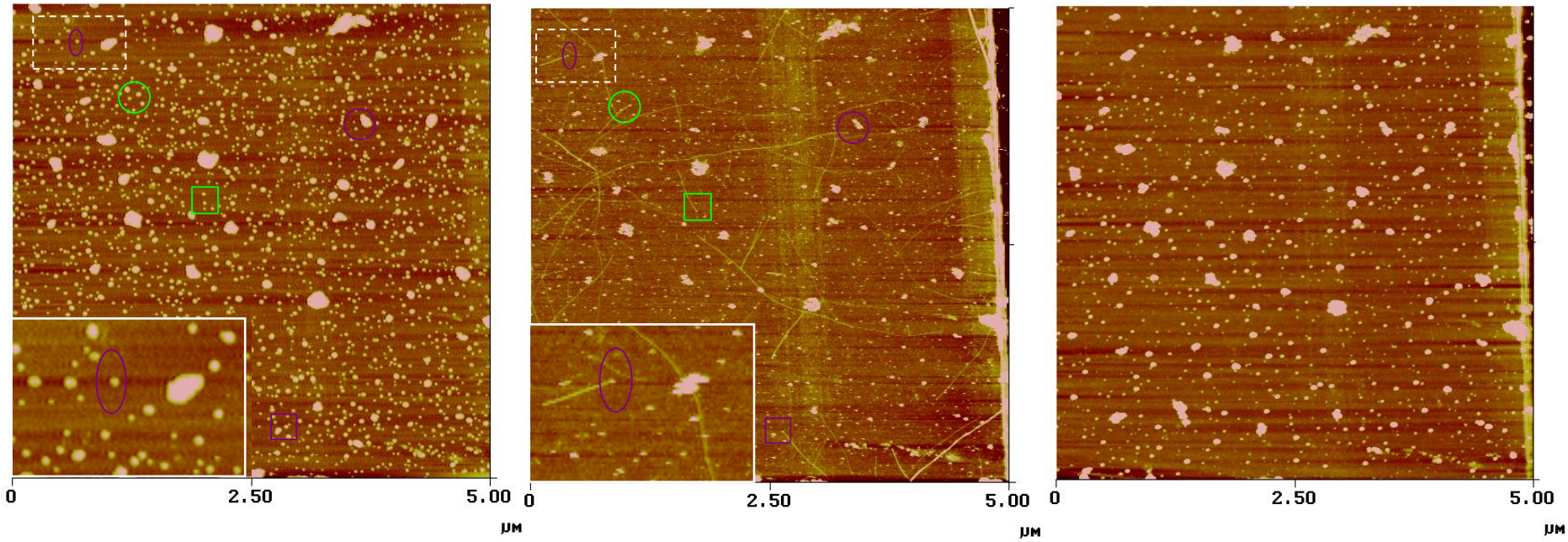

On Al_2O_3/Si surface

A) original nanoparticles B) after CVD C) after heated in air

Control on diameters of SWNTs

ELSEVIER

14 August 1998

Chemical Physics Letters 292 (1998) 567–574

CHEMICAL PHYSICS LETTERS

Chemical vapor deposition of methane for single-walled carbon nanotubes

Jing Kong [a]

[a] *Department of*
[b] *NASA Ar*

Rece

Table 1
Summary of results of methane CVD experiments using s

Catalyst composition	Support material	SWN
Fe_2O_3	alumina	yes
Fe_2O_3	silica	yes
CoO	alumina	yes
CoO	silica	no
NiO	alumina	no
NiO	silica	no
NiO/CoO	alumina	no
NiO/CoO	silica	yes

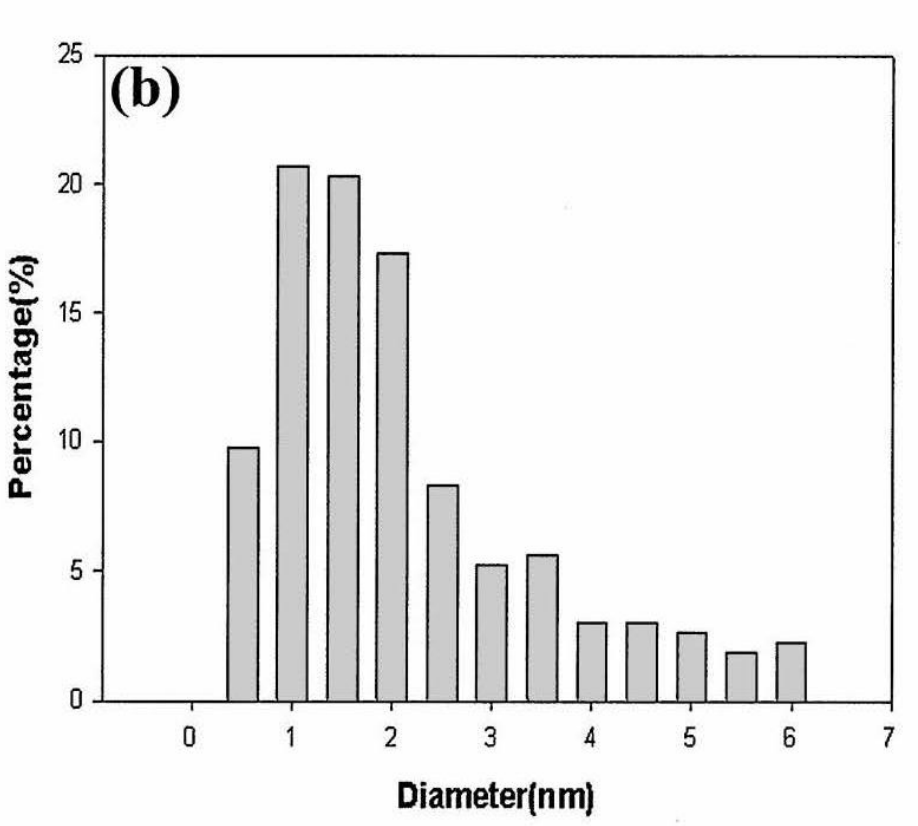

Fe-Mo Catalysts

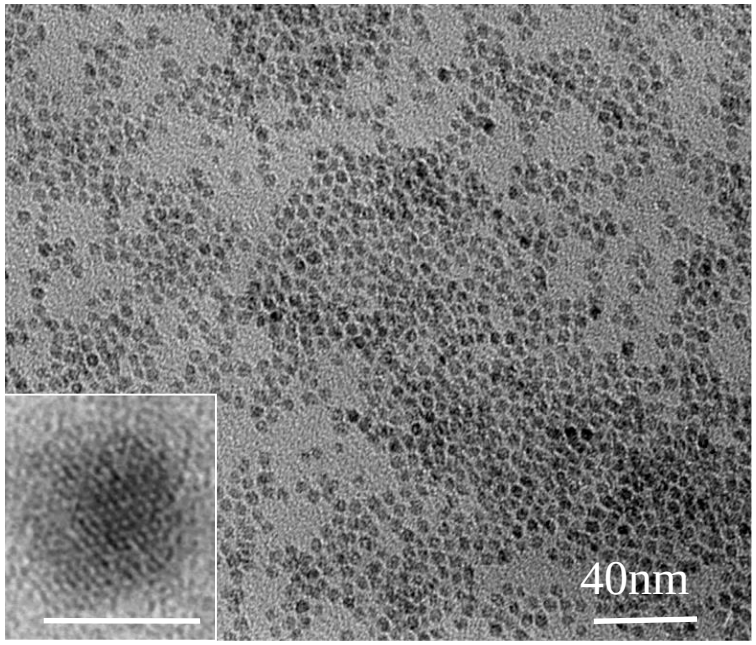

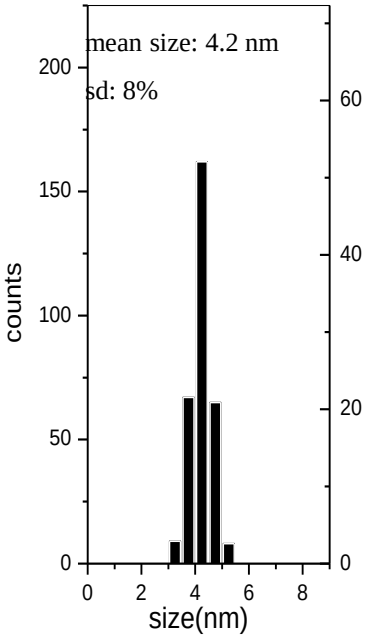

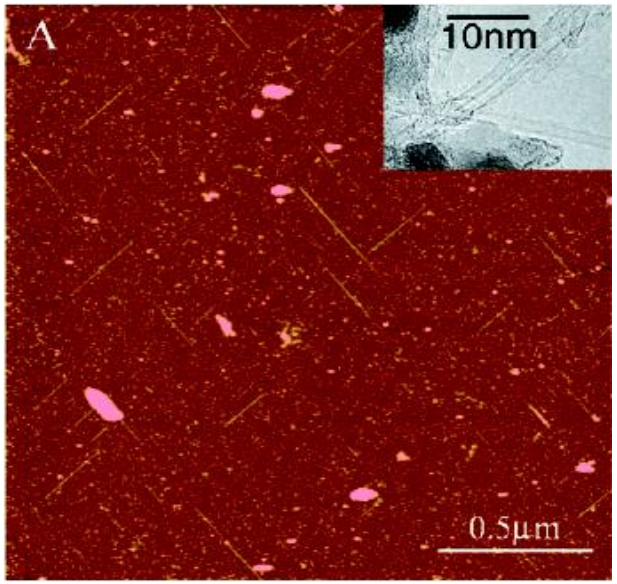

Fe-Mo nanoparticles prepared by the decomposition of carbonyl compounds in solution, and the SWNTs grown from these particles

Y. Li, J. Liu, Y. Wang, Z. L. Wang, ***Chem. Mater.***, 2001, 13(3), 1008-1014.

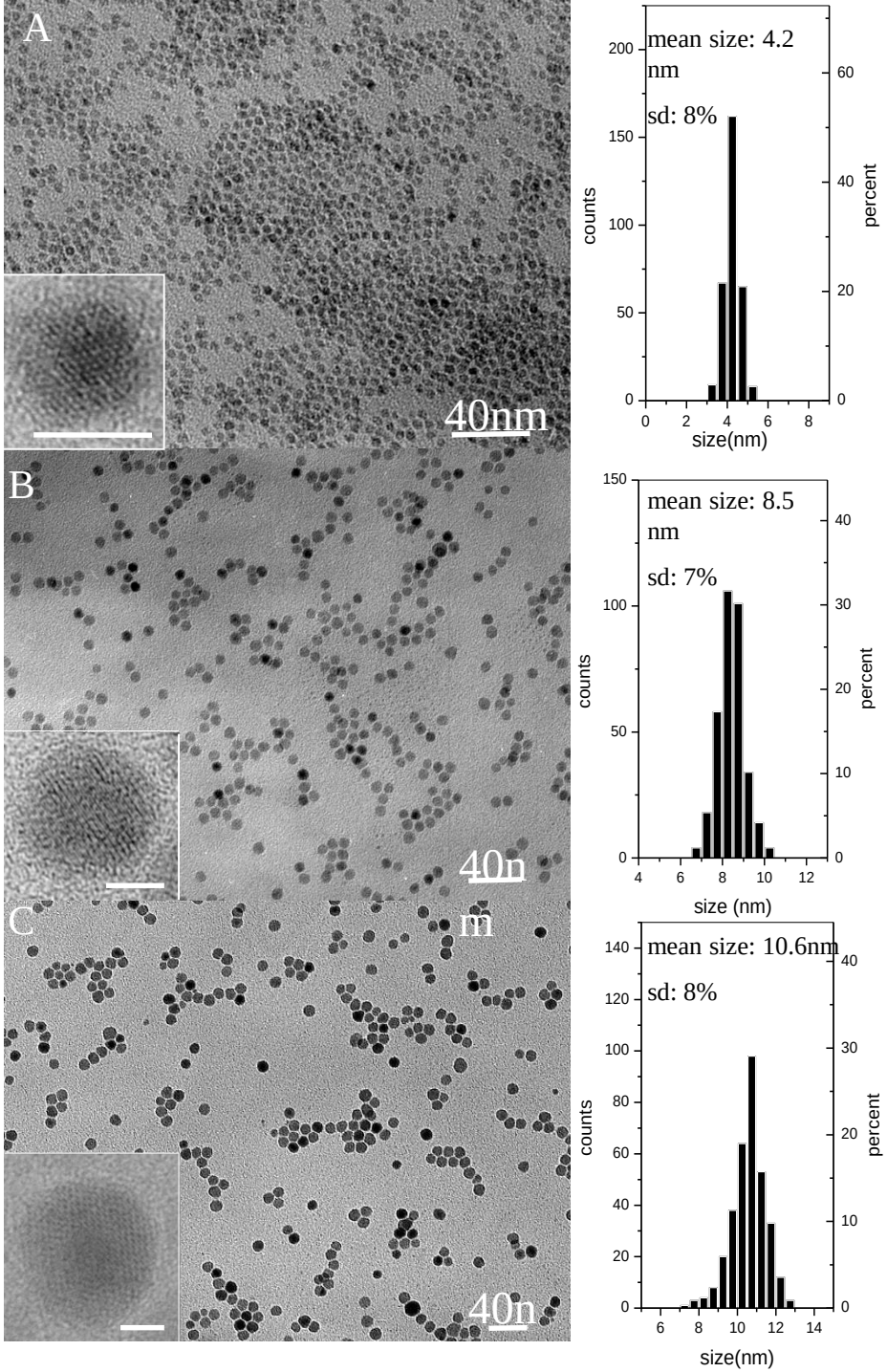
A
40nm
mean size: 4.2 nm
sd: 8%
counts
percent
size(nm)
B
40n
m
mean size: 8.5 nm
sd: 7%
counts
percent
size (nm)
C
40n
mean size: 10.6nm
sd: 8%
counts
percent
size(nm)

Sizes of the monodispersed Fe-Mo nanoparticles and the CVD result by using the particles as catalysts

No.		A	B	C	D	E	F	G	H	I
Size/nm		3.3	4.2	4.5	5.0	5.9	6.7	7.6	8.5	10.6
Tube	On surface	N	Y	Y	Y	N	N	N	N	N
growth	powder	N	Y	Y	Y/N	N	N	N	N	N

Catalysts for Surface growth of SWNTs (2)

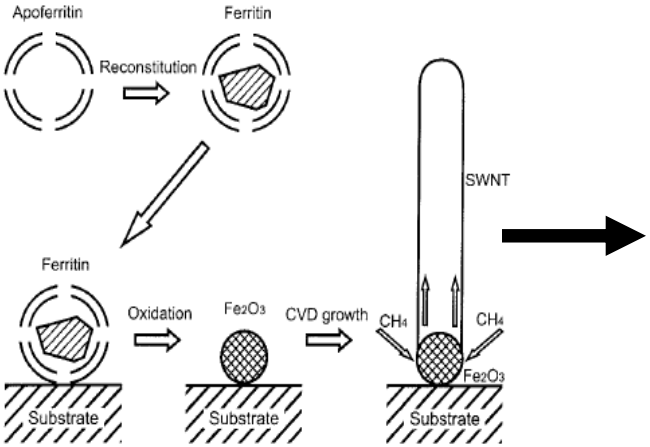

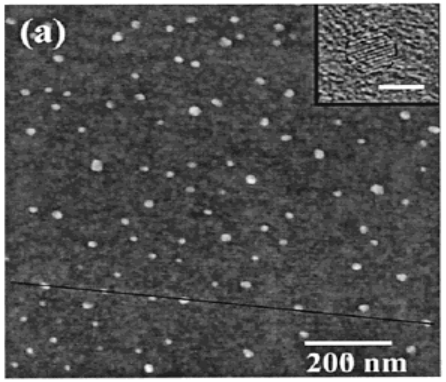

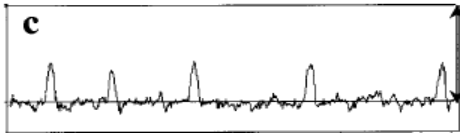

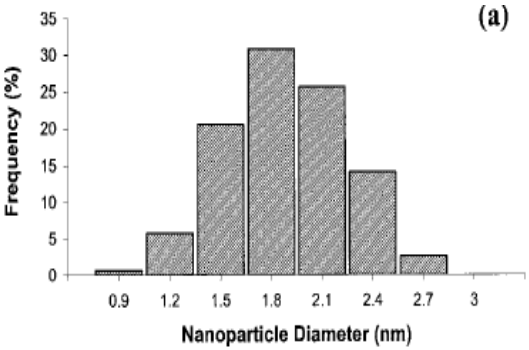

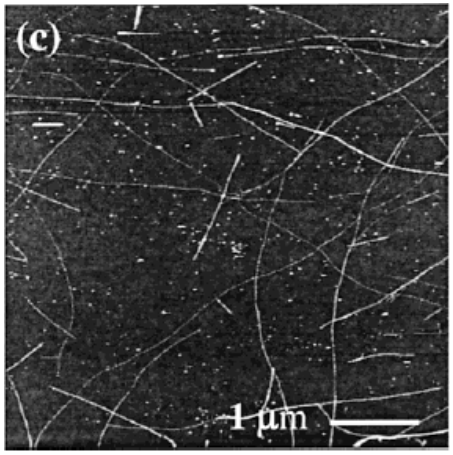

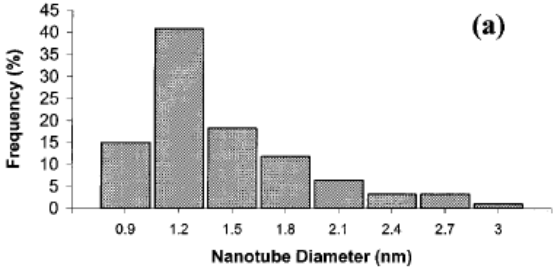

Hongjie Dai, et al., J. Phys. Chem. B 2001, 105, 11424

Control SWNT diameter by catalysts

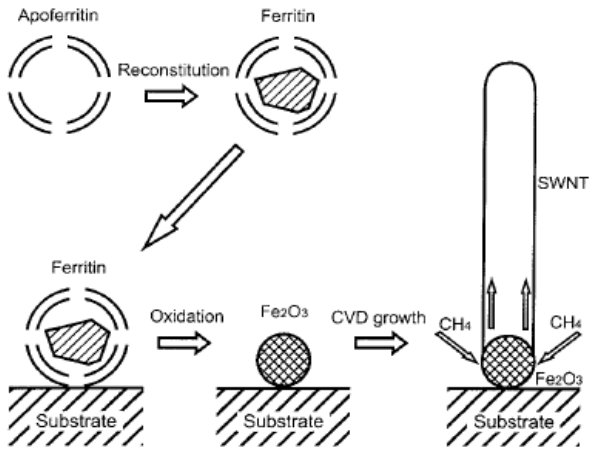

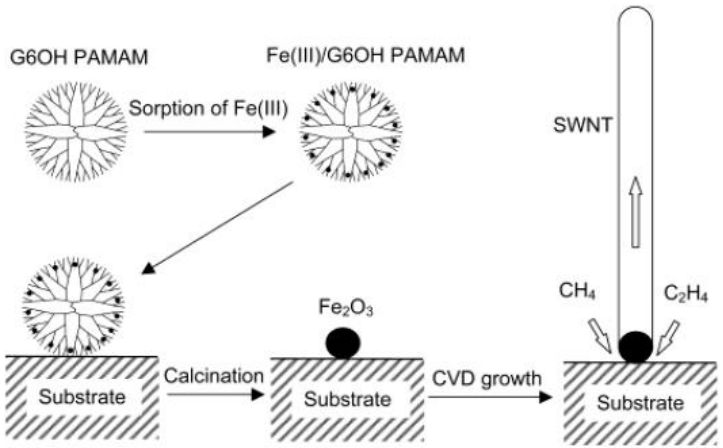

催化剂

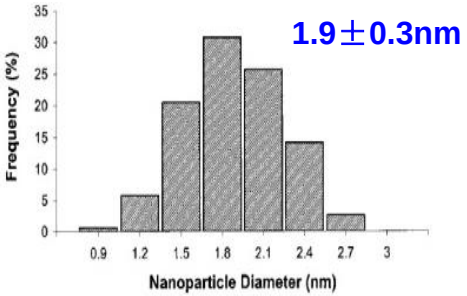

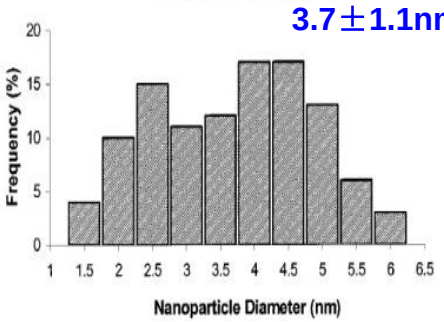

碳纳米管

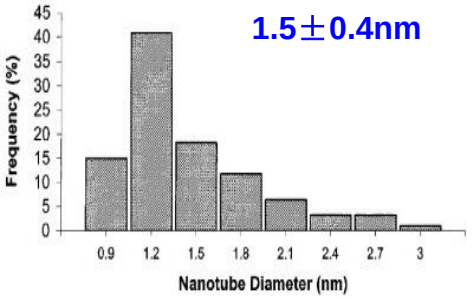

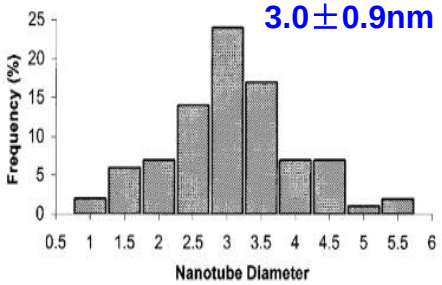

Hongjie Dai, et al., J. Phys. Chem. B 2001, 105, 11424;
J. Phys. Chem. B, **2002**, 106, 12361-12365

Using polyacid cluster as catalyst precursor

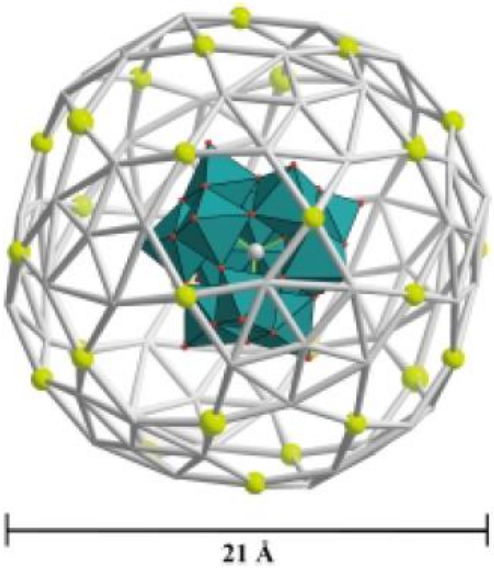

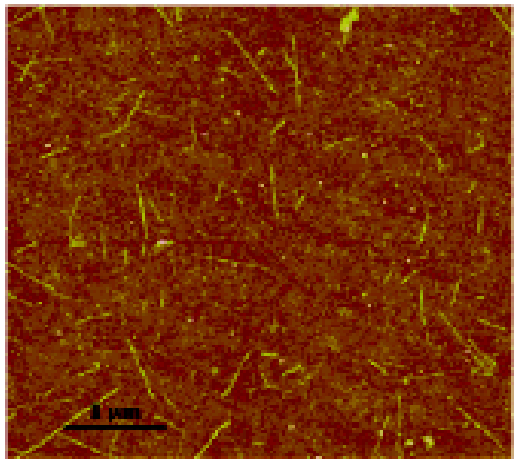

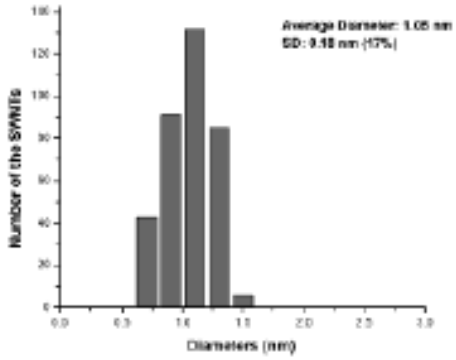

$$[H_xPMo_{12}O_{40} \subset H_4Mo^{VI}_{72}Fe^{III}_{30}(CH_3COO)_{15}O_{254}(H_2O)_{98}] \cdot \text{ca. } 60\,H_2O$$

$$\mathbf{1} \equiv \mathbf{1a} \cdot \text{ca. } 60\,H_2O$$

Jie Liu, et al., J. AM.CHEM.SOC, 2002, 124, 13688

Orientation

Growth of Oriented ultra-long SWNTs on surfaces

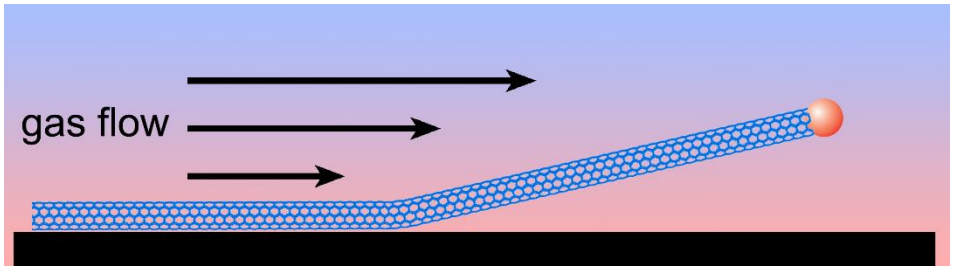

"Kite" Mechanism

Fast-heating; Large feeding gas flow

By Jie Liu et al.

? Question: Is fast-heating and large feeding gas flow really essential for the growth of ultralong SWNTs?

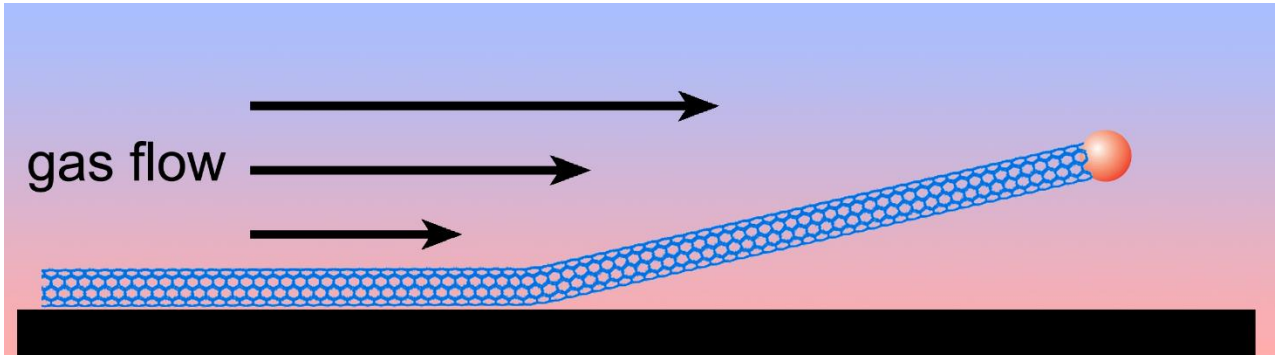

$\mathrm{Ri} = \Delta\rho g h / \rho v^2$ Buoyant effect is strong enough to lift the tube up

$Re = \rho v d / \mu$ Stable lamellar flow is favorite for the growth

Fluid Mechanics tells us: NO

Ultra-low feeding gas guided non-fast-heating CVD growth of oriented ultra-long SWNTs (1)

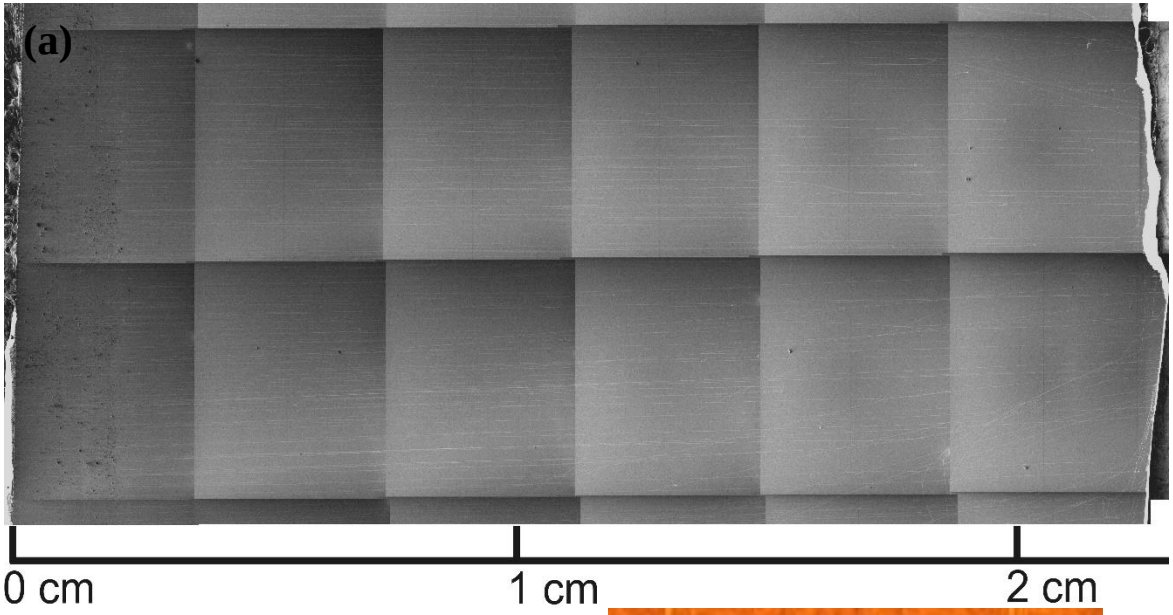

1.5~6 sccm

0.3~1.2mm/s

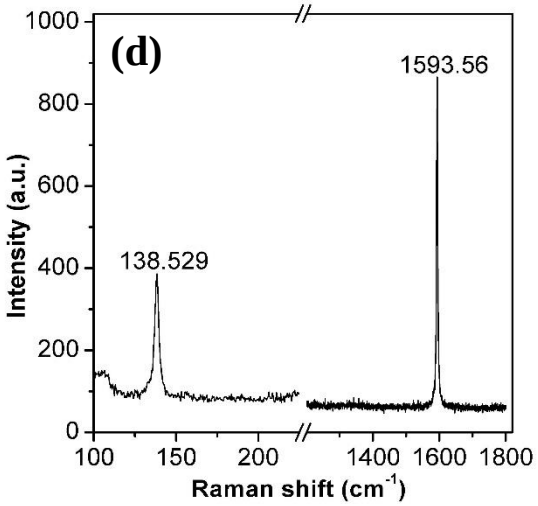

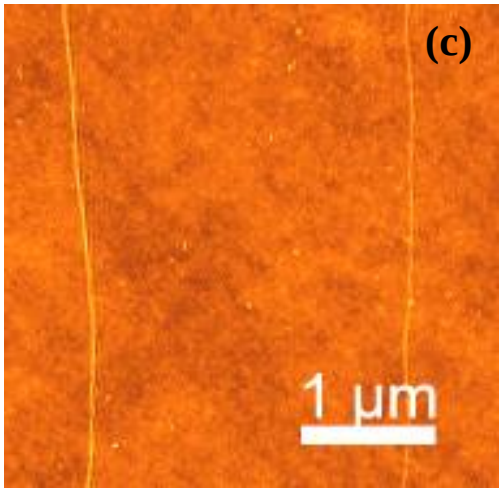

Z. Jin, H. Chu, J. Wang, J. Hong, W. Tan, **Y. Li***; ***Nano Letters 2007***, *7, 2073-2079.*

Ultra-low feeding gas guided non-fast-heating CVD growth of oriented ultra-long SWNTs

How long can an individual SWNT be?

18.5 cm

X. Wang/Q. Li*/Y. Li ***Nano Lett.*** 2009, 3137

1.5~6 sccm 0.3~1.2mm/s

Z. Jin/ **Y. Li***; ***Nano Letters 2007***, *7, 2073.*

Ultra-low feeding gas guided non-fast-heating CVD growth of oriented ultra-long SWNTs (3)

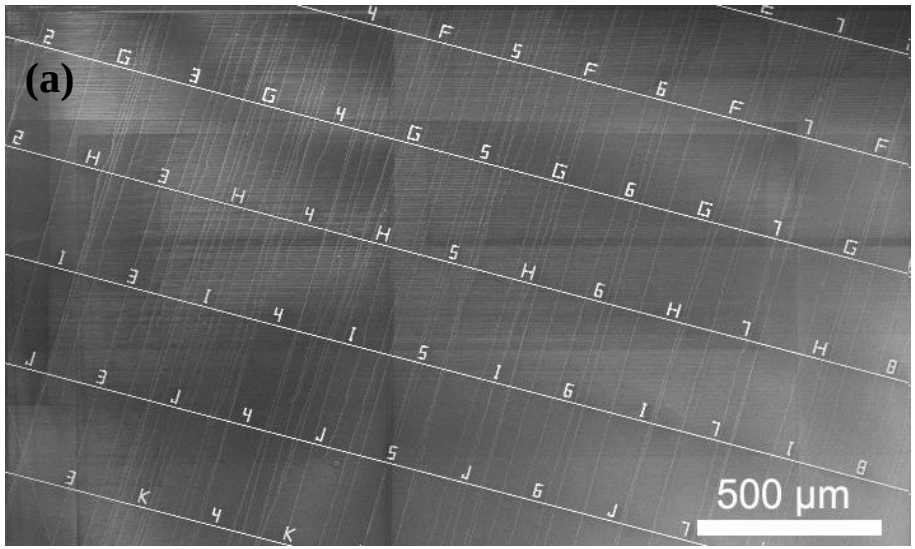

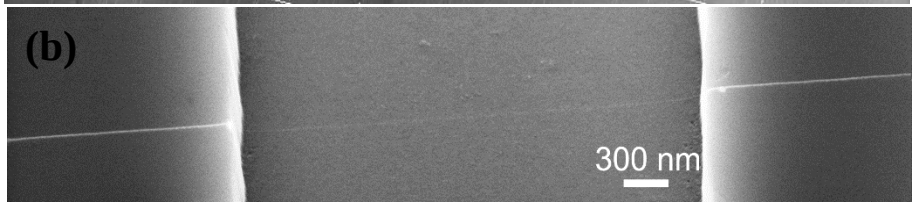

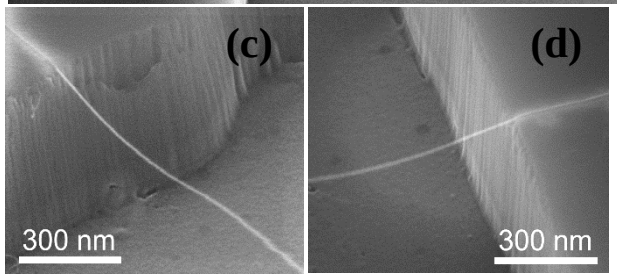

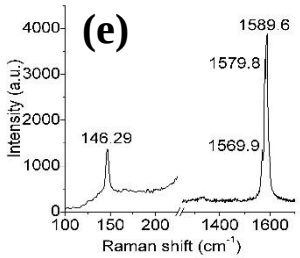

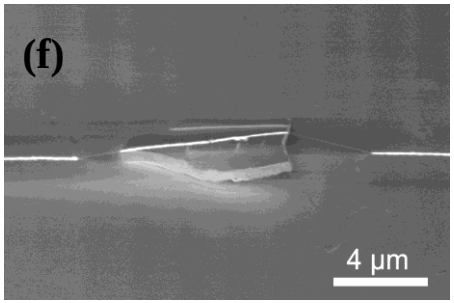

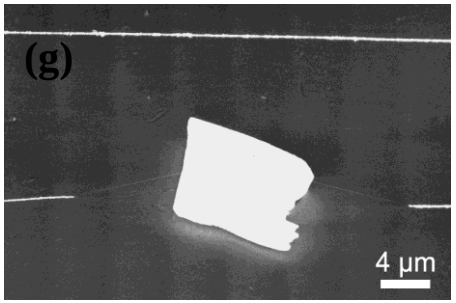

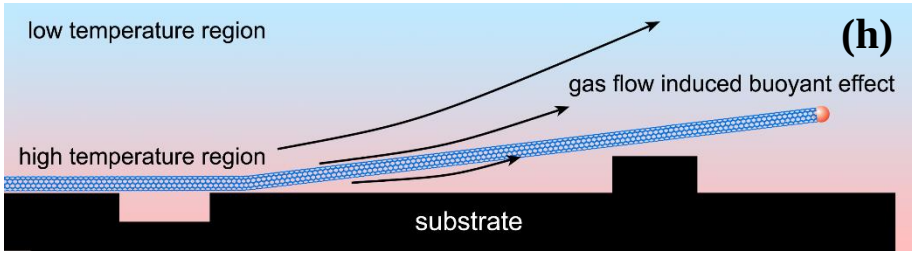

Z. Jin, H. Chu, J. Wang, J. Hong, W. Tan, **Y. Li***; ***Nano Letters 2007***, *7, 2073-2079.*

Ultra-low feeding gas guided non-fast-heating CVD growth of oriented ultra-long SWNTs (4)

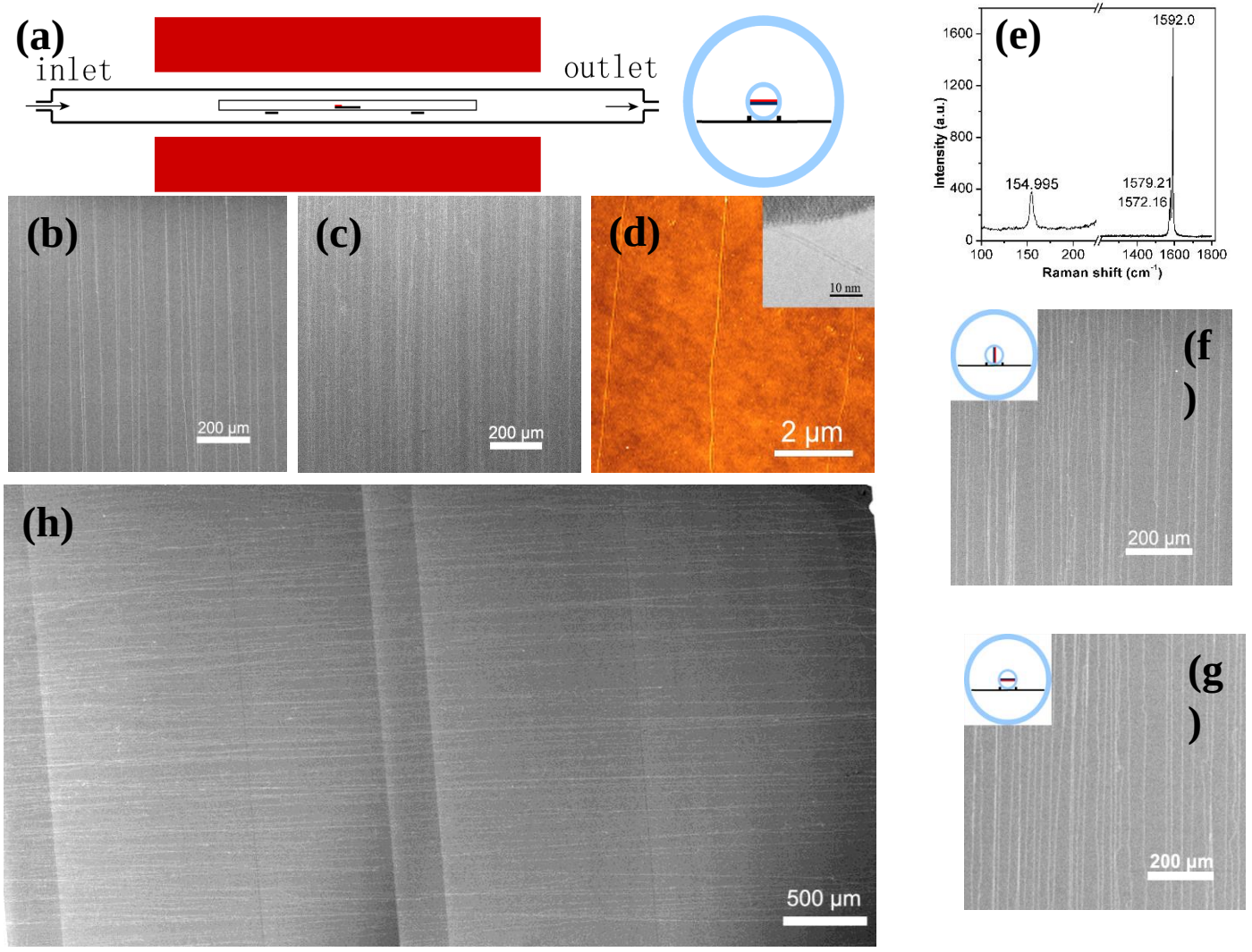

Z. Jin, H. Chu, J. Wang, J. Hong, W. Tan, **Y. Li***; ***Nano Letters 2007***, *7, 2073-2079.*

Ultra-low feeding gas guided non-fast-heating CVD growth of oriented ultra-long SWNTs (5)

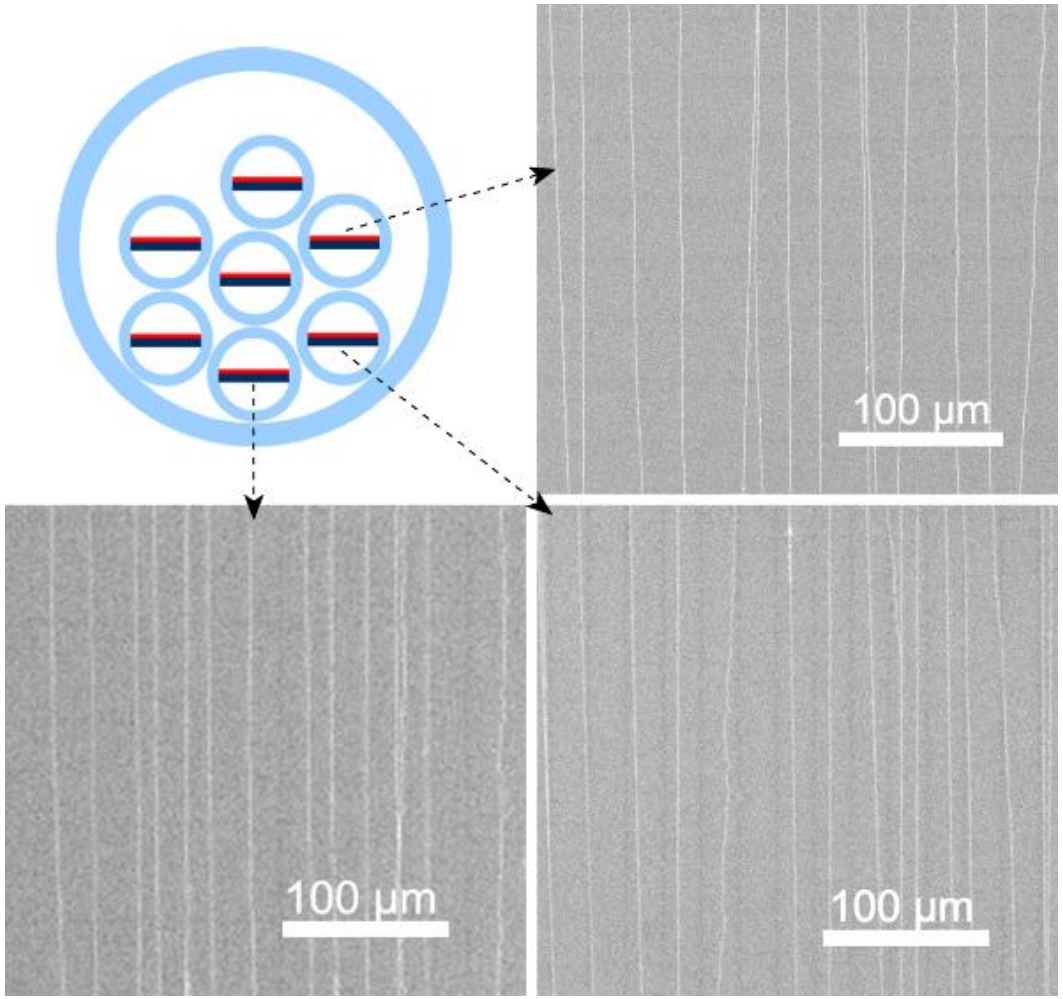

Z. Jin, H. Chu, J. Wang, J. Hong, W. Tan, **Y. Li***; ***Nano Letters 2007***, *7, 2073-2079.*

Flexible orientation control of SWCNT arrays by gas flow (1)

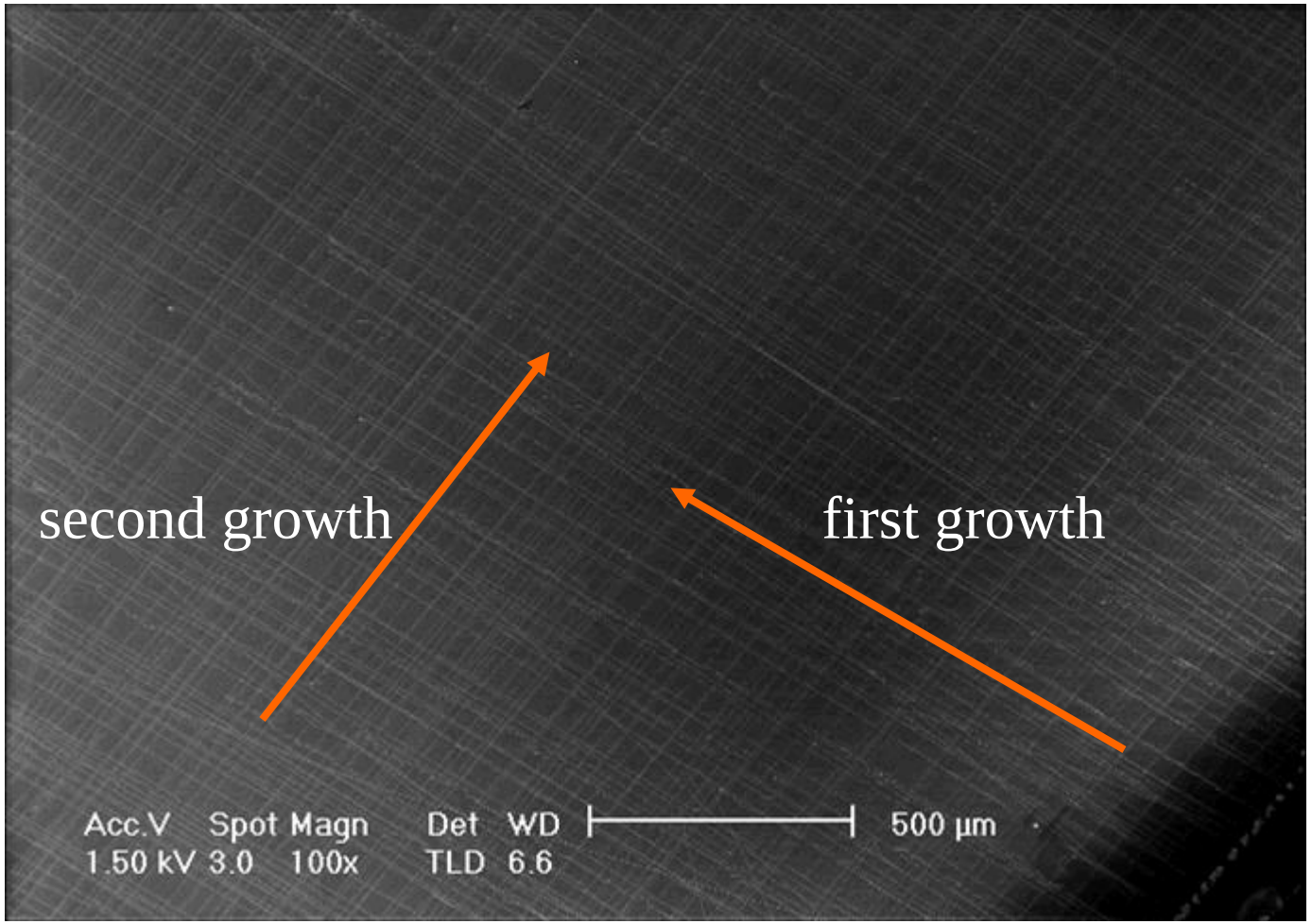

Y. Liu, J. Hong, Y. Zhang, R. Cui, J. Wang, W. Tan, **Y. Li*; *Nanotechnology 2009***, 20,185601

Flexible orientation control of SWCNT arrays by gas flow (2)

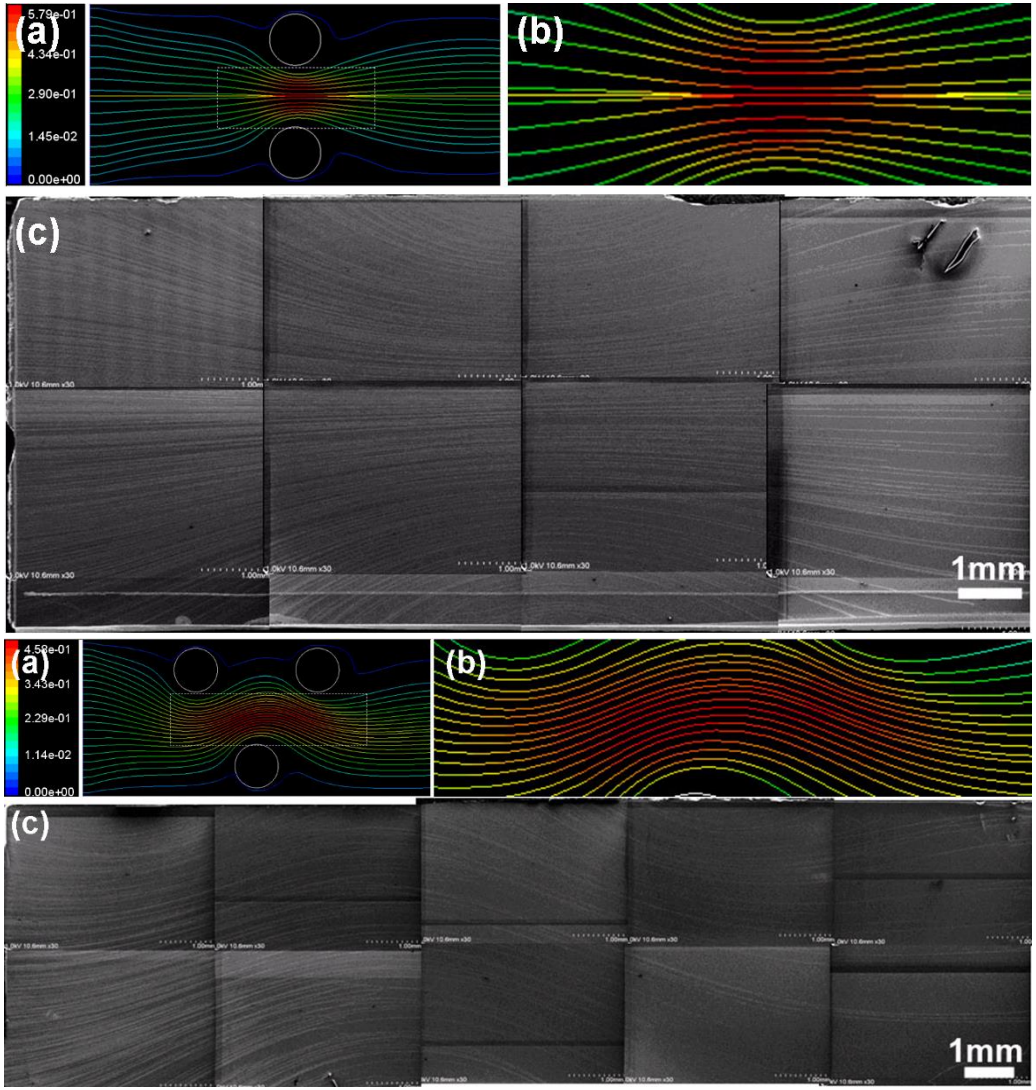

Y. Liu, J. Hong, Y. Zhang, R. Cui, J. Wang, W. Tan, **Y. Li*;** ***Nanotechnology 2009***, 20,185601

Copper Catalyzing Growth of SWNTs on Substrates

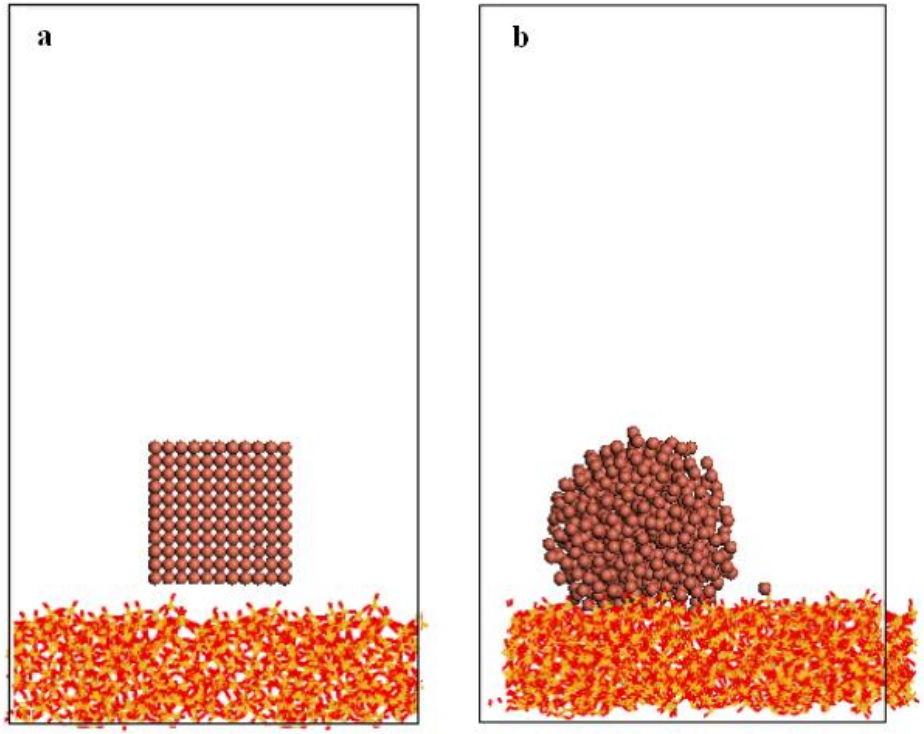

MD simulation

$Cu\text{-}SiO_2$

177 kcal/mol

$Fe\text{-}SiO_2$

390 kcal/mol

W. Zhou, Z. Han, J. Wang, Y. Zhang, Z. Jin, X. Sun, Y. Zhang, C. Yan, **Y. Li***; ***Nano Letters 2006***, 6 (12): 2987-2990.

Copper Catalyzing Growth of SWNTs on Substrates

Carbon source: ethanol

Fe

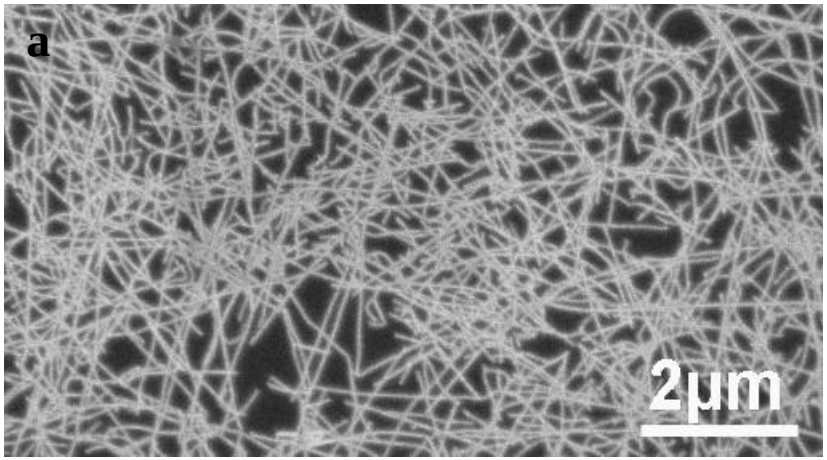

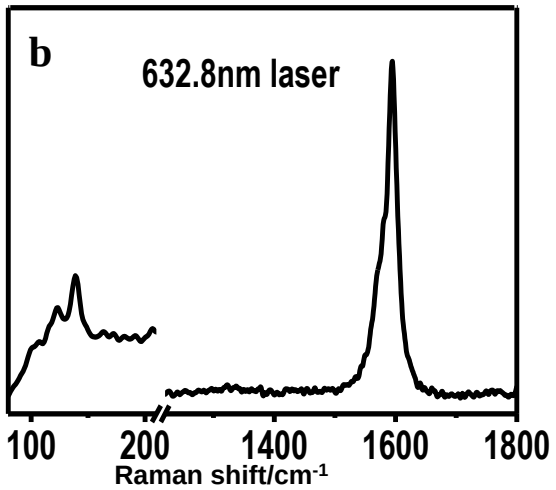

Cu

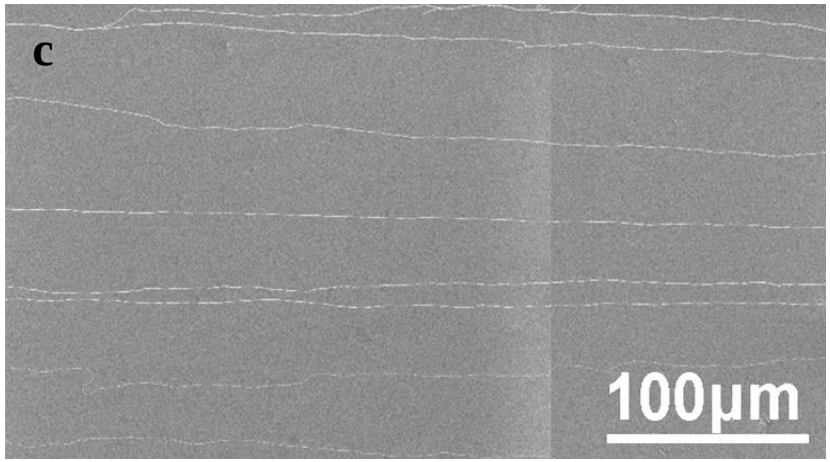

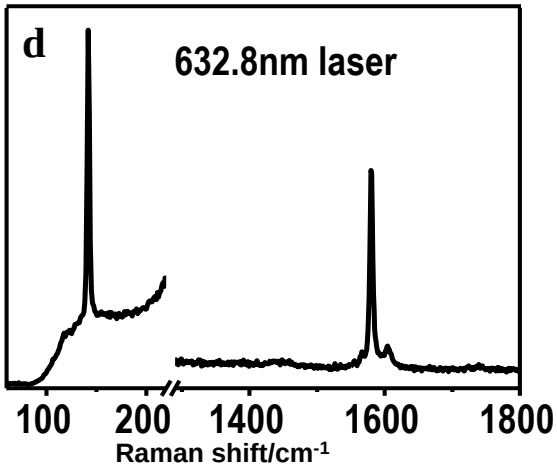

Nano Letters, 2006

Comparison between Cu and Fe as catalysts for SWNT growth

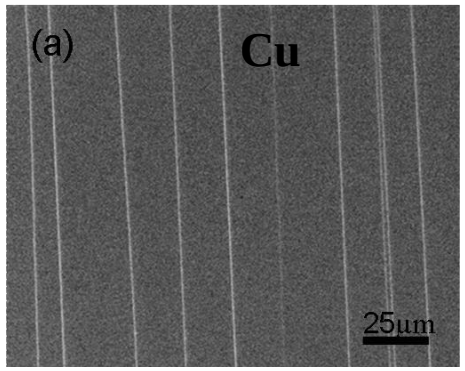

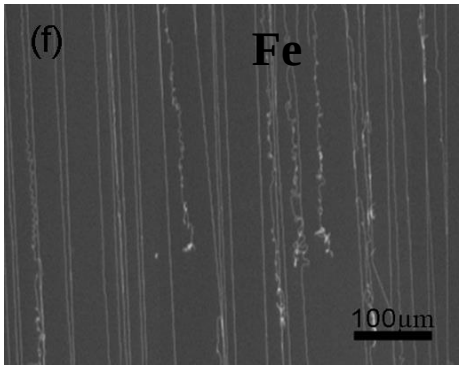

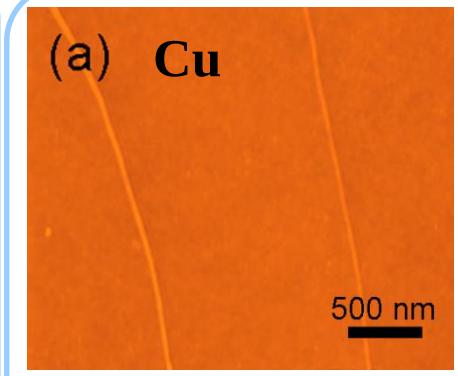

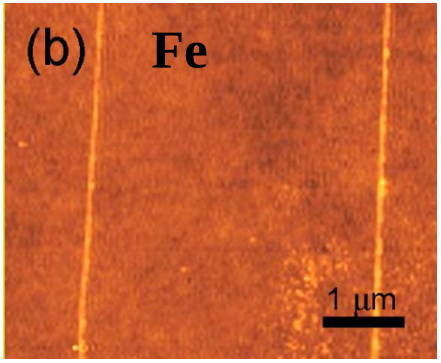

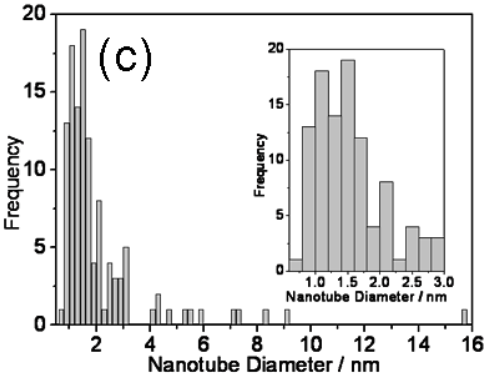

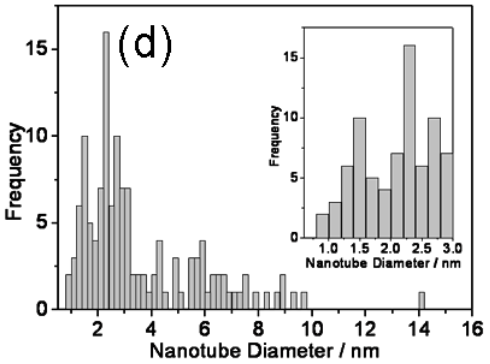

<3.0 nm 85%
>3.0 nm 15%
1.5 ± 0.5 nm
80%>1cm

<3.0 nm 58%
>3.0 nm 42%
2.1 ± 0.6 nm
40%>1cm

SWNTs obtained by using Cu as catalysts are straight, longer, cleaner, and with narrower dimameter distribution.

W. Zhou/**Y. Li*** ; ***Nano Lett.* 2006**, 2987

R. Cui/**Y. Li***; ***JPCC* 2010**, 114, 15547

Y. Li* et al., Adv. Mater. 2010, 22, 1508

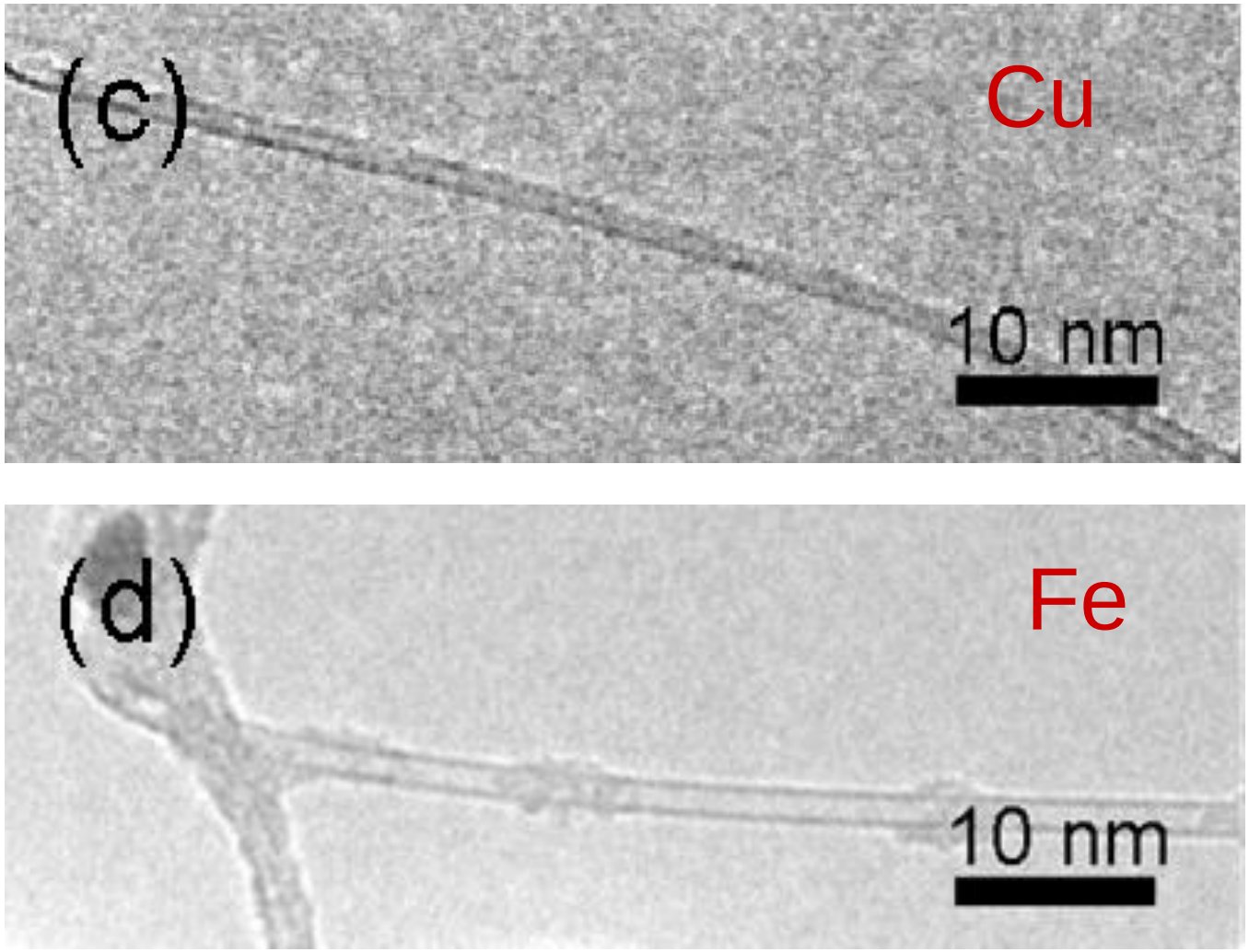

R. Cui, **Y. Li*** et al., ***JPCC* 2010**, **114,** 15547.

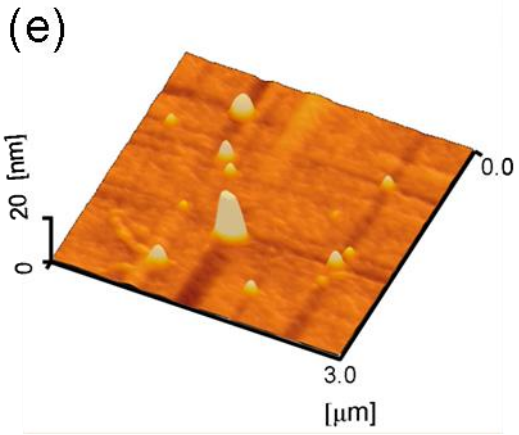

originally

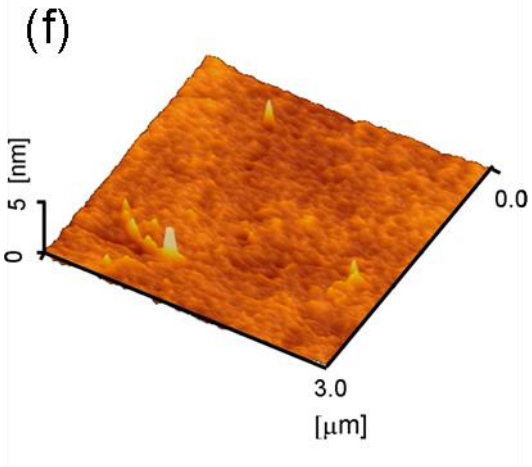

After reduced in H_2 for 15 min at 900 °C

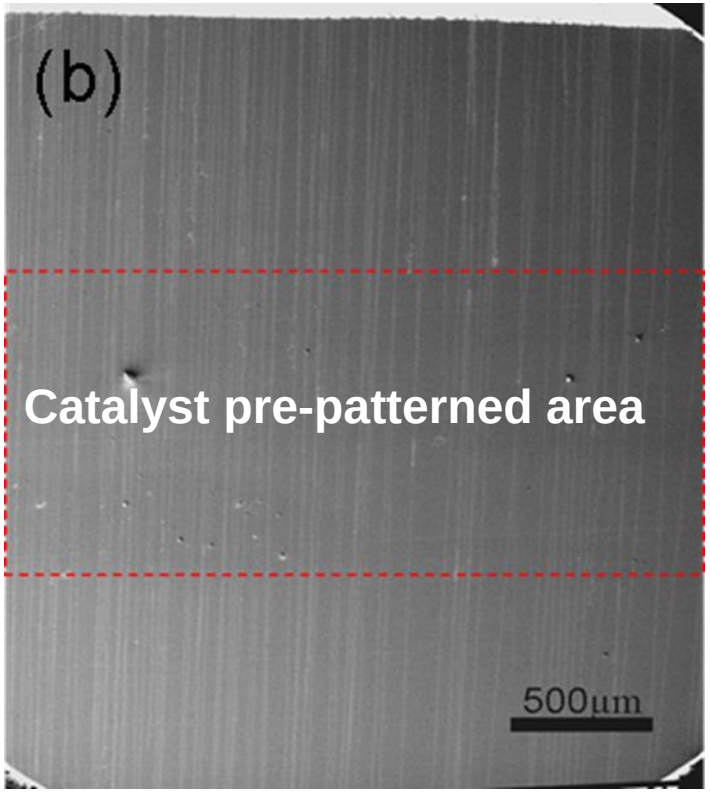

R. Cui/ **Y. Li*** , ***JPCC* 2010**, **114,** 15547.

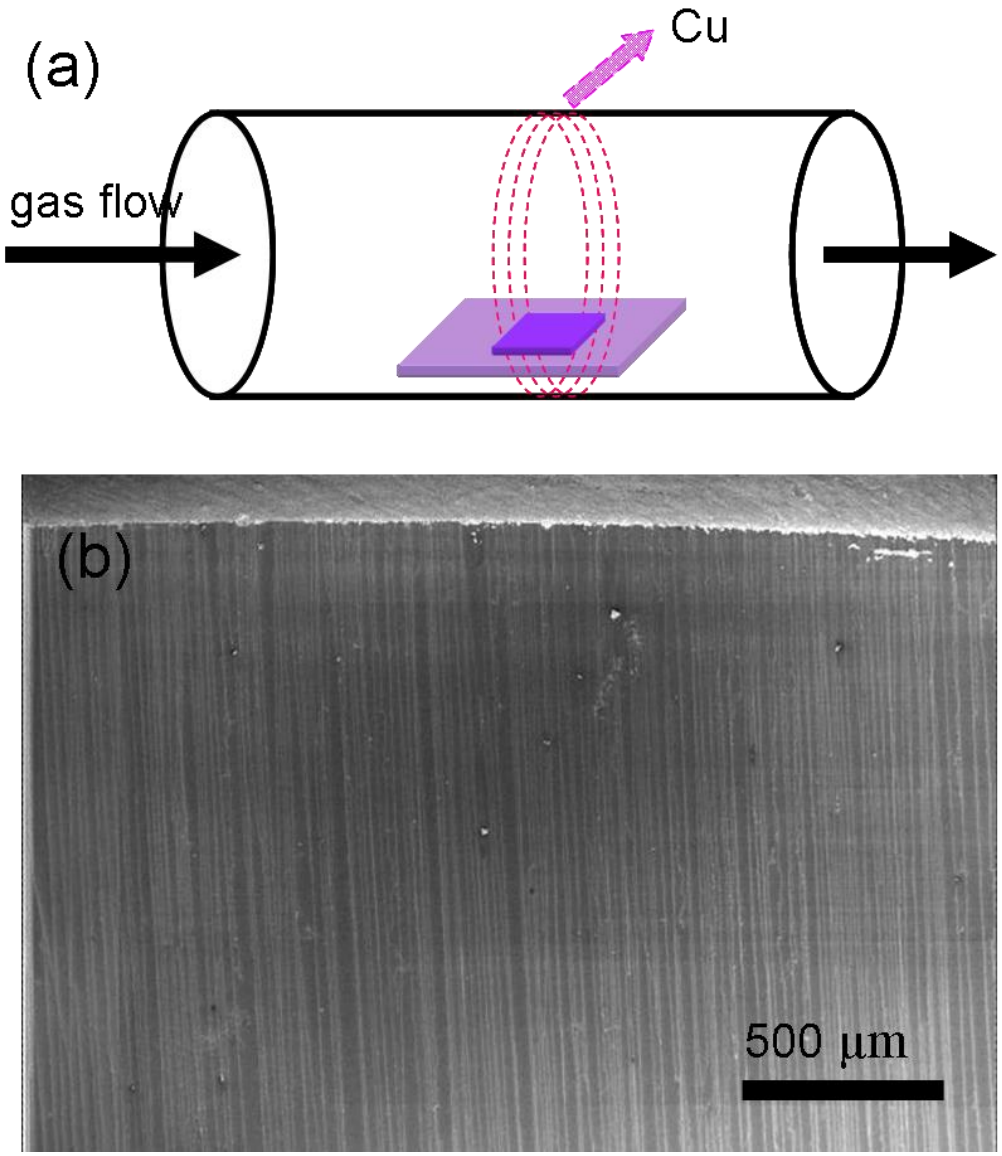
(a)
Cu
gas flow
(b)
500 μm

Fe

Cu

Lattice-oriented growth of SWNTs

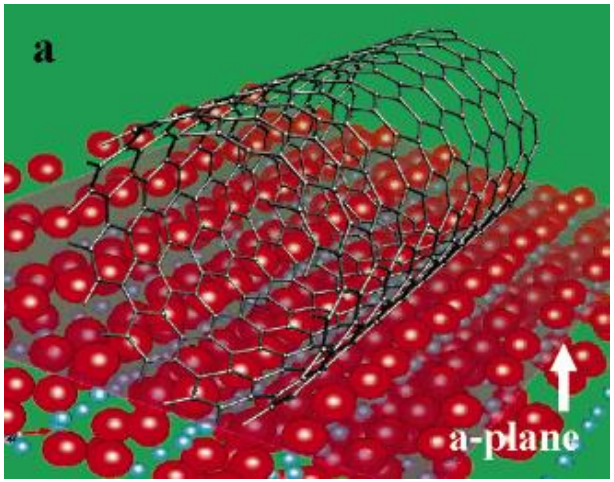

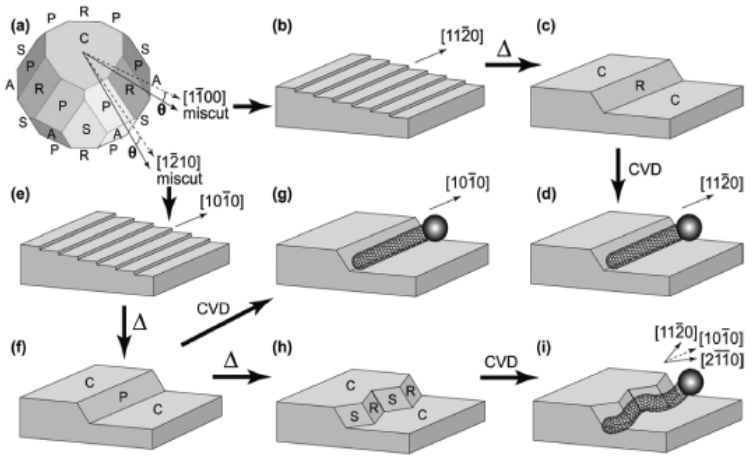

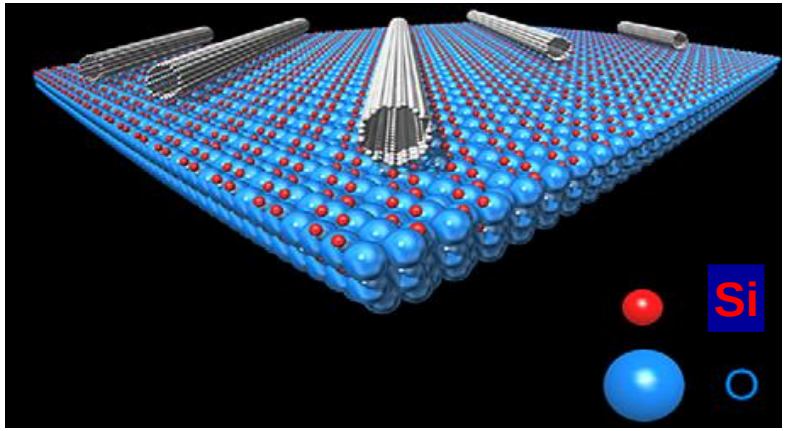

Zhou, Rogers, Joselevich

Dense SWNT arrays grown on ST-cut quartz

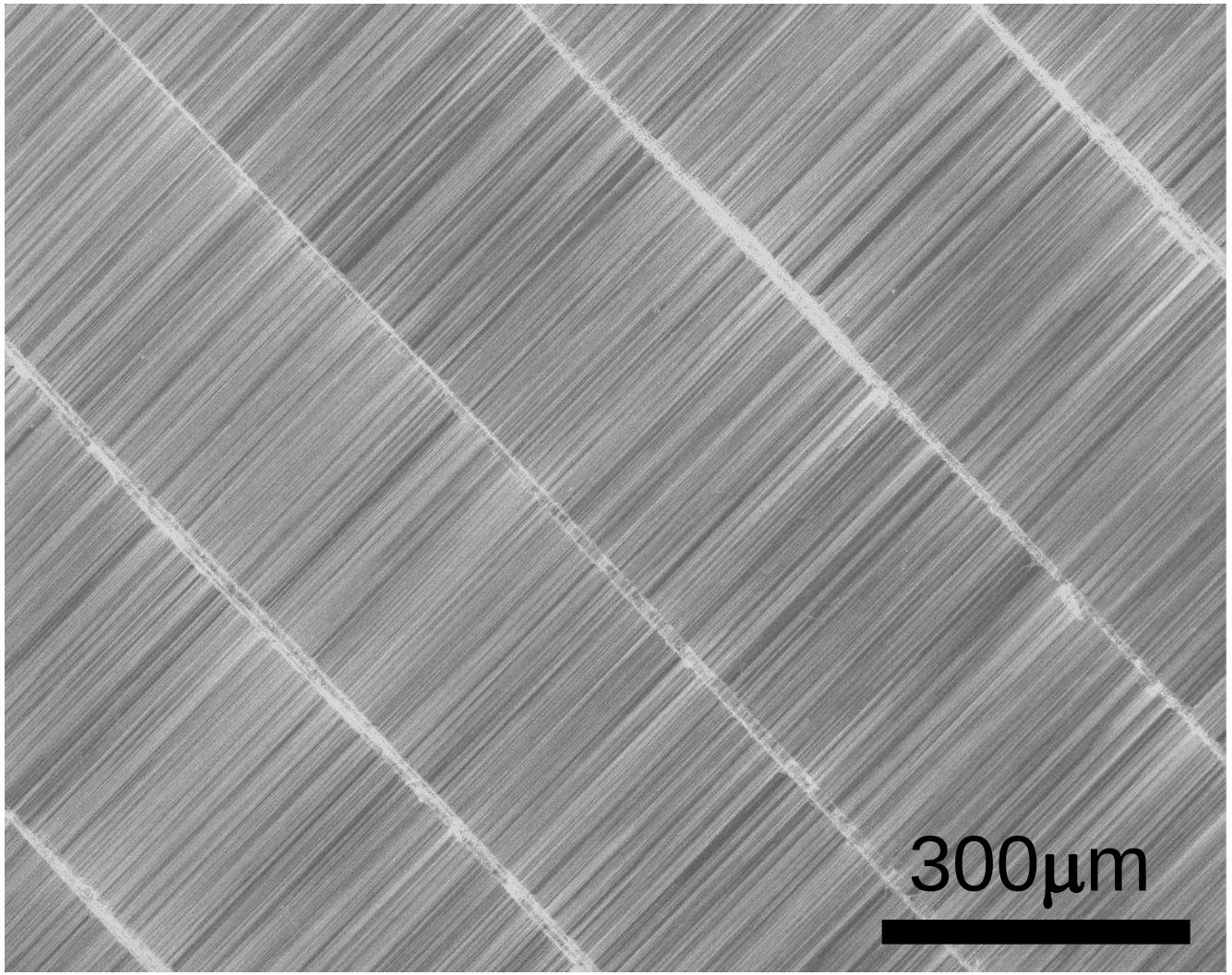

Y. Li* et al. ***Adv. Mater., 2010,*** 22,1508-1515.

Orientation of SWNTs depends on substrate lattice

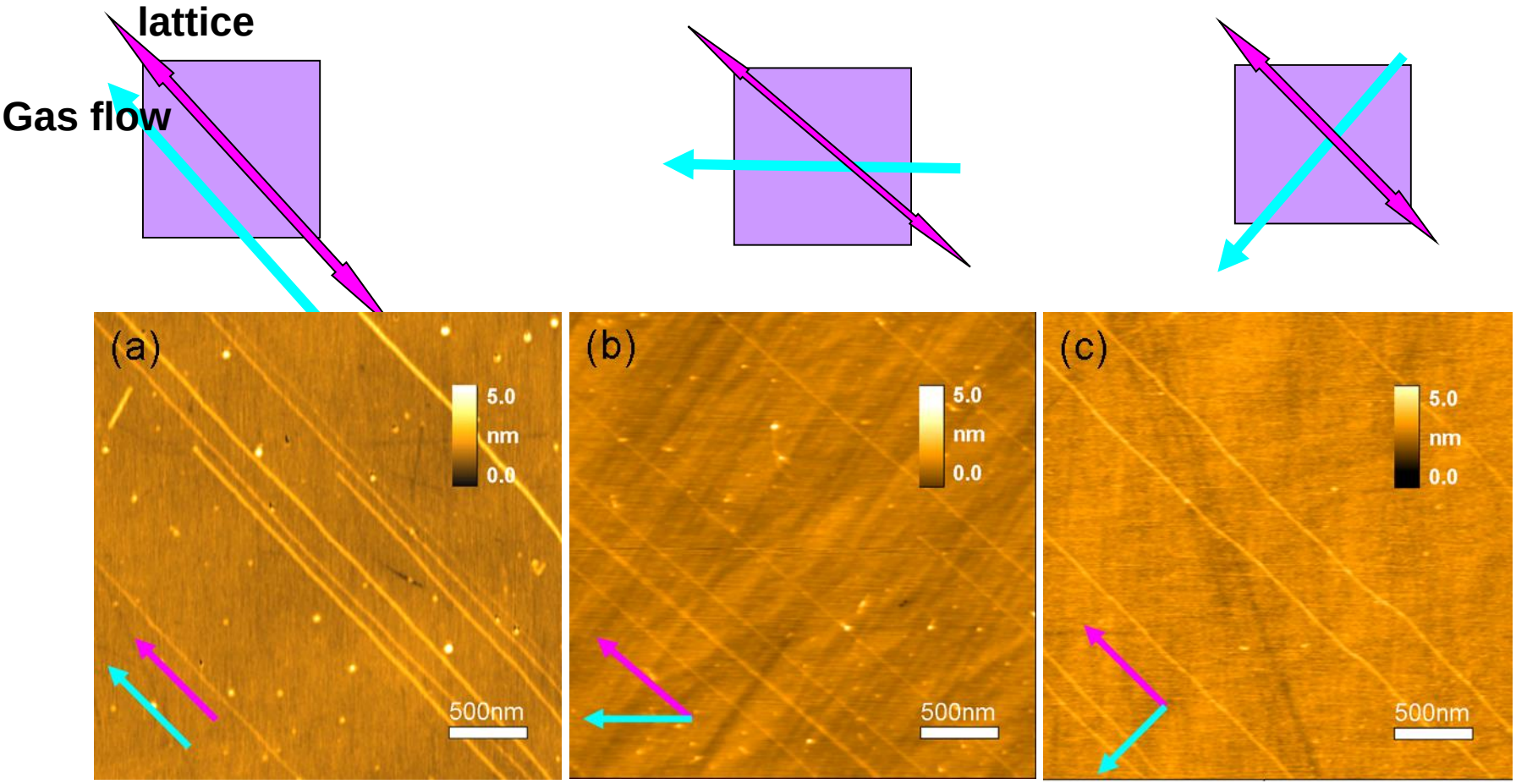

Molecular nanoclusters as catalyst precursors

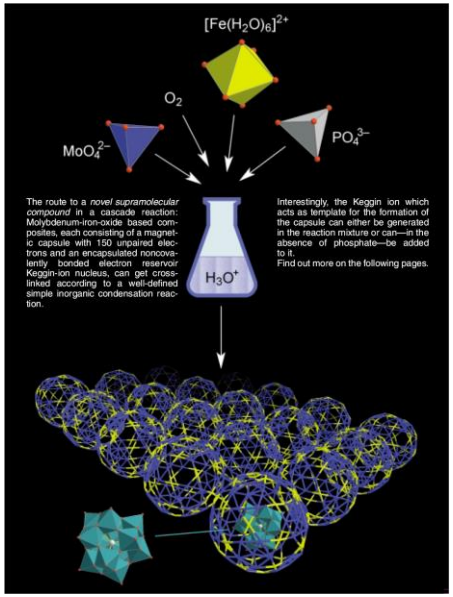

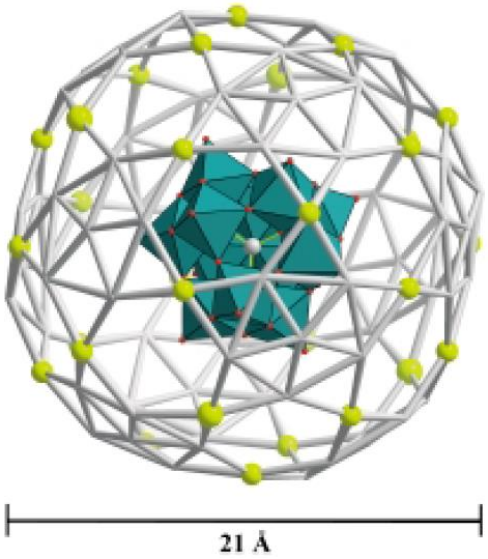

$$[H_xPMo_{12}O_{40} \subset H_4Mo^{VI}_{72}Fe^{III}_{30}(CH_3COO)_{15}O_{254}(H_2O)_{98}] \cdot \text{ca. } 60\,H_2O$$

$Mo_{72}Fe_{30}$

Identical structure and size

Achim Muller et al. ***Angew. Chem. Int. Ed. 2000, 39***, 3413

SWNT arrays grown at different temperatures

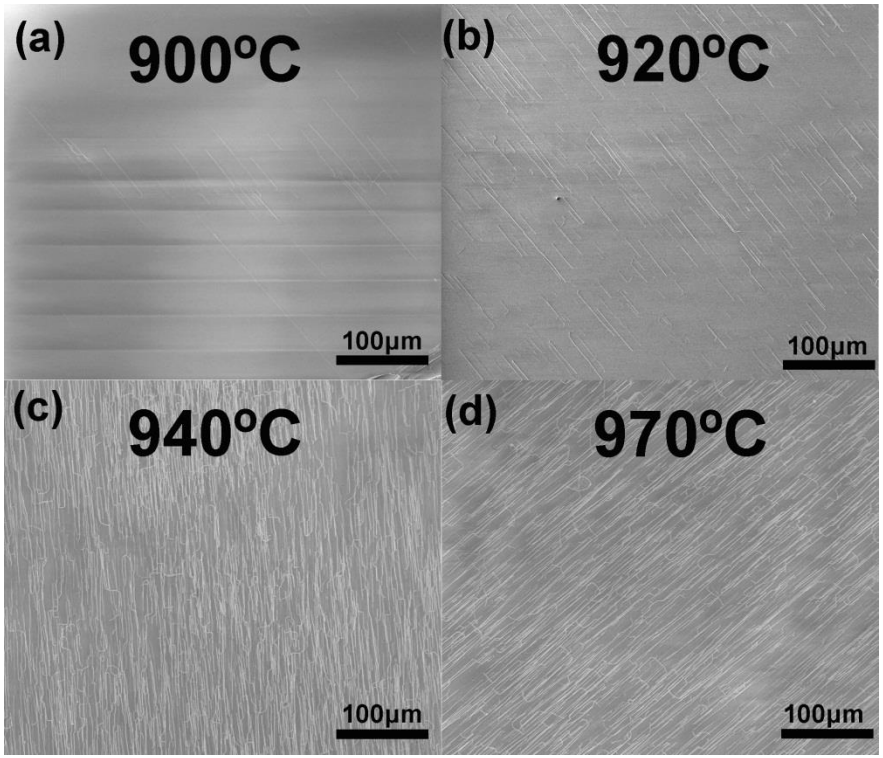

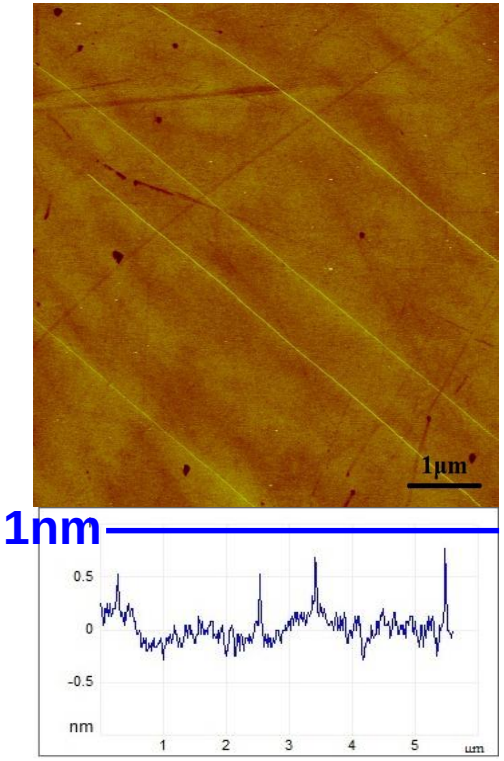

920 ℃

Diameter distribution of SWNTs

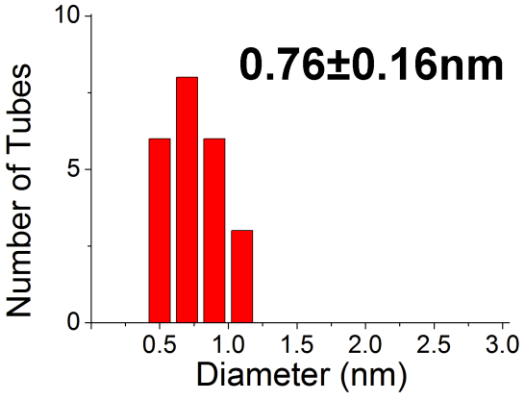

(a) 900°C

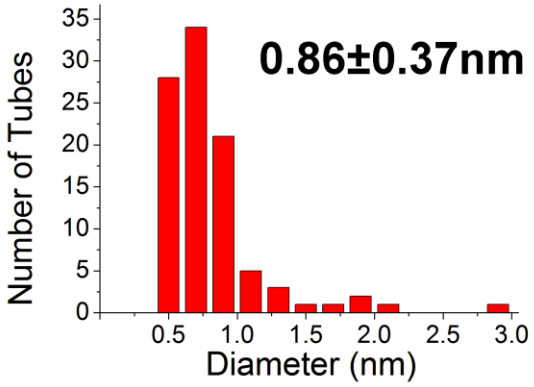

(b) 920°C

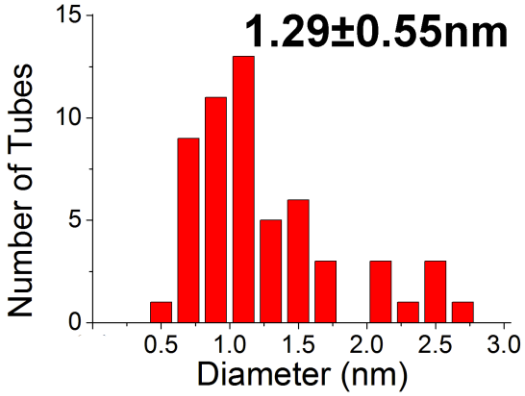

(c) 940°C

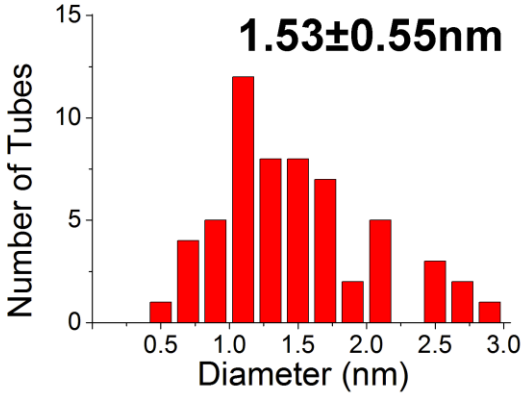

(d) 970°C

With the increase of growth temperature, the diameter of SWNTs increases together with a broadened diameter distribution.

Diameter distribution of catalyst particles

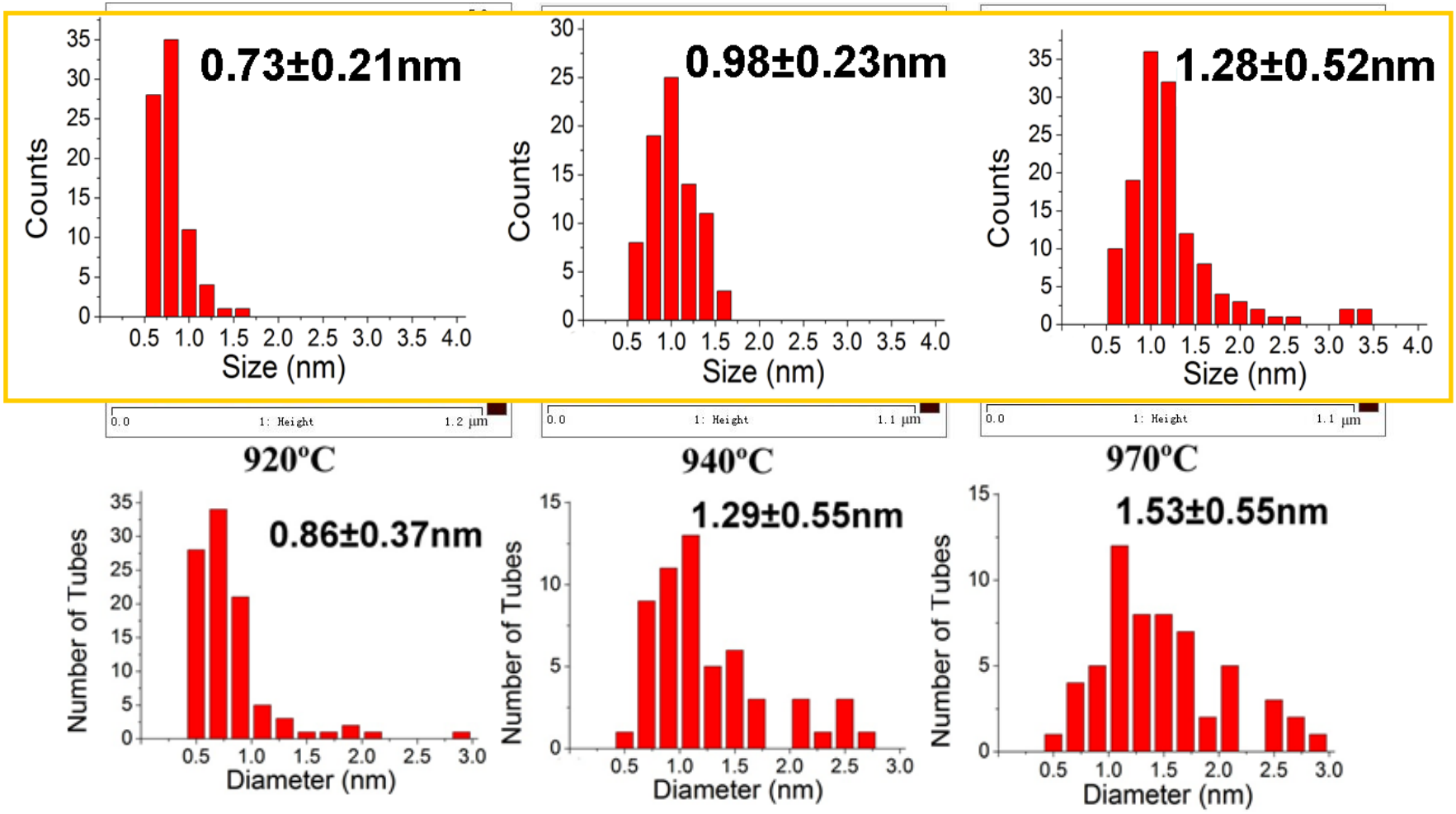

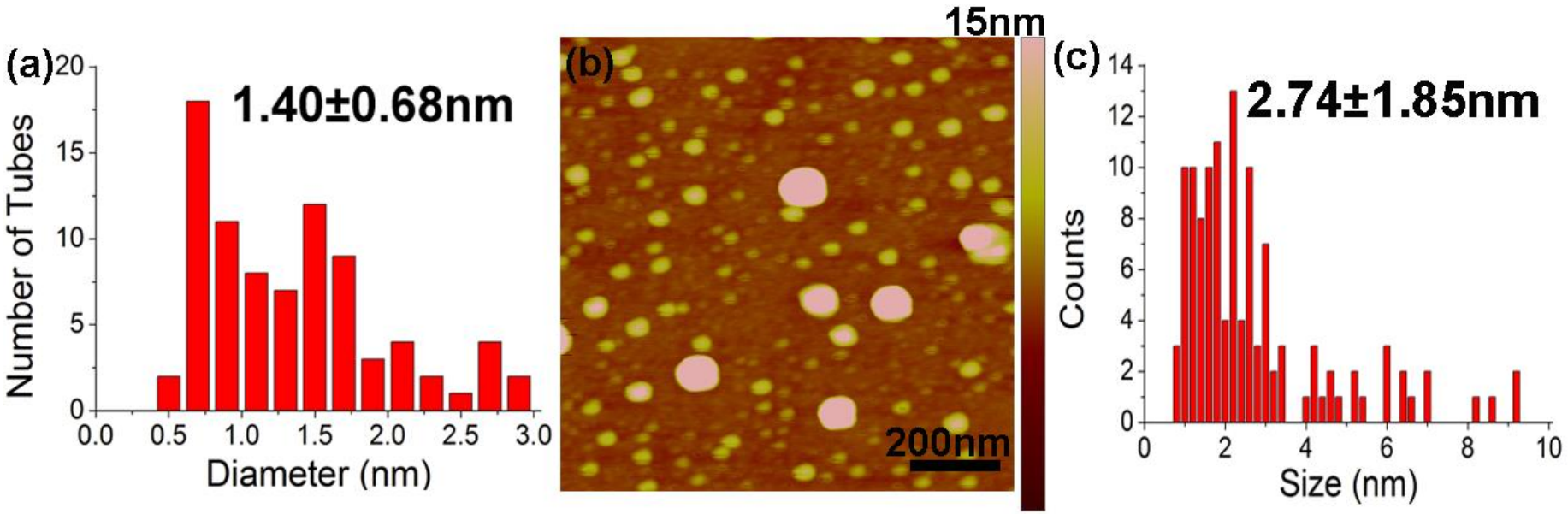

(a) Diameter distribution of SWNTs grown at 920 ºC using a mixture of Fe and Mo compounds as catalyst precursors. (b,c) AFM image and size distribution of the mixture of Fe and Mo compounds after H_2 reduction at 920 ºC

Super-growth SWNT forests

10mm

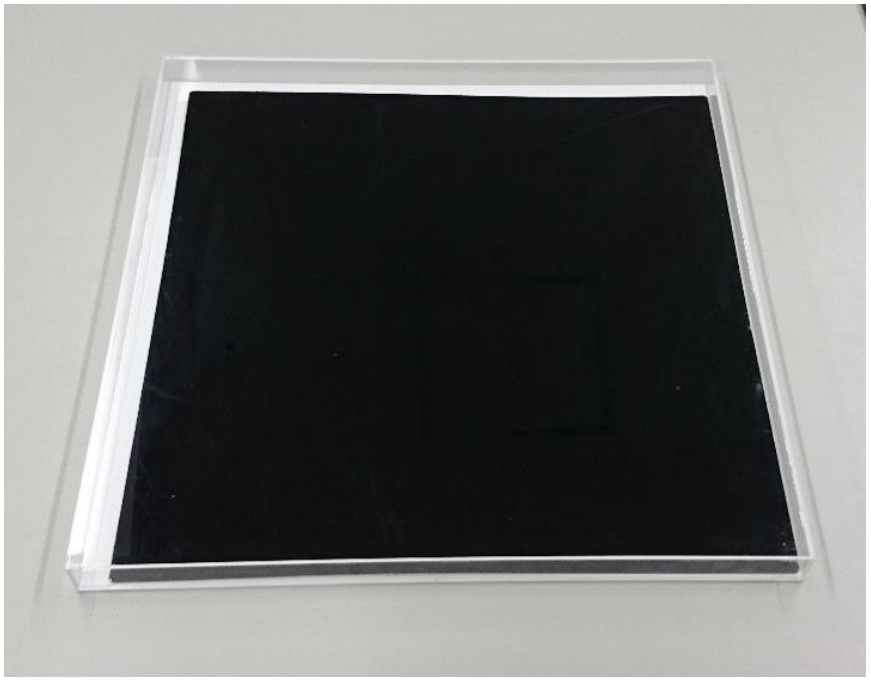

50cm

Kenji Hata, Don Futaba et al, AIST

Science 2004, 306, 1362–1364

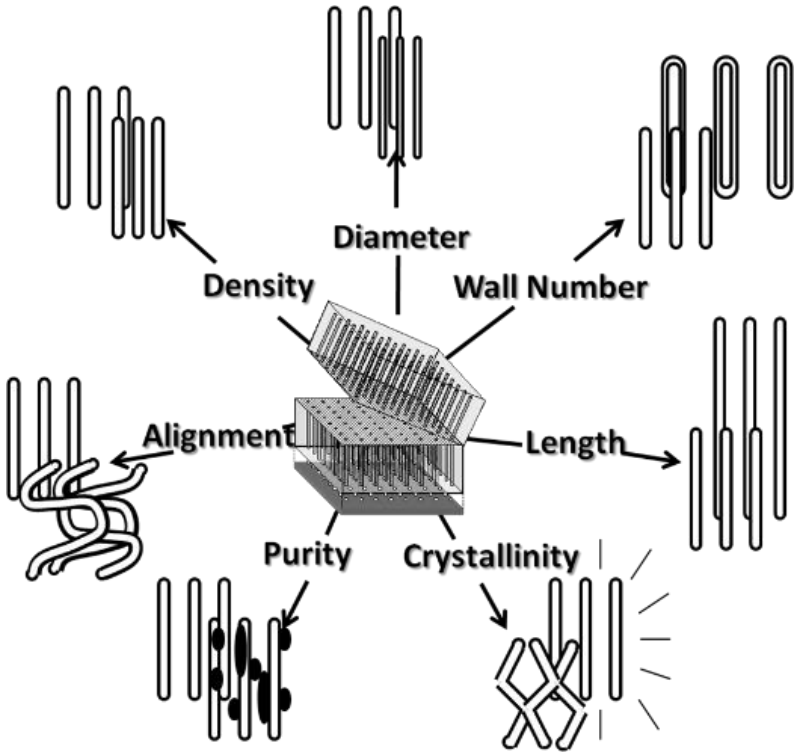
Diameter
Density
Wall Number
Alignment
Length
Purity
Crystallinity

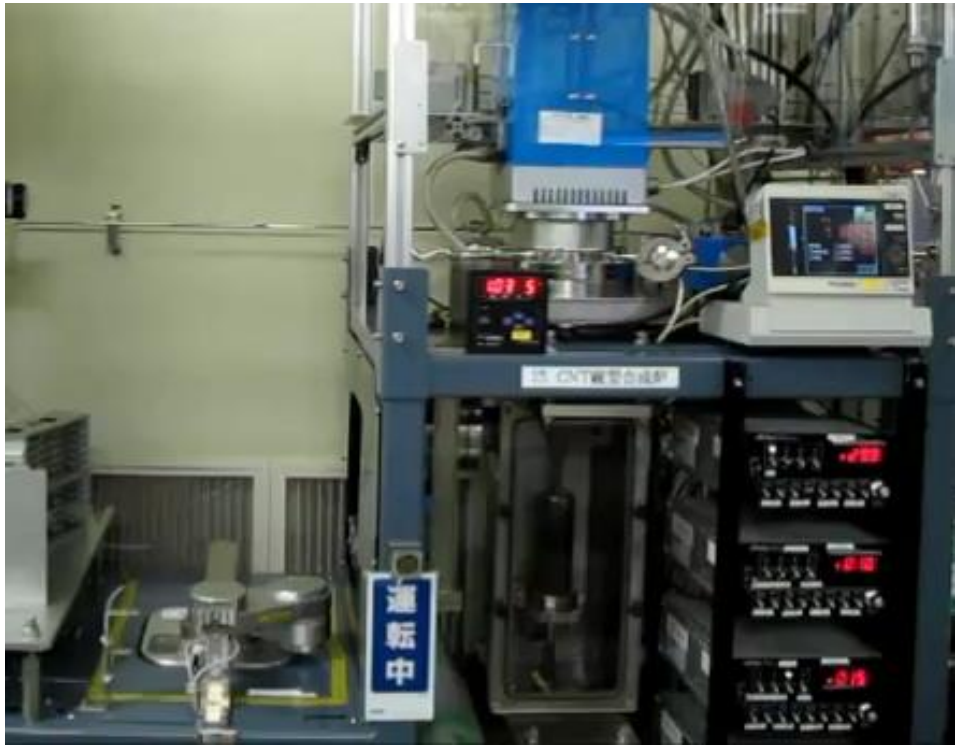
運転中

Role of water in super-growth:

Keep the catalyst nanoparticles active!

---etch carbon

---inhibit Ostwald ripening of catalyst nanoparticles

Water-Assisted Highly Efficient Synthesis of Impurity-Free Single-Walled Carbon Nanotubes

Kenji Hata,*† Don N. Futaba,* Kohei Mizuno, Tatsunori Namai, Motoo Yumura, Sumio Iijima

We demonstrate the efficient chemical vapor deposition synthesis of single-walled carbon nanotubes where the activity and lifetime of the catalysts are enhanced by water. Water-stimulated enhanced catalytic activity results in massive growth of superdense and vertically aligned nanotube forests with heights up to 2.5 millimeters that can be easily separated from the catalysts, providing nanotube material with carbon purity above 99.98%. Moreover, patterned, highly organized intrinsic nanotube structures were successfully fabricated. The water-assisted synthesis method addresses many critical problems that currently plague carbon nanotube synthesis.

Single-walled carbon nanotubes (SWNTs) are a key aspect in the emerging field of nanotechnology; however, large-scale synthesis is still limited because of the difficulties in synthesizing SWNTs. Current synthesis methods suffer from the production of impurities that must be removed through purifications steps, which can damage the nanotubes. Dispersion of SWNTs in solutions for further processing also presents challenges because the smooth-sided tubes readily aggregate and form parallel bundles or ropes as a result of van der Waals interactions. We report a rational yet simple and general synthetic approach that concurrently addresses these problems, in which the activity and lifetime of the catalysts are dramatically enhanced by the addition of a controlled amount of water vapor in the growth atmosphere.

We wanted to find a weak oxidizer that would selectively remove amorphous carbon but would not damage the nanotubes at the growth temperature, because coating of the catalyst particles by amorphous carbon during chemical vapor deposition (CVD) reduces their activity and lifetime (*1*). We found that water acts in promoting and preserving catalytic activity. SWNTs were grown by ethylene CVD by using Ar or He with H_2 that contained a small and controlled amount of water vapor (*2*). Balancing the relative levels of ethylene and water was crucial to maximize catalytic lifetime. Water-assisted growth was successfully carried out on various catalysts that generate SWNTs, including Fe nanoparticles (*3*) from $FeCl_3$ and sputtered metal thin films (Fe, Al/Fe, Al_2O_3/Fe, Al_2O_3/Co) on Si wafers, quartz, and metal foils, which demonstrates the generality of our approach.

Water-stimulated catalytic activity results in the growth of dense and vertically aligned SWNT forests with millimeter-scale height in a 10-min growth time. Our best result to date is 2.5 mm in 10 min (Fig. 1, A and B). In contrast with standard ethylene CVD growth, where the catalysts are only active for about 1 min, a height increase of the forests has been observed after 30 min for water-assisted growth. The SWNT/catalyst weight ratio exceeds 50,000%, more than 100 times as high as that of the high-pressure carbon monoxide (HiPco) process (*4*). Provided that the amount of water is well controlled, growths are highly reproducible.

A close examination (Fig. 1C) at the ledge of the SWNT forest illustrates that the nanotubes are densely packed and vertically aligned from the substrate. Low-resolution transmission electron microscopy (TEM) studies (Fig. 1D) of the as-grown forest reveal the presence of only thin nanotubes and the absence of metallic particles and supporting materials that usually comprise a major constituent of as-grown material. High-resolution TEM studies (Fig. 1E and fig. S1) show that the nanotubes are clean SWNTs free from amorphous carbon and metal particles. We have taken hundreds of high-resolution TEM images, and double- or multi-walled carbon nanotubes (MWNTs) were rarely found. Raman spectra (fig. S2) at 514 nm excitation showed clear radial breathing mode peaks (RBM), which confirmed the existence of SWNTs. The sizes of the SWNTs were estimated from the peaks to be in the range of 1 to 3 nm, in agreement with those measured by TEM.

The SWNT forest structure can be easily removed from the substrate with, for example, a razor blade (movie S1). After removal, the substrate is still catalytically active and can grow SWNT forests again, indicating a root-growth mode and the presence of the catalysts on the substrate. Thermo-gravimetric analysis (TGA) was implemented on 10 mg of the as-grown material (Fig. 2A). No measurable residue remained after heating above 750°C, indicating very high purity. The combustion range of the SWNTs was 550°C to 750°C, with the peak weight reduction occurring at 700°C, a result very similar to that of purified, high-quality SWNTs synthesized by a laser-oven method (*5*). Quantitative elemental analysis with x-ray fluorescence spec-

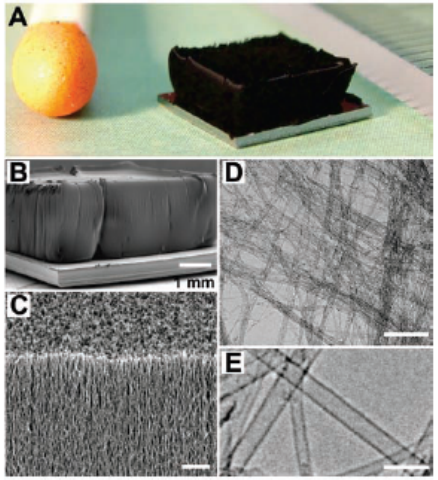

Fig. 1. SWNT forest grown with water-assisted CVD. (**A**) Picture of a 2.5-mm-tall SWNT forest on a 7-mm by 7-mm silicon wafer. A matchstick on the left and ruler with millimeter markings on the right is for size reference. (**B**) Scanning electron microscopy (SEM) image of the same SWNT forest. Scale bar, 1 mm. (**C**) SEM image of the SWNT forest ledge. Scale bar, 1 μm. (**D**) Low-resolution TEM image of the nanotubes. Scale bar, 100 nm. (**E**) High-resolution TEM image of the SWNTs. Scale bar, 5 nm.

Research Center for Advanced Carbon Materials, National Institute of Advanced Industrial Science and Technology (AIST), Tsukuba, 305-8565, Japan.

*These authors contributed equally to this work
†To whom correspondence should be addressed. E-mail: kenji-hata@aist.go.jp

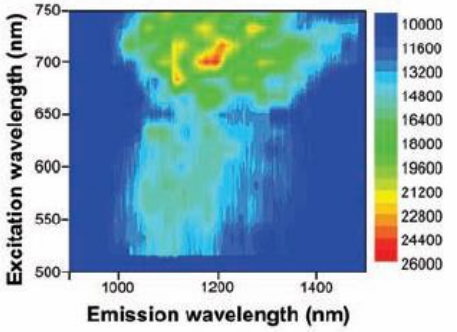

Fig. 3. Contour plot of fluorescence intensity versus excitation and emission wavelengths for the as-grown SWNT forest sample.

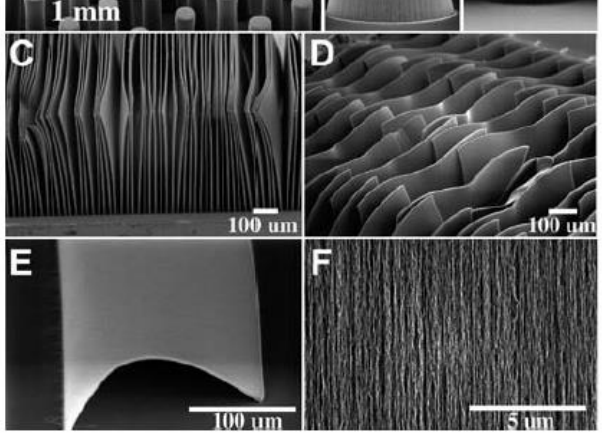

of the sheet face.

REPORTS

height close to 1 mm. A close examination (Fig. 4B) shows that the pillars are standing vertically from the substrate. Notably, the cross section of the SWNT structure corresponds well with the patterned catalyst (inset of Fig. 4A), and thus it is possible to fabricate arbitrary shapes of organized SWNT structures in which the base is lithographically defined and the height is controlled by the growth time. To further explore this unusual opportunity, we templated rows of catalytic stripe patterns and succeeded in growing pseudo two-dimensional organized SWNT structures (Fig. 4, C and D) that resemble sheets. A close investigation of a sheet face (Fig. 4F) reveals that the SWNTs are well aligned, with high uniformity. Some of these sheets are curved like pages in a book, which demonstrates their flexibility. This aspect is highlighted in Fig. 4E, in which an isolated thin SWNT sheet 5 μm thick was fabricated. Although this sheet formed a well-organized structure, its flexibility allowed it to bow and touch the surface, a point that suggests these thin sheets could be arbitrarily laid down, for example, by mechanical forces, gas flows, or electric fields.

Our approach is applicable to other synthesis methods developed for the mass production of SWNTs, such as rotary kiln, floating catalyst, and fluidized bed, addressing simultaneously such critical problems as scalability, purity, and cost. Thus, our approach represents an advance toward a realization of large-scale SWNT material. Additionally, our SWNTs are pure enough for use in various fields ranging from biology and chemistry to magnetic research. Highly pure SWNTs could be grown into scaled-up macroscopic organized structures with defined shape, be it a three-dimensional complex structure or a two-dimensional flexible sheet; potential applications include optical polarizers and field-emitter arrays for flat-panel displays.

References and Notes

1. S. Helveg *et al.*, *Nature* **427**, 426 (2004).
2. Material and methods are available as supporting material on *Science* Online.
3. H. Choi *et al.*, *Nano Lett.* **3**, 157 (2003).
4. M. Cinke *et al.*, *Chem. Phys. Lett.* **365**, 69 (2002).
5. W. I. Chiang *et al.*, *J. Phys. Chem. B* **105**, 8297 (2001).
6. M. J. O'Connell *et al.*, *Science* **297**, 593 (2002).
7. K. Tohji *et al.*, *Nature* **383**, 679 (1996).
8. K. Tohji *et al.*, *J. Phys. Chem. B* **101**, 1974 (1997).
9. A. Cao, X. Zhang, C. Xu, D. Wu, B. Wei, *J. Mater. Res.* **16**, 3107 (2001).
10. We thank Y. Kakudate for x-ray analyses, T. Yokoi for assistance with spectrofluorimetric measurements, K. Suenaga, K. Urita for some TEM observations, and T. Okazaki and M. Yudasaka for helpful discussions. Partial support by the New Energy and Industrial Technology Development Organization (NEDO) Nano Carbon Technology project and the use of the AIST Nano-Processing Facility are acknowledged.

Supporting Online Material

www.sciencemag.org/cgi/content/full/306/5700/1362/DC1
Materials and Methods
Figs. S1 and S2
Movie S1

7 September 2004; accepted 21 October 2004

Available online at www.sciencedirect.com
SCIENCE DIRECT®
Chemical Physics Letters 385 (2004) 298–303
CHEMICAL PHYSICS LETTERS
www.elsevier.com/locate/cplett

Growth of vertically aligned single-walled carbon nanotube films on quartz substrates and their optical anisotropy

Yoichi Murakami [a], Shohei Chiashi [a], Yuhei Miyauchi [a], Minghui Hu [b], Masaru Ogura [b], Tatsuya Okubo [b,c], Shigeo Maruyama [a,*]

[a] Department of Mechanical Engineering, The University of Tokyo, 7-3-1 Hongo, Bunkyo-ku, Tokyo 113-8656, Japan
[b] Department of Chemical System Engineering, The University of Tokyo, 7-3-1 Hongo, Bunkyo-ku, Tokyo 113-8656, Japan
[c] PRESTO, JST, 7-3-1 Hongo, Bunkyo-ku, Tokyo 113-8656, Japan

Received 23 November 2003; in final form 5 December 2003
Published online: 22 January 2004

Abstract

Films of vertically aligned single-walled carbon nanotubes (SWNTs) with a few micrometer thickness were g
chemical vapor deposition (CVD) on quartz substrates. Low-temperature CVD from ethanol was performed
mono-dispersed Co–Mo catalyst of ≈1.0–2.0 nm prepared on quartz substrates by a dip-coating method. Contin
catalysts with Ar/H_2 (3% H_2) during CVD was essential for generating dense enough SWNTs with vertical al
alignment was clearly demonstrated by anisotropic optical absorption and transmission characteristics in additio
by FE-SEM, TEM and resonance Raman scattering.

Ethanol: C_2H_5OH

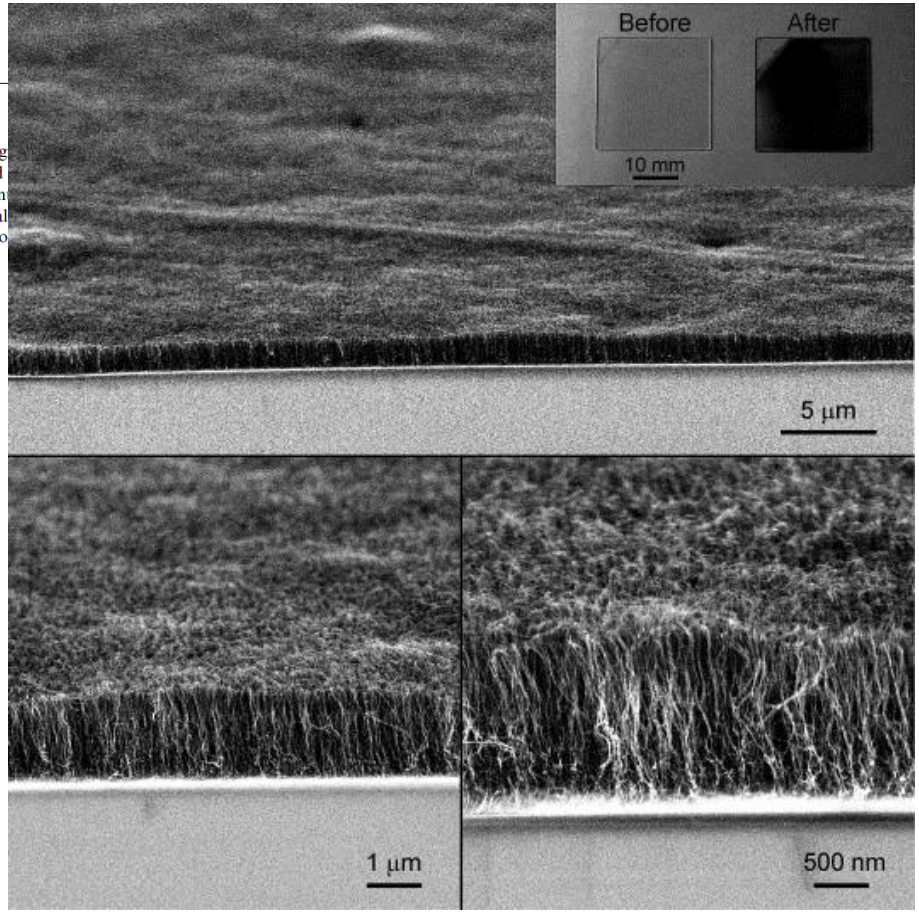

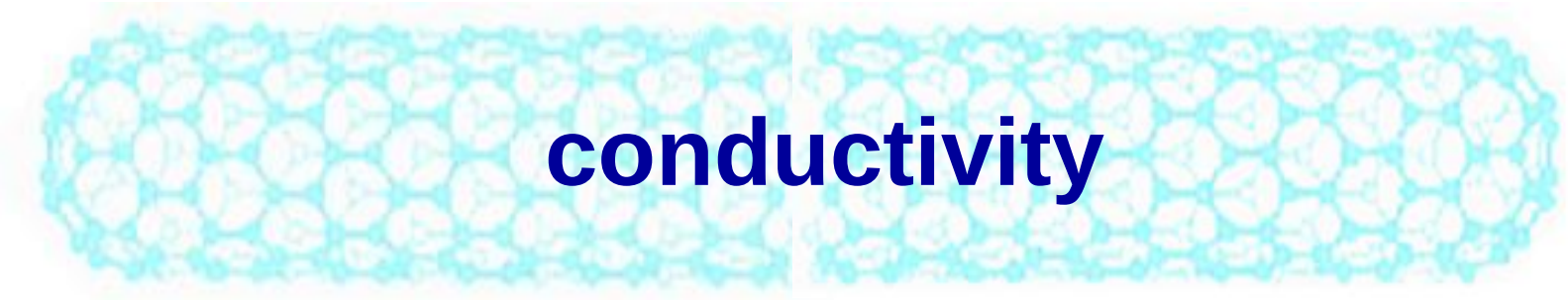
conductivity

Conductivity control: selective growth of semiconducting SWNTs

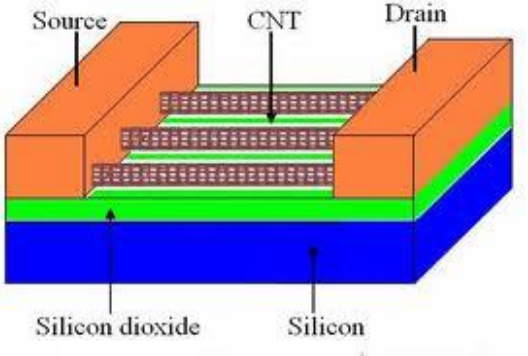

- **Semiconducting SWNTs are needed for build FETs**
- **Normal SWNT sample is the mixture of metallic and semiconducting tubes**

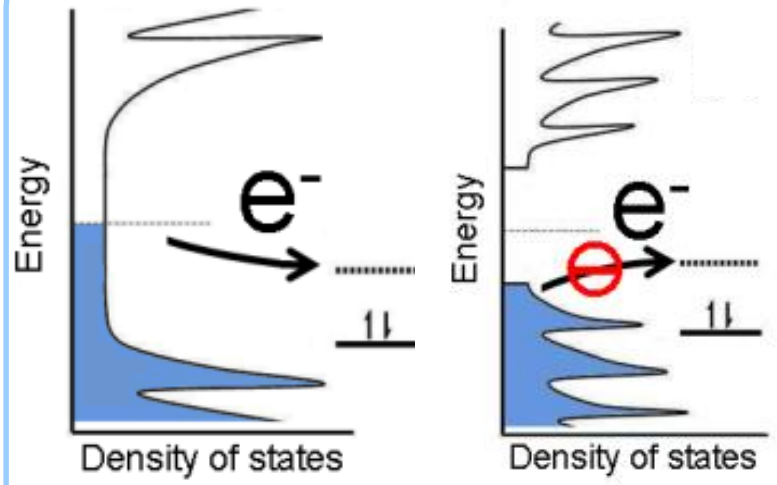

The ionization energy of metallic SWNTs is smaller.

How can we selectively grow pure semiconducting SWNTs?

Our strategy:
selectively inhibit metallic tubes while growing

Growing s-SWNTs by adding methanol to the carbon stocks

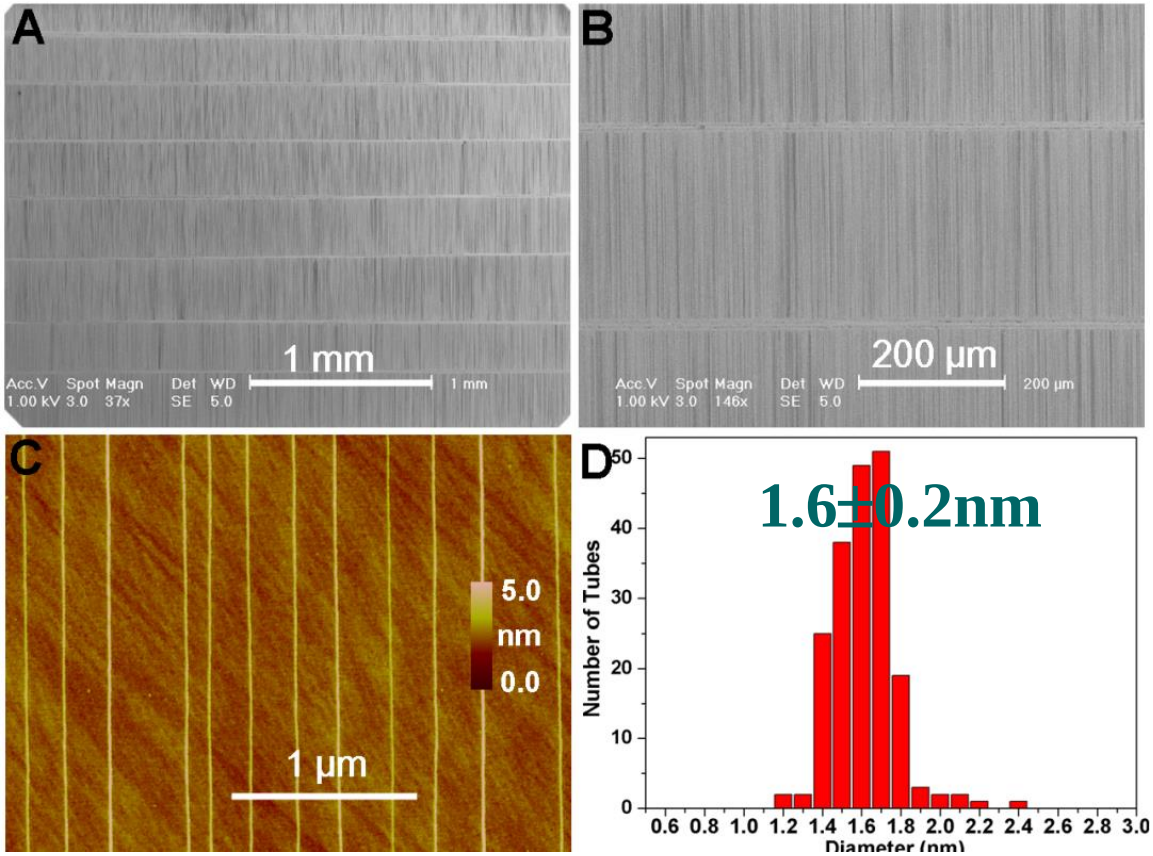

Quartz substrate

C_2H_5OH+CH_3OH

$CH_3OH \Rightarrow \bullet OH$

***Nano Lett.* 2009**, 9, 800-805.

Growing s-SWNTs by adding methanol to the carbon stocks

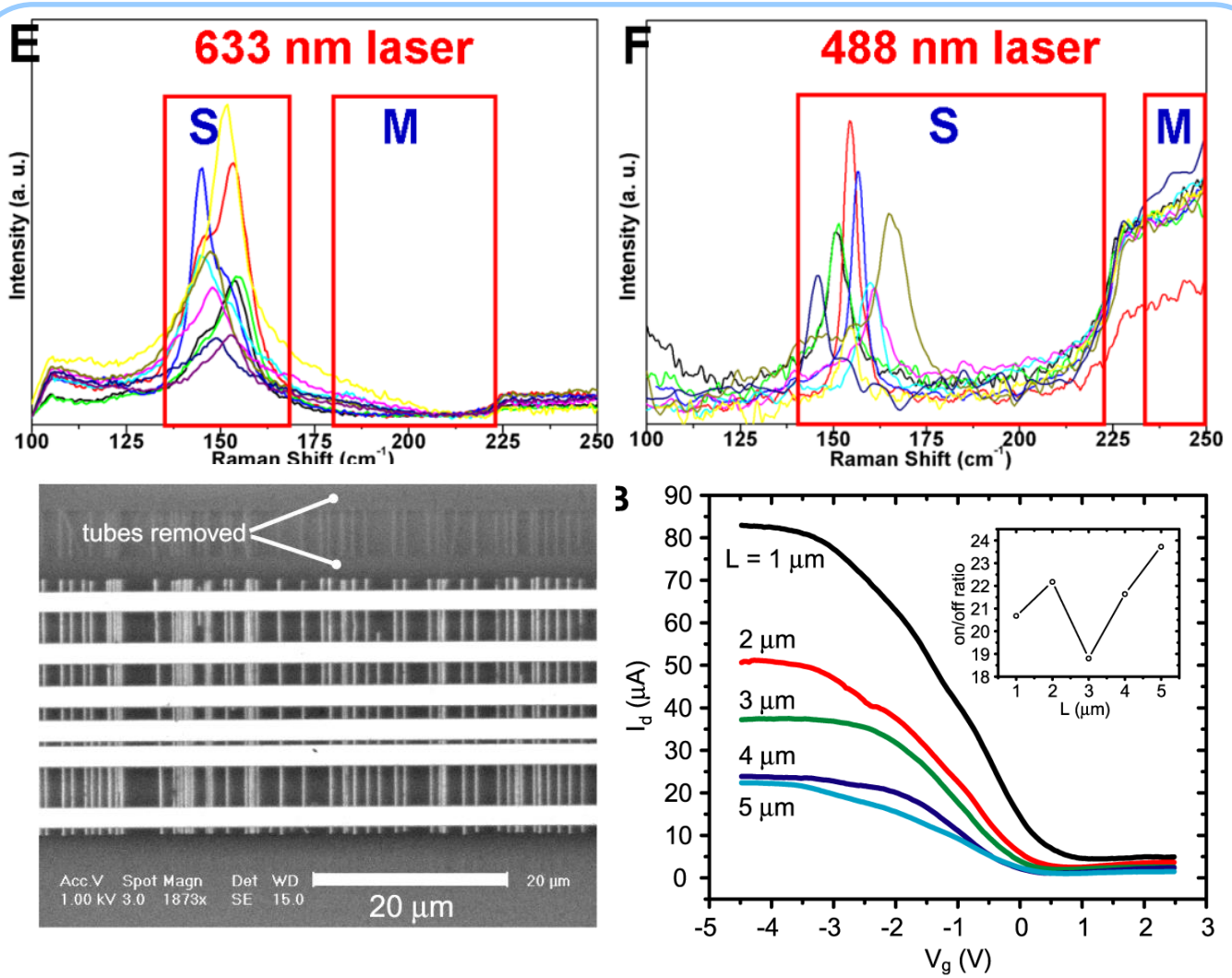

Content of s-SWNTs: 95-98%

***Nano Lett.* 2009**, 9, 800-805.

Catalyst: Cu

Substrate: quartz

Carbon source:

C_2H_5OH+CH_3OH

$CH_3OH \Rightarrow \bullet OH$

oxidant

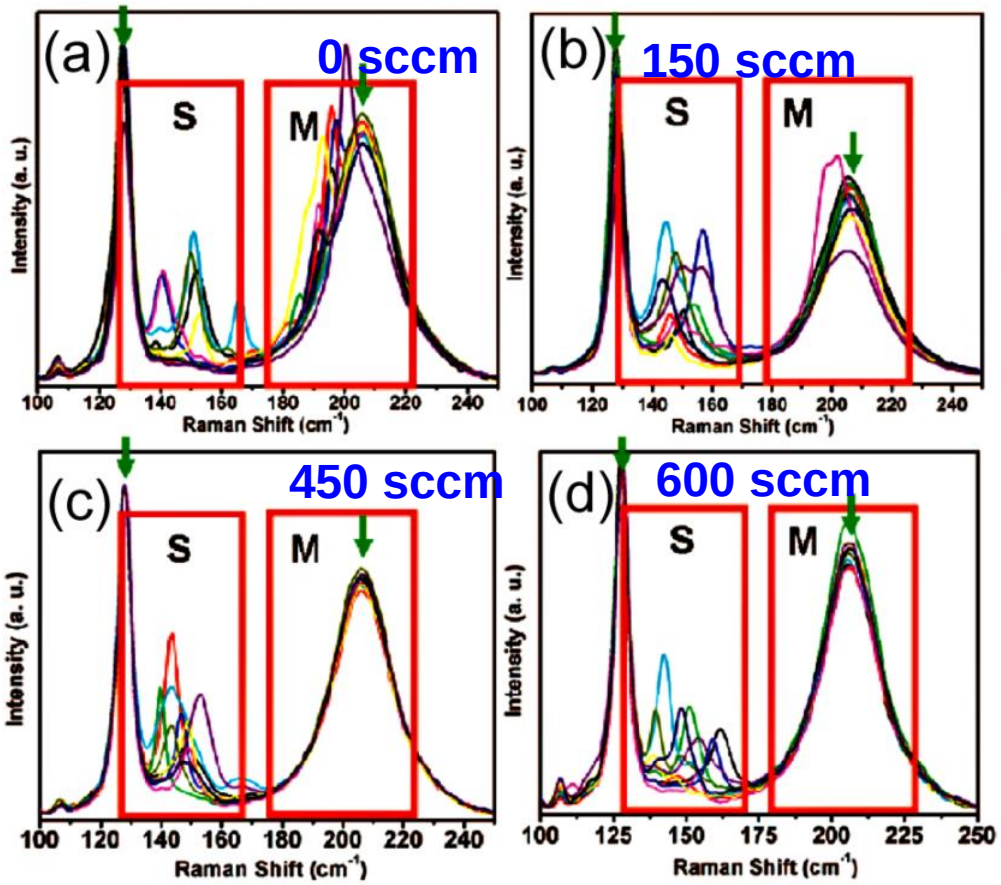

The content of semiconducting SWNTs increases with the methanol concentration.

L. Ding/Y. Li*/J. Liu*; ***Nano Lett.*** **2009**, 9, 800-805

Inhibit the formation of metallic tubes by the addition of O_2

O_2 增加

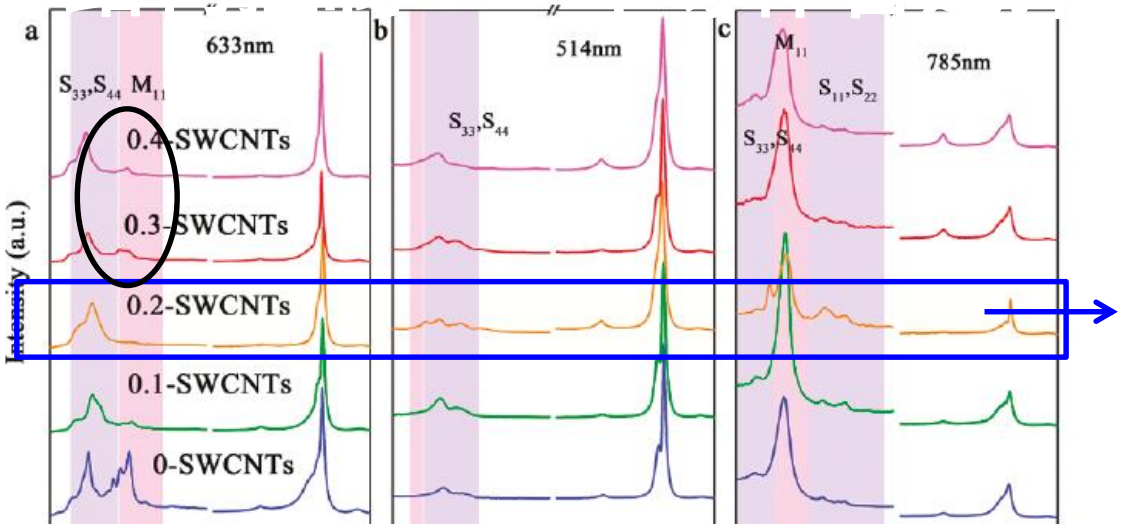

Optimized O_2 content

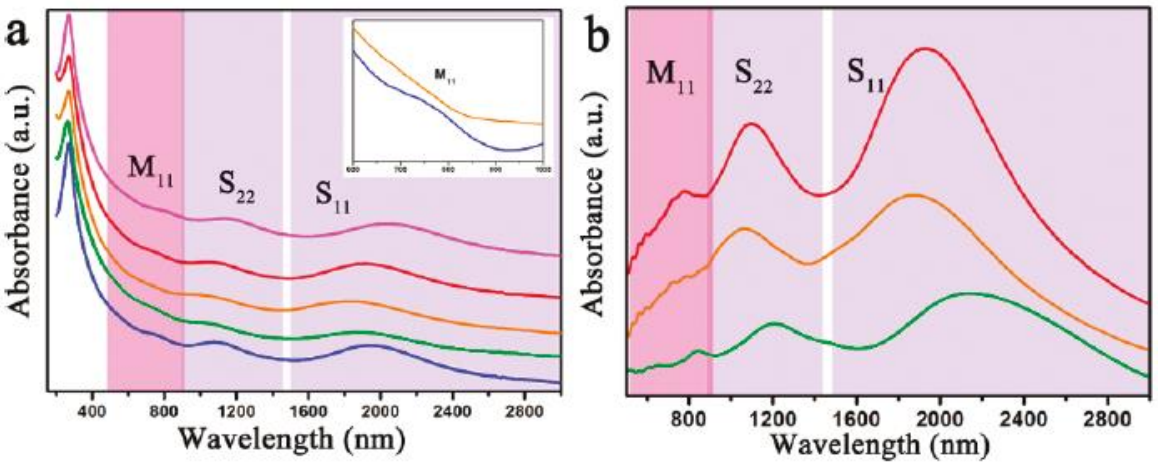

H. Cheng, ***J. AM. CHEM. SOC.* 2011, 133,** 5232.

Questions:

- **Can we obtain firm evidence for the proposed mechanism?**
- **How can we improve the flexibility and reliability of this process?**

Oxidative catalyst support ?!

It should be much easier to handle the solid state catalyst support than the gas phase oxidants.

Our new strategy:

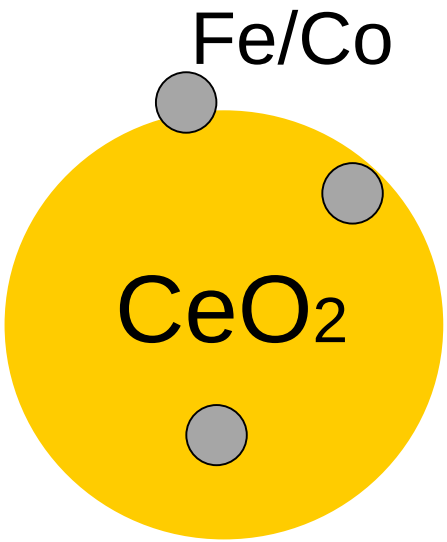

Oxidative catalyst support ?!

It should be much easier to handle the solid state catalyst support than the gas phase oxidants.

X. Qin/…/ **Y. Li***; ***Nano Lett. 2014***, 14, 512-517.

Control experiment——Fe/SiO_2

532nm

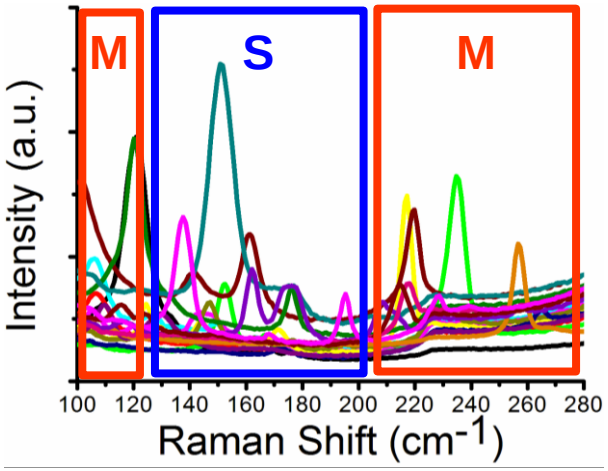

72% 84/117

633nm

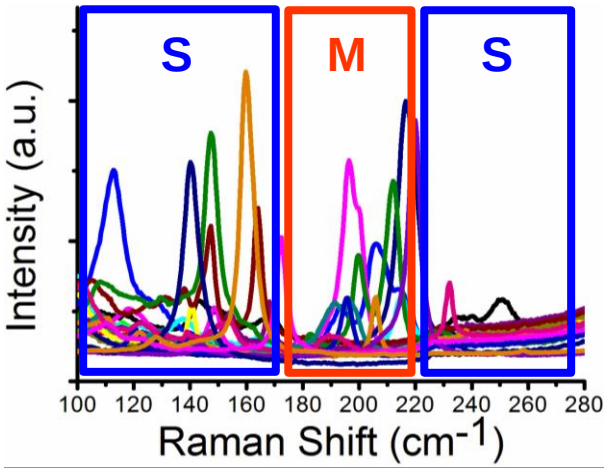

58% 89/154

785nm

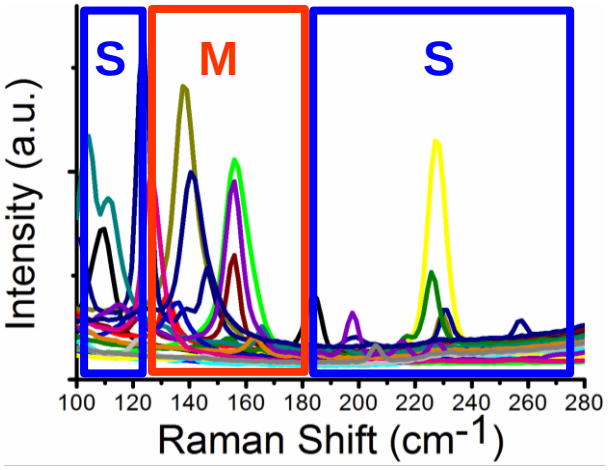

52% 89/170

The theoretical content of s-SWNTs is 67%.

X. Qin/…/ **Y. Li***; ***Nano Lett. 2014***, 14, 512-517.

Ceria supported catalysts at different reduction time

10 min **0 min**

532nm

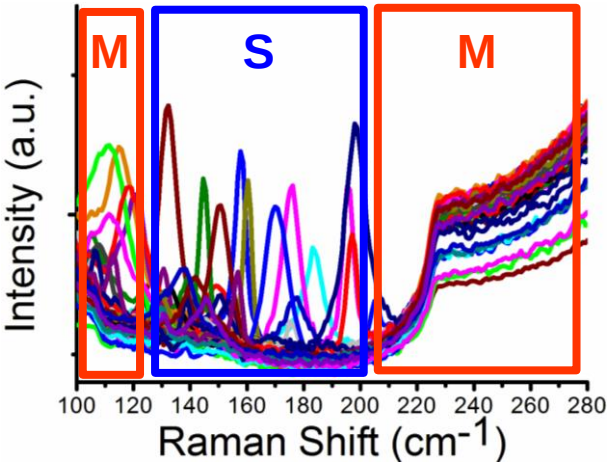

84% 74/88

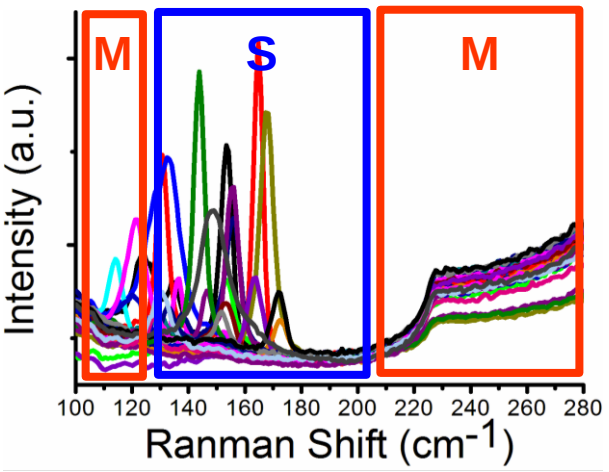

94% 45/48

633nm

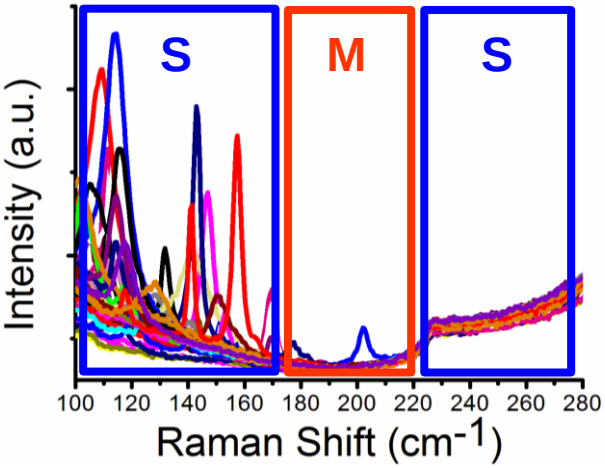

99% 102/103

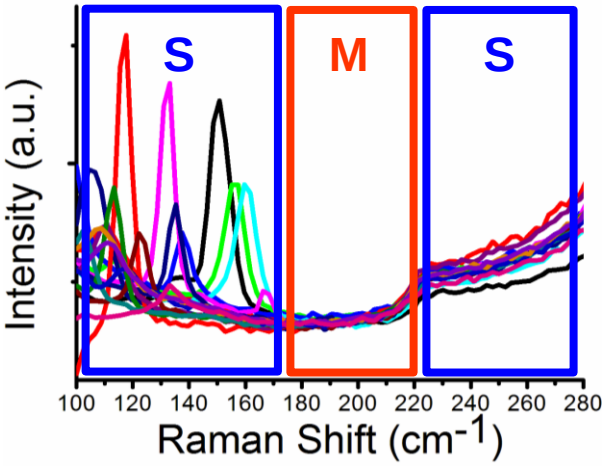

100% 39/39

Statistics on SWNTs grown with catalysts treated in different ways

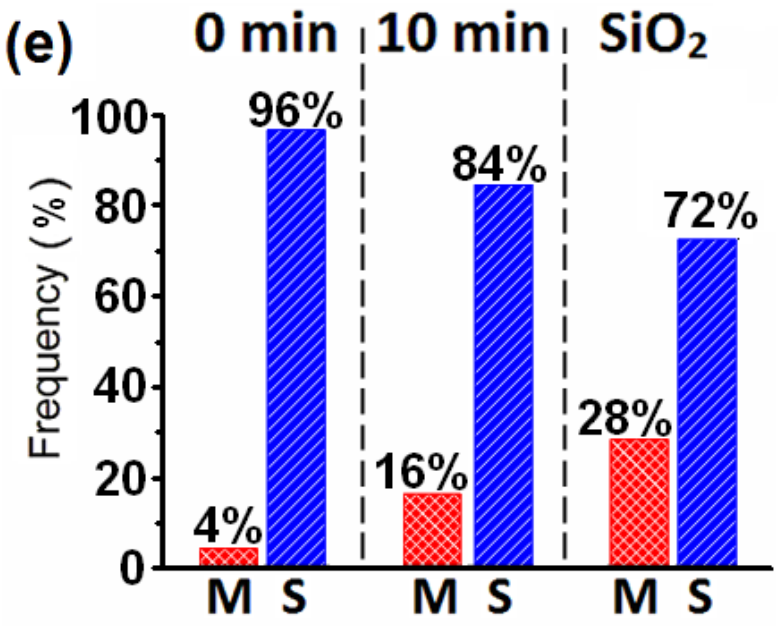

532nm

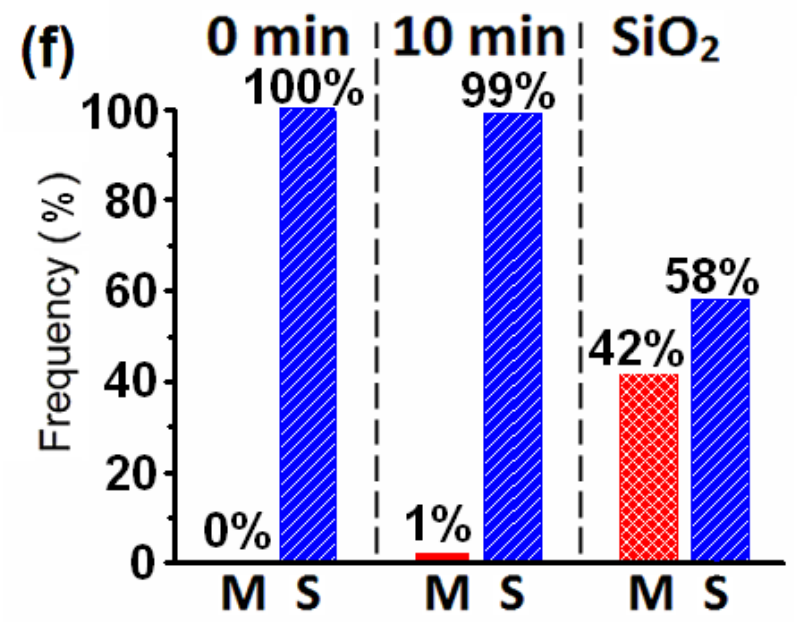

633nm

X. Qin/…/ **Y. Li***; ***Nano Lett. 2014***, 14, 512-517.

Ultralong SWNTs

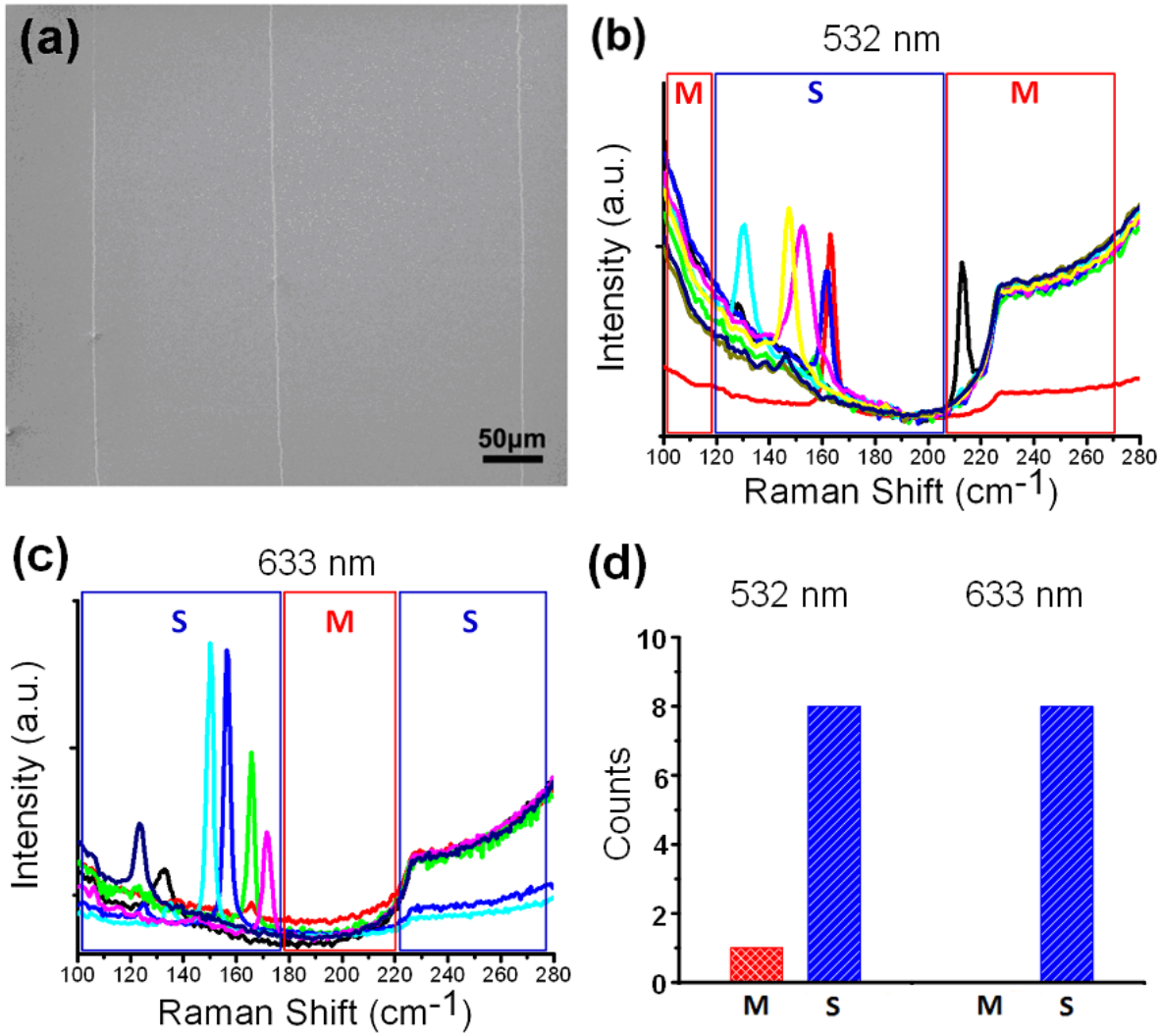

Chirality selective growth

materials	Si	Ge	GaAs	InAs	InSb	CNT
Electron mobility	1600	3900	9200	9200	40000	>100,000
hole mobility	430	1900	400	400	500	>100,000
bandgap	1.12	0.66	1.424	0.36	0.7	0.4-2

International Technology Roadmap for Semiconductors

Carbon-based Nanoelectronics to include carbon nanotubes and graphene

For additional resources and detailed road mapping for ITRS as promising technologies targeting commercial demonstration in the 5-10 year horizon.

ITRS 2009 edition

Slides from www.ITRS.net

NANO LETTERS

Sub-10 nm Carbon Nanotube Transistor

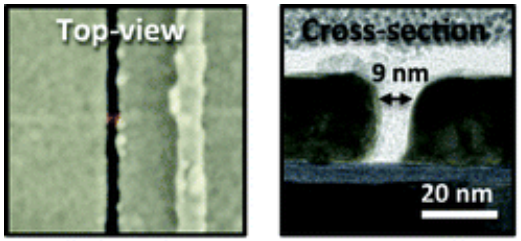

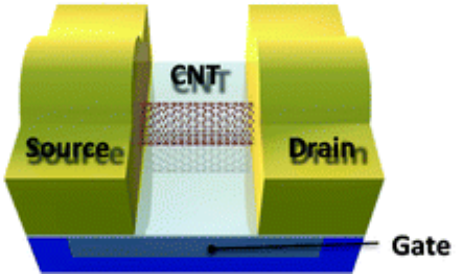

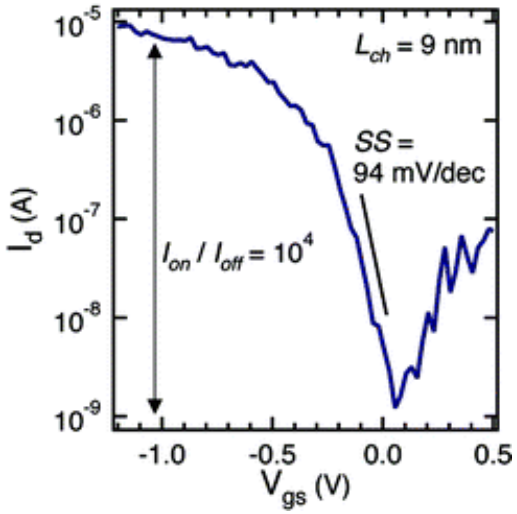

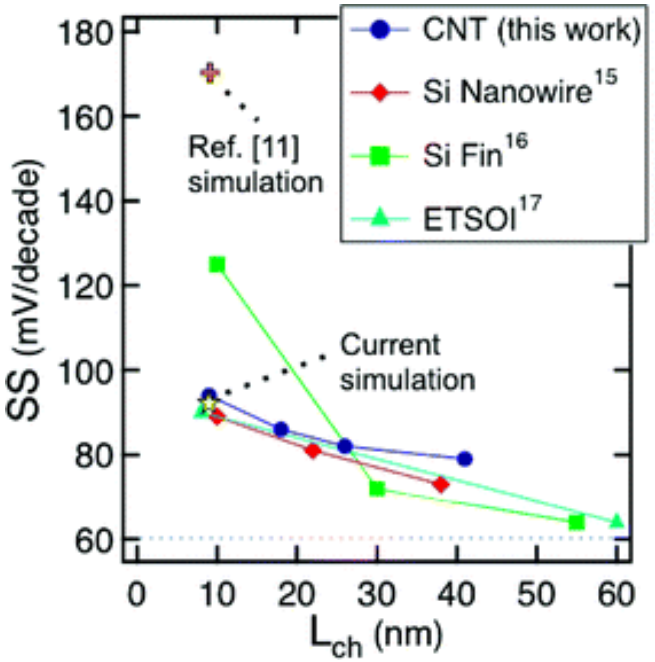

The 9 nm CNT transistor outperformed the best competing silicon devices with more than four times the diameter-normalized current density at a low operating voltage of 0.5 V. It also exhibits an impressively small inverse subthreshold slope of 94 mV/decade, which is remarkably lower than Si.

A. Franklin et al., *Nano Lett.* 2012, 12, 758

nature International weekly journal of science
Home | News & Comment | Research | Careers & Jobs | Current Issue | Archive | Audio & Video

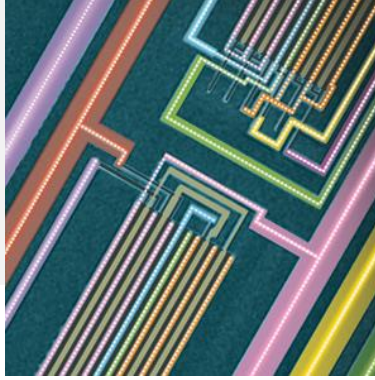

Carbon Nanotube Computer

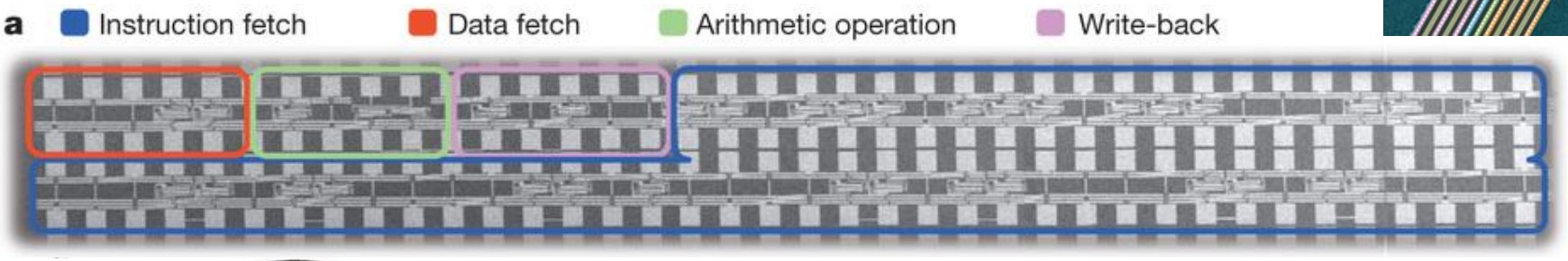

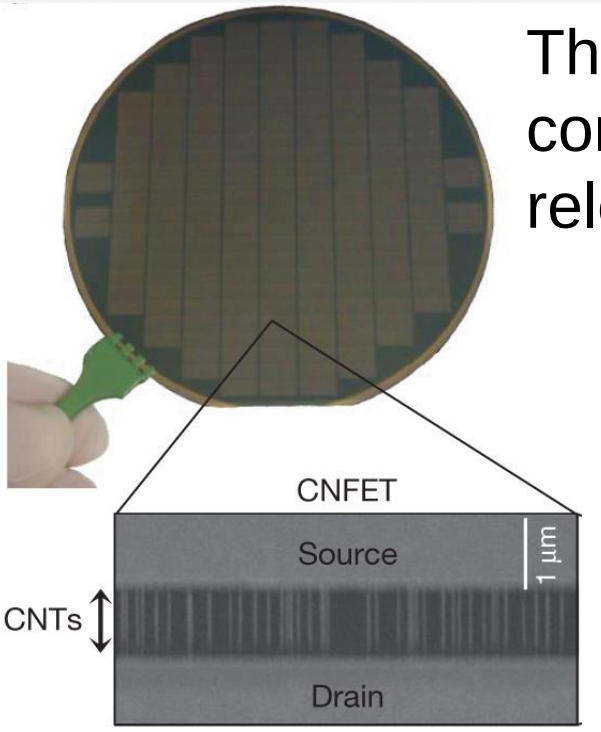

The carbon nanotube processor is comparable in capabilities to the Intel 4004 released in 1971.

- Grow SWNT arrays on quartz wafer
- Transfer SWNTs onto silicon wafer
- Apply a voltage to burn metallic tubes

M. Shulaker et al., *Nature.* 2013, 501, 525

nature International weekly journal of science
Home | News & Comment | Research | Careers & Jobs | Current Issue | Archive | Audio & Video

Aaron D. Franklin **27 June 2013**

Electronics: The road to carbon nanotube transistors

- **Carbon nanotubes**
  - **0.0001% metallic CNTs**
  - **density: 125 CNTs per μm**

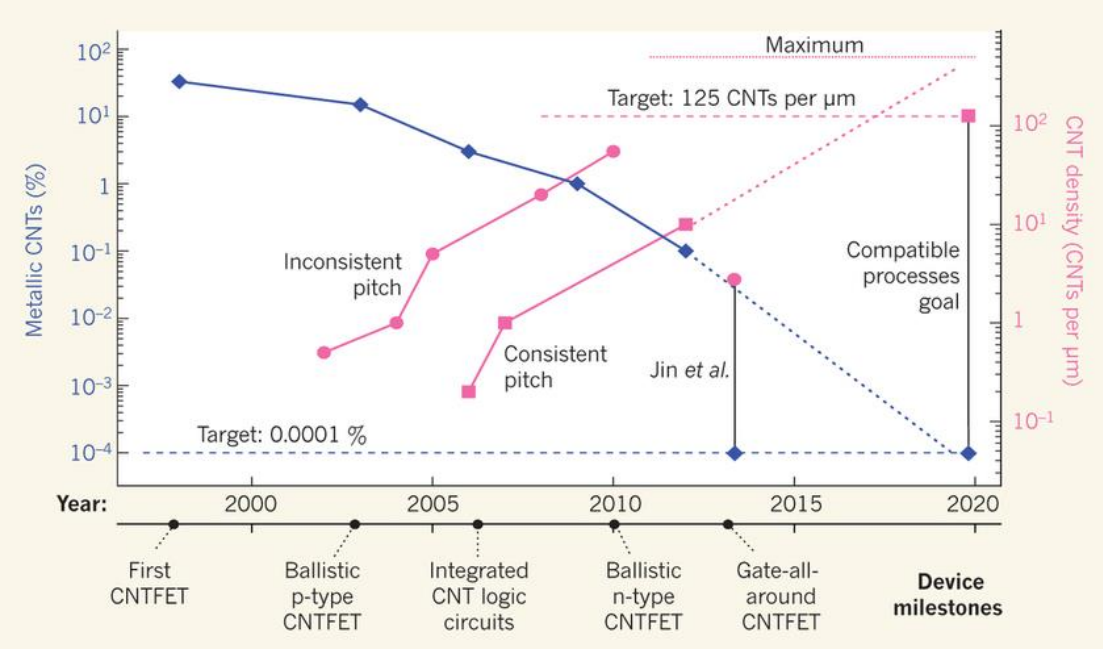

Phaedon Avouris: Carbon-Based Electronics

Nature nanotechnology, 2, 605, 2007

How soon do we expect to see these developments? What is the bottleneck in the development of nanotubes, graphene and indeed in any high-end nanotechnology? **The main hurdle is our current inability to produce large amounts of identical nanostructures.** Nanotubes come in many sizes and structures and the same is true of many other nanostructures. …… ***there is no reliable way to directly produce a single CNT type such as will be needed in a large integrated system.*** ……

Chirality controlled growth of SWNTs

---- Ultimate goal for SWNT growth

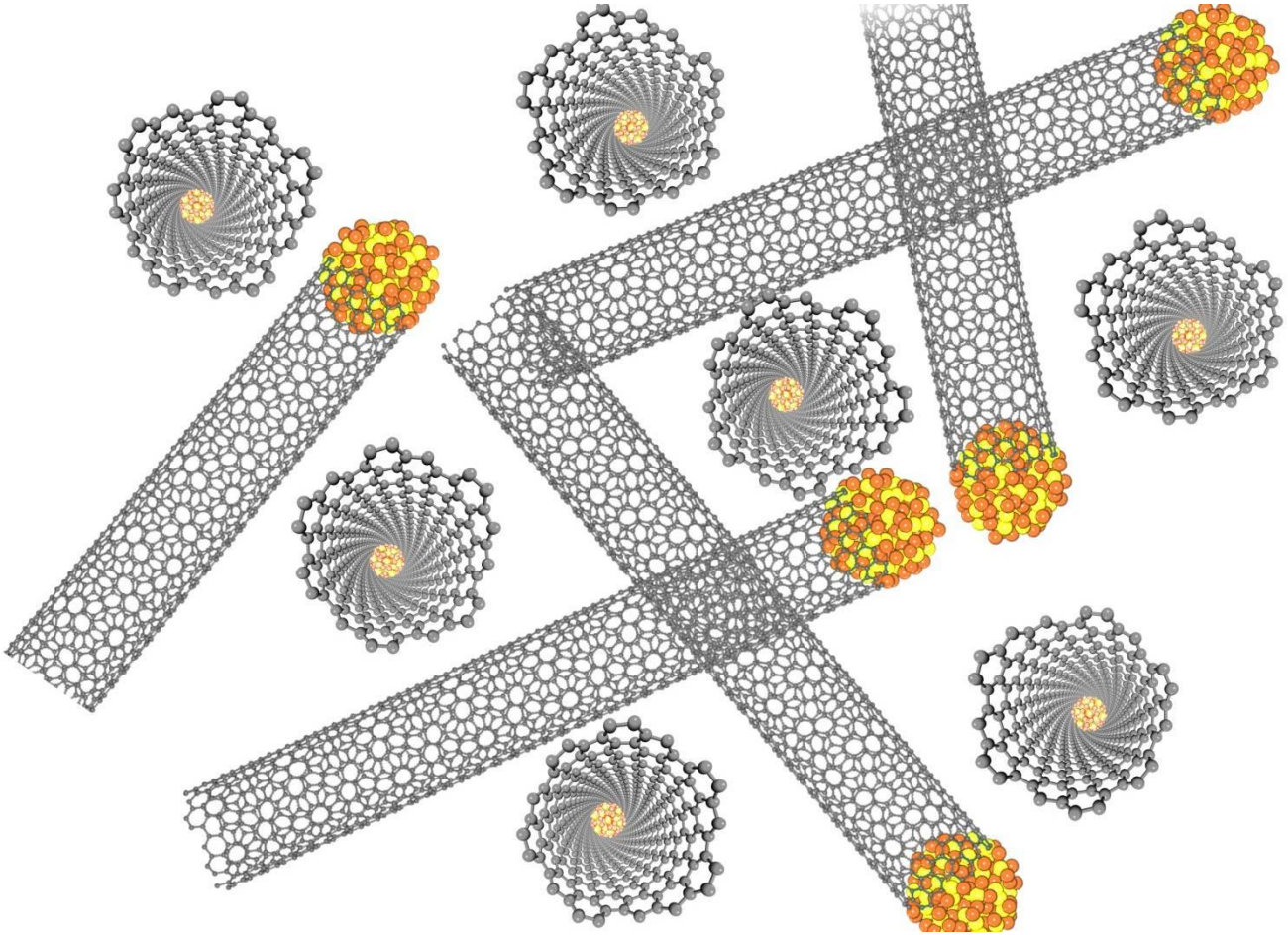

Using segments of tubes as seeds to grow SWNTs with the same chirality

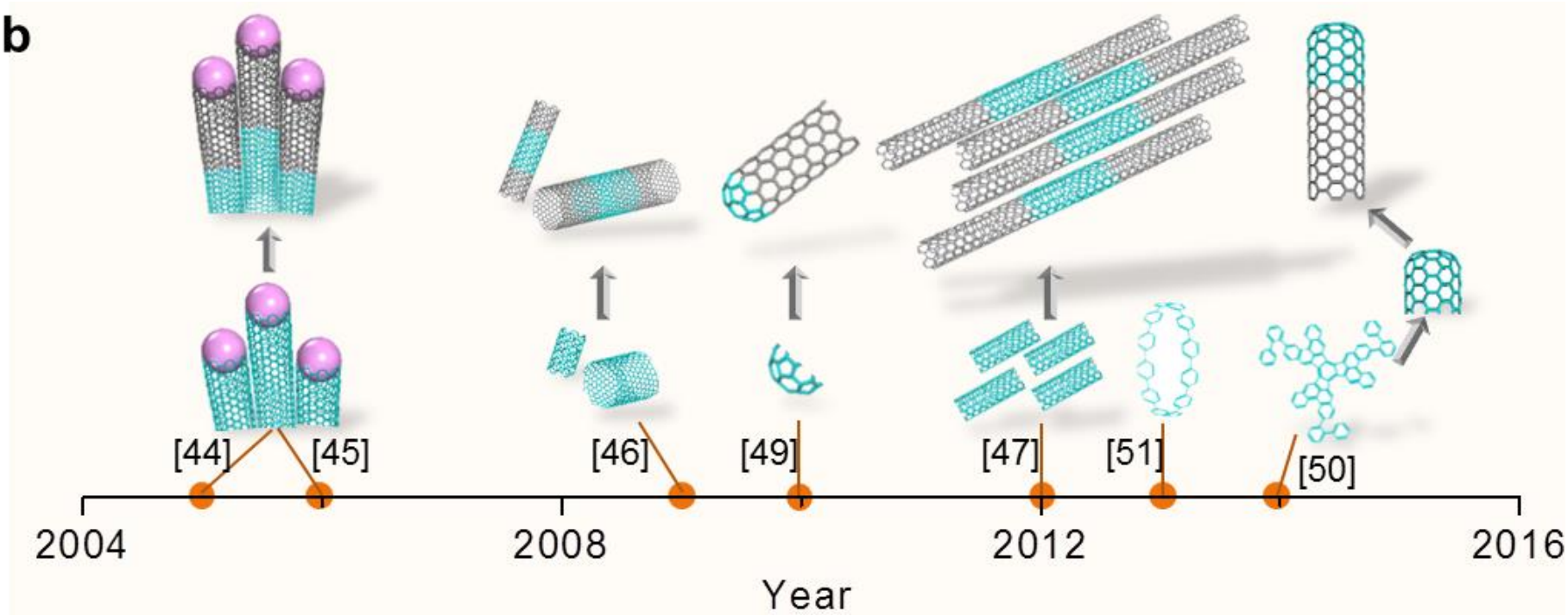

R. Smalley, J. Zhang, C. Zhou, R. Falser et al.

Challenge: efficiency

The Highest Selectivity Ever Reported

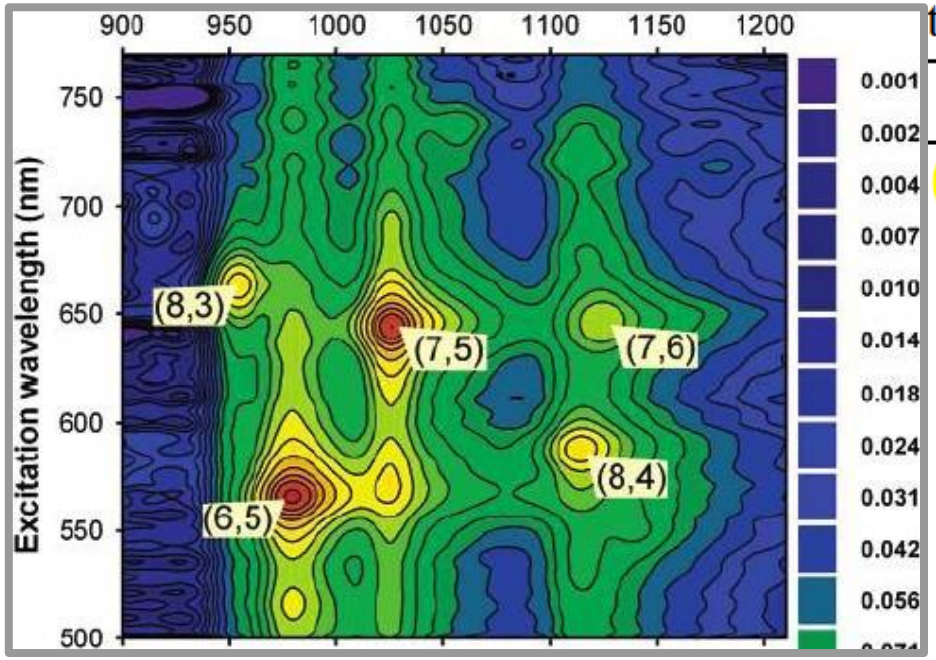

t	SiO_2				MgO
	700	750	800	850	750
(6,5)	54%	42%	55%	6%	19%
(8,4)	4%	16%	4%	6%	12%
(7,5)	8%	8%	6%	10%	26%
(7,6)	8%	7%	6%	15%	13%
(8,6)			1%	10%	2%
(8,7)			2%	13%	2%
(6,6)	14%	19%	15%	17%	22%
(7,7)	13%	10%	10%	14%	3%
(8,8)				6%	

Co-Mo Catalysts

Proposed mechanism:

The presence of molybdenum oxides stabilized the Co nanoparticles and made the particles small and uniform.

D. E. Resasco, ***J. Am. Chem. Soc*. 2003**, 125, 11186; ***JPC B* 2006,** *110,* 2108.

Chemical Vapor Deposition

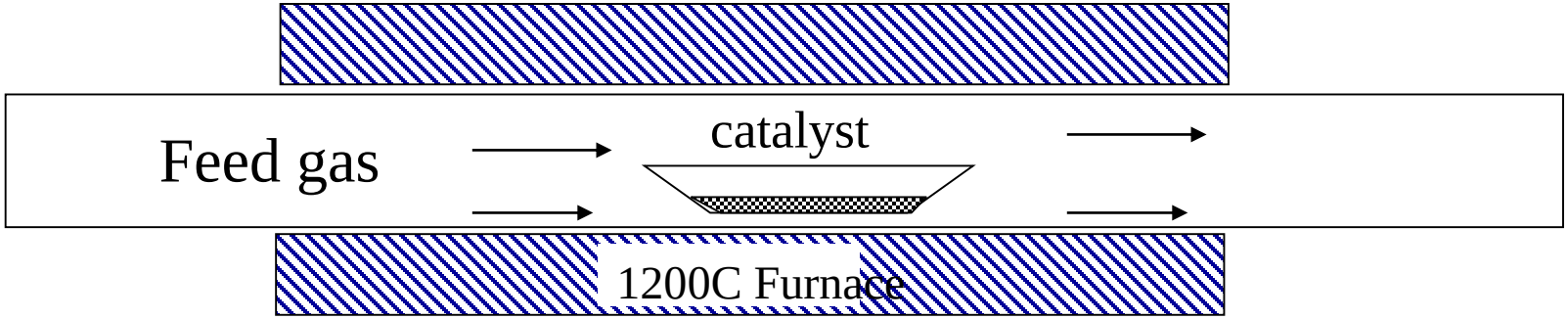

Feed Stock Gas:	CO, CH_4, C_2H_5OH etc.
Catalyst:	Fe, Ni, Co, **Cu, Pb** etc.
Temperature:	800 – 1100 ºC

ELSEVIER

14 August 1998

Chemical Physics Letters 292 (1998) 567–574

CHEMICAL PHYSICS LETTERS

Chemical vapor deposition of methane for single-walled carbon nanotubes

Jing Kong [a], Alan M

[a] *Department of Chemistry, Sta*
[b] *NASA Ames Research C*

Received 1 May 19

Table 1
Summary of results of methane CVD experiments using sup

Catalyst composition	Support material	SWNTs
Fe_2O_3	alumina	yes
Fe_2O_3	silica	yes
CoO	alumina	yes
CoO	silica	no
NiO	alumina	no
NiO	silica	no
NiO/CoO	alumina	no
NiO/CoO	silica	yes

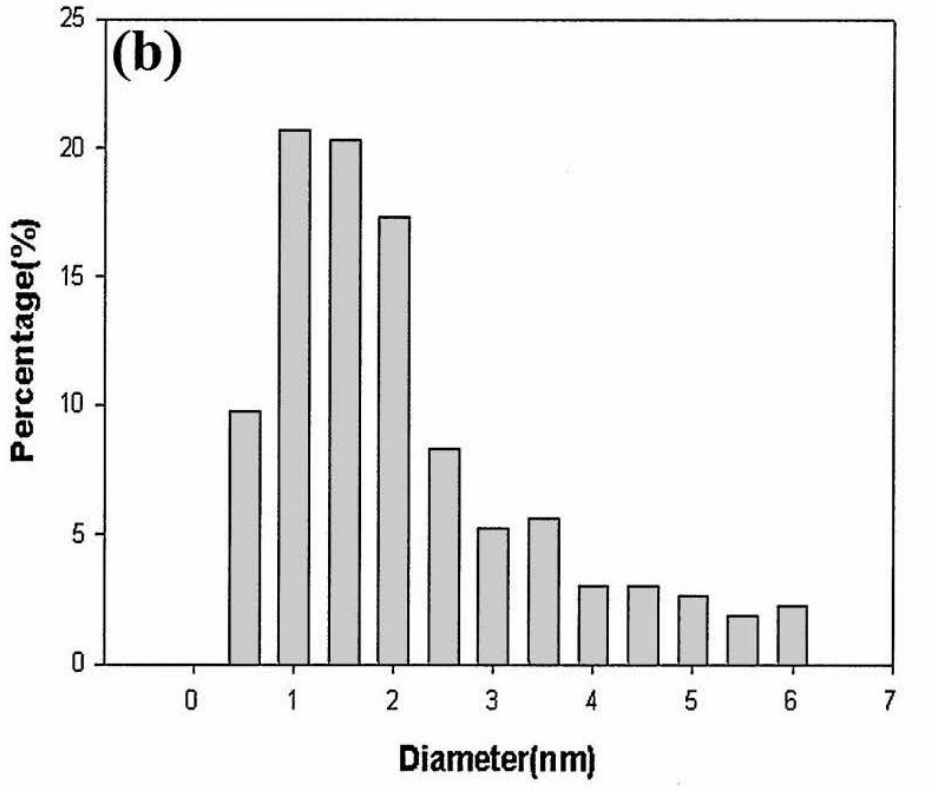

VLS growth of SWNTs catalyzed by metallic nanoparticles

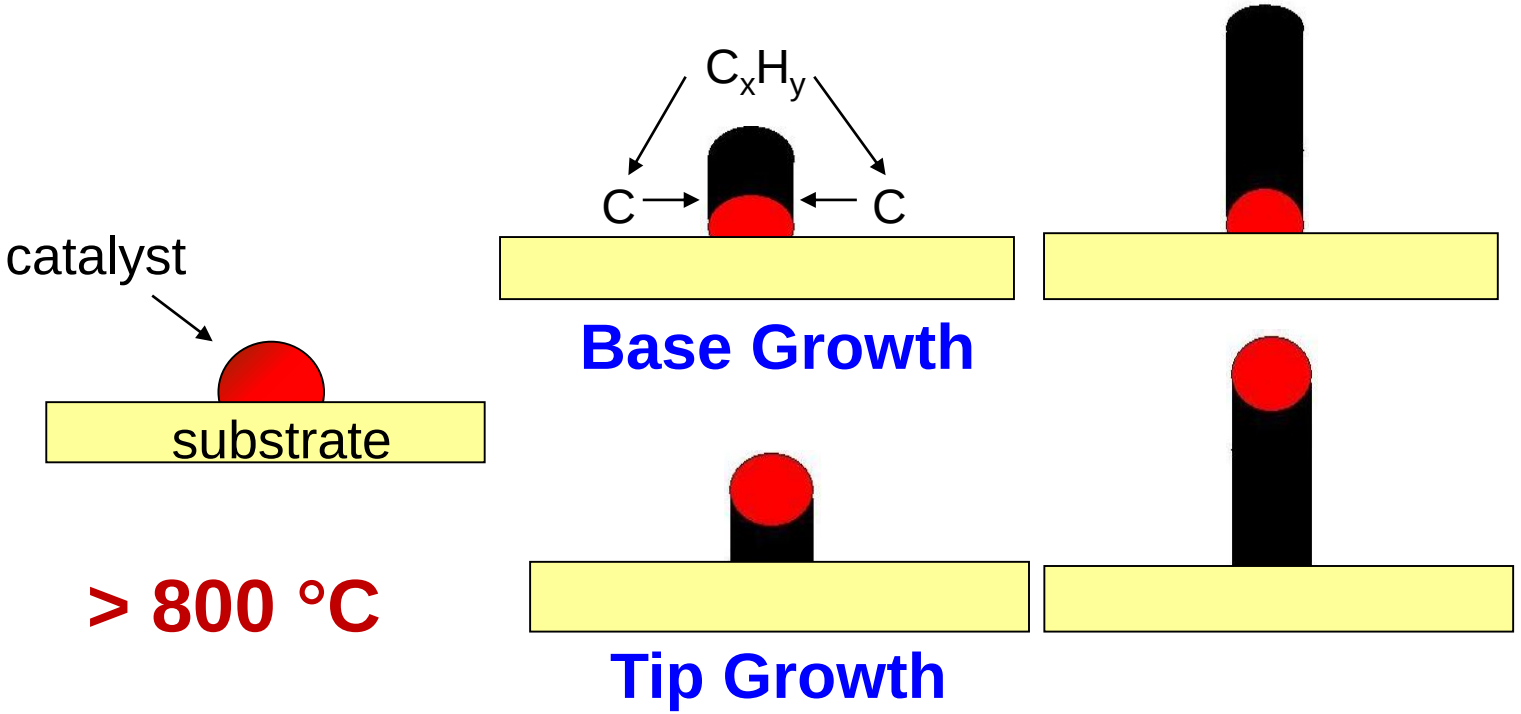

Roles of the catalysts:

- to catalyze the decomposition of carbon feeding stocks
- to initiate the nucleation and growth of nanotubes

1. Composition of catalysts

Selective growth of (6,5) SWNTs with Co-Mo Catalysts

	support		SiO_2				MgO
	temp (°C)		700	750	800	850	750
(*n*,*m*) species	semicond	(6,5)	54%	42%	55%	6%	19%
		(8,4)	4%	16%	4%	6%	12%
		(7,5)	8%	8%	6%	10%	26%
		(7,6)	8%	7%	6%	15%	13%
		(8,6)			1%	10%	2%
		(8,7)			2%	13%	2%
	metallic	(6,6)	14%	19%	15%	17%	22%
		(7,7)	13%	10%	10%	14%	3%
		(8,8)				6%	

The highest chirality selectivity ever reported.

Proposed mechanism:

The presence of molybdenum oxides stabilized the Co nanoparticles and made the particles small and uniform.

D. E. Resasco et al., ***JPC B* 2006,** *110,* 2108.

Selective growth of (6,5) SWNTs with Fe-Cu Catalysts

FeCuCAT: (6,5)
Fe: Cu:
MgO=2:0.4:40
600°C, CO 50sccm

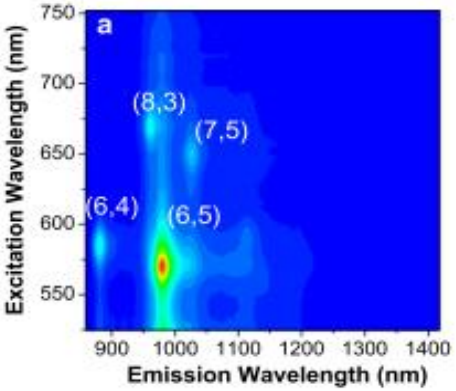

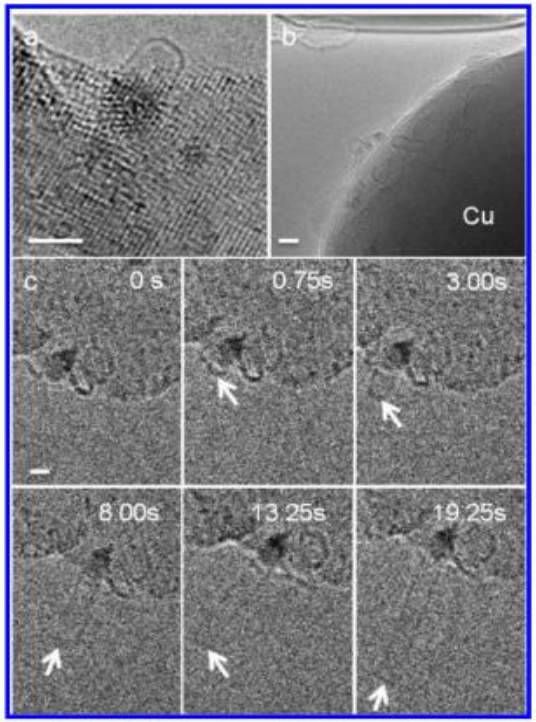

Cu play an important role in the Fe reduction process.

In situ TEM image showing the growth of SWNTs on metallic Cu-supported Fe particles

Proposed mechanism:

SWNTs grew from Fe nanocrystals, Cu made Fe nanocrystals small and uniform.

He, M*,*Carbon,* **2012**, 52, 590
He, M.*; Kauppinen, E. I*, *Chem. Mater*., **2012,** 24, 1796

2. Carbon stocks

Tune the chirality composition by carbon precursor

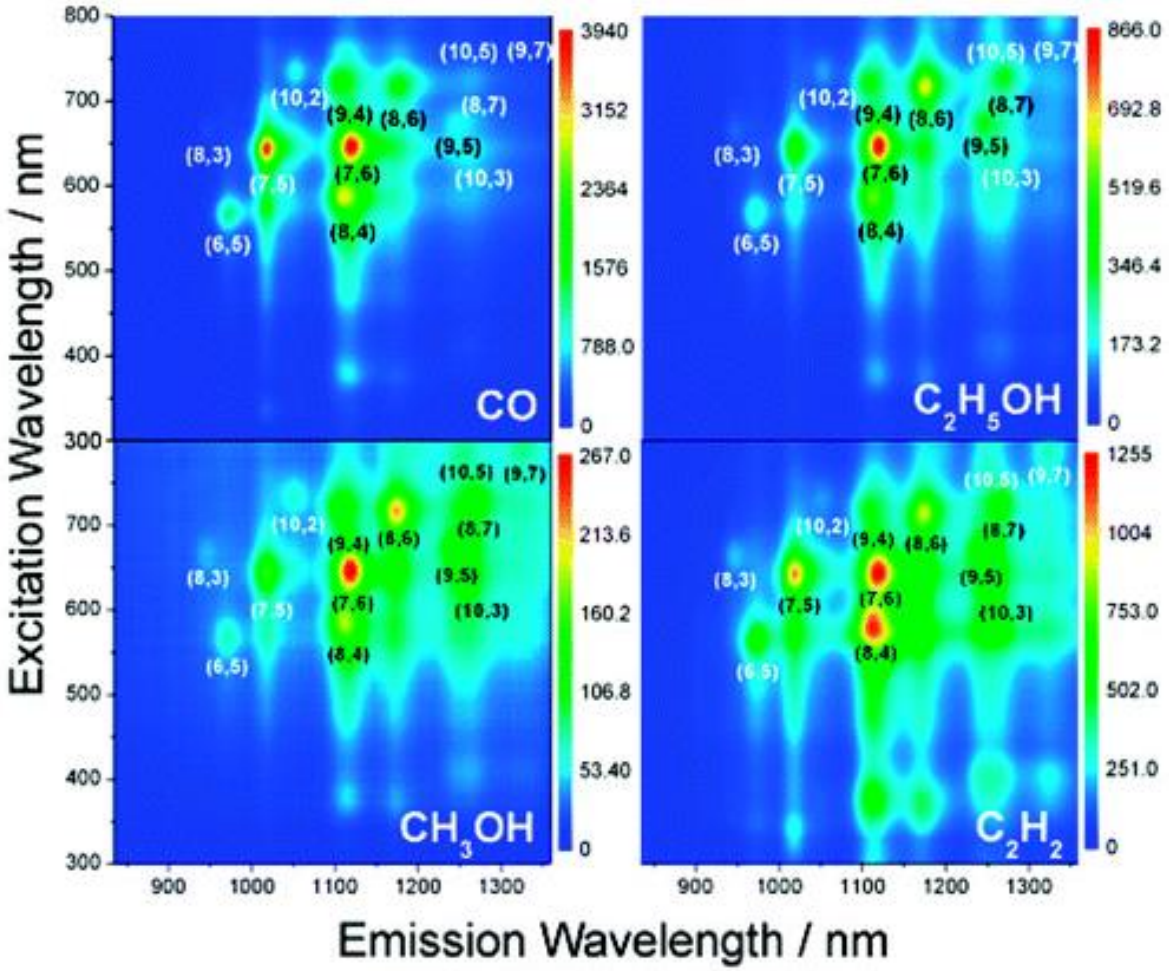

CoMo

Y. Chen *et al.*, *J. Am. Chem. Soc.* 2007, 129, 9014

3. Carbon feeding & active catalyst particles

Tune the diameter of SWNTs by carbon feeding

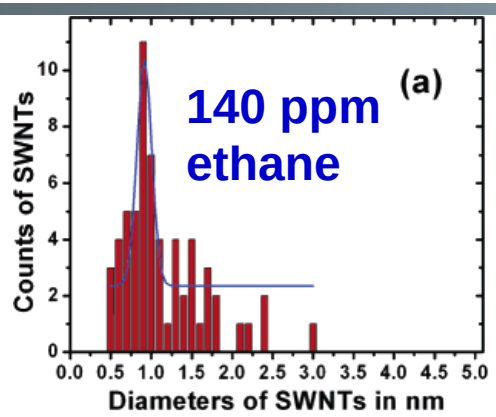

0.91±0.18 nm

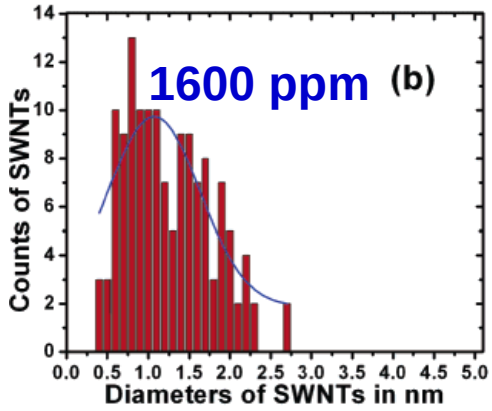

1.07±1.12 nm

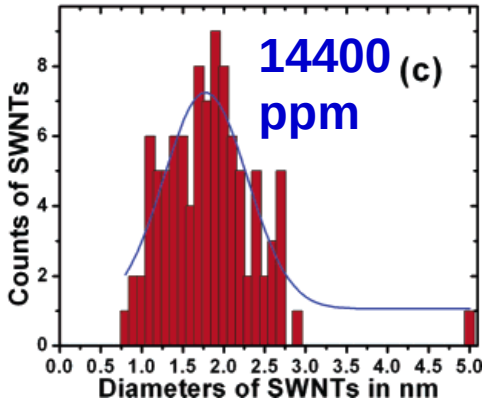

1.78±1.02 nm

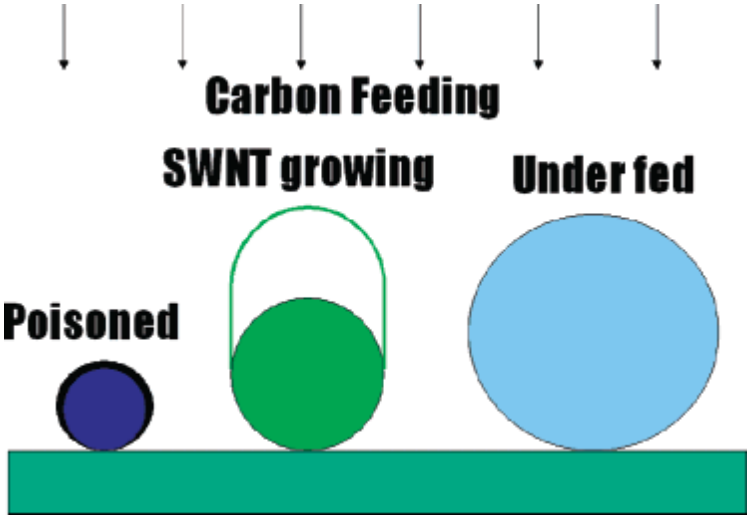

J. Liu et al., J. Phys. Chem. B 2006, 110, 20254

Diameter distribution of FeMo catalyst particles and SWNTs

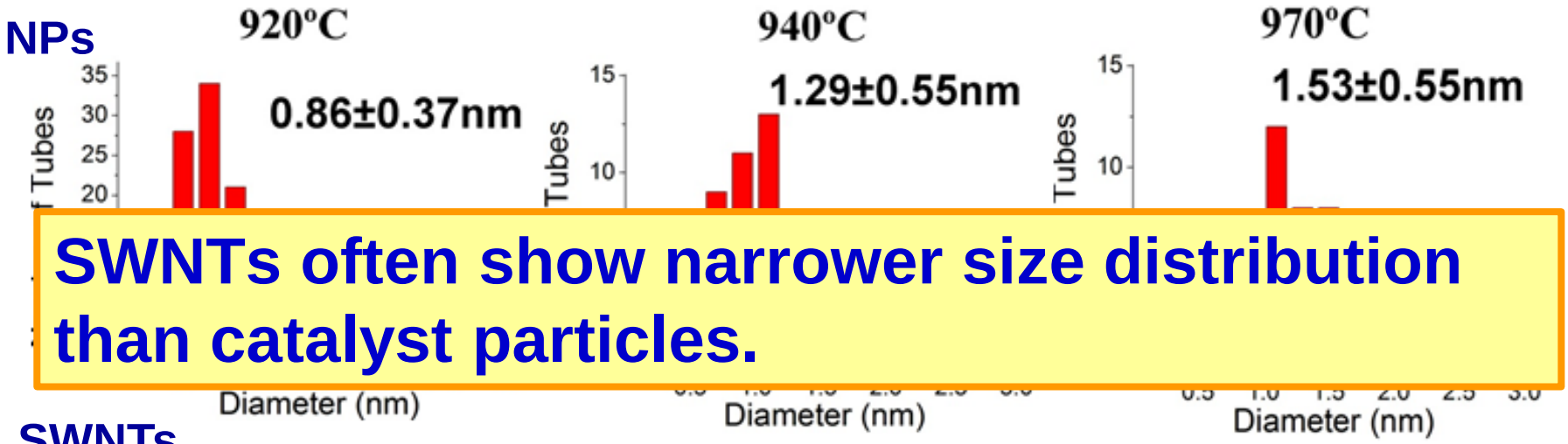

SWNTs often show narrower size distribution than catalyst particles.

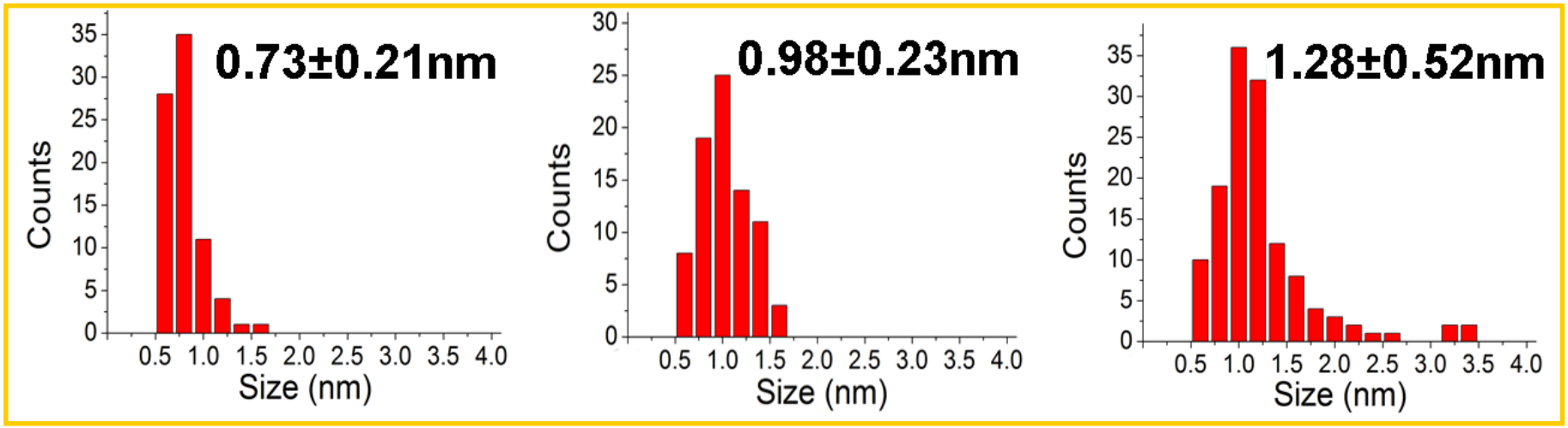

F.Peng/…/**Y. Li***

4. Catalysts are mobile

Catalysts' behavior during CVD: Cu

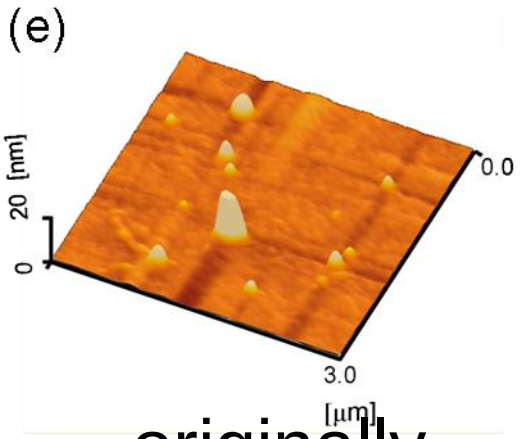

originally

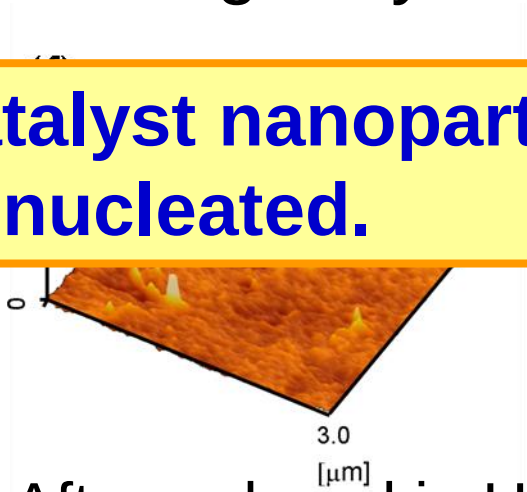

After reduced in H_2 for 15 min at 900 ºC

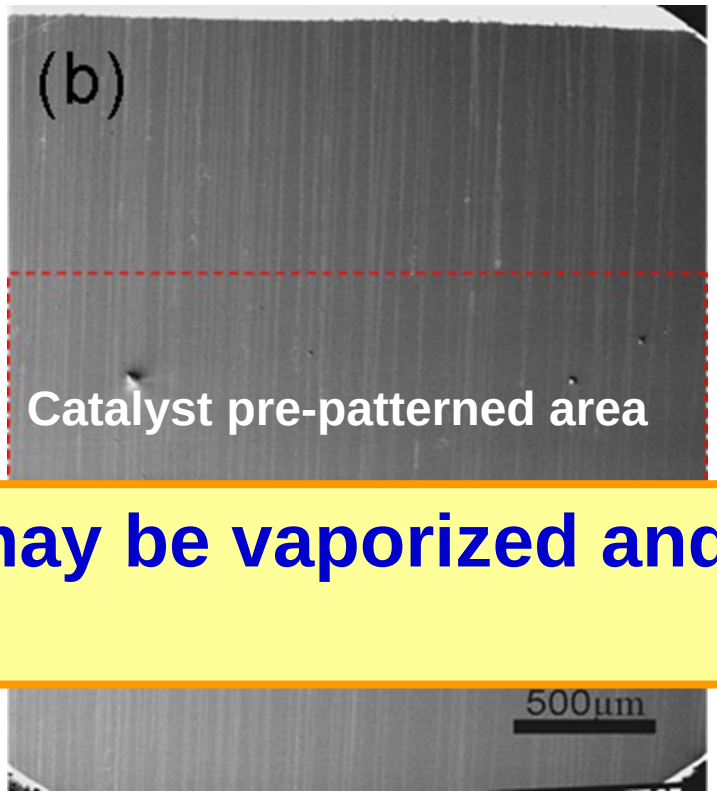

Catalyst nanoparticles may be vaporized and re-nucleated.

W. Zhou/**Y. Li*** ; ***Nano Lett.* 2006**, 2987

R. Cui/**Y. Li*** , ***JPCC* 2010, 114,** 15547.

5. Structure of catalysts

VSS growth of SWNTs

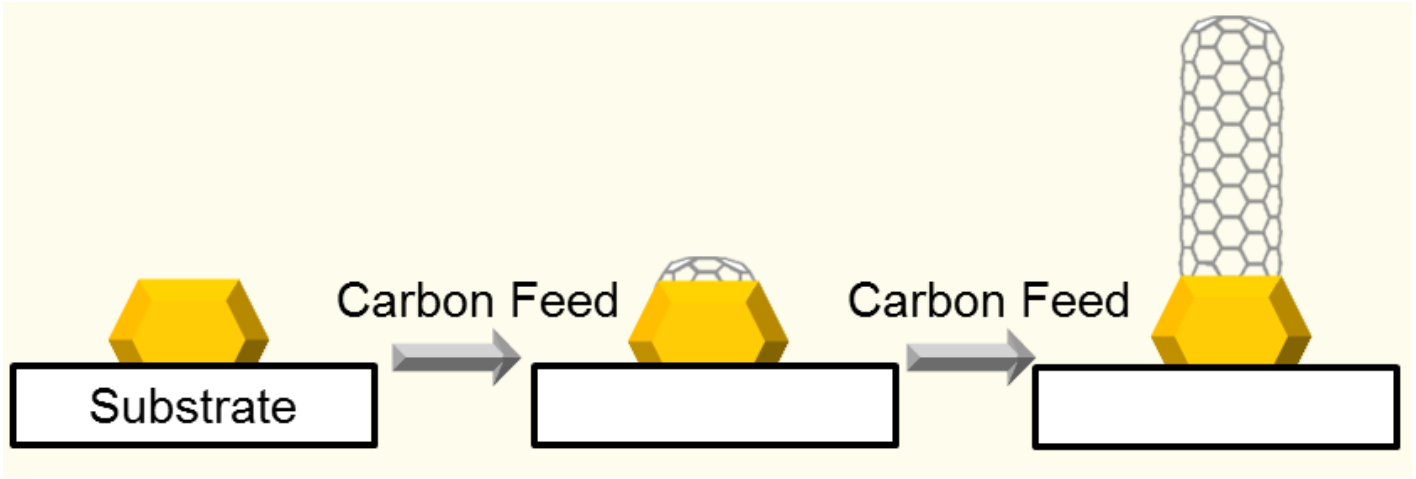

Vapor-Solid-Solid

Use the catalyst as a structural template for SWNT

Using Ni-Fe alloy to adjust the chirality distribution

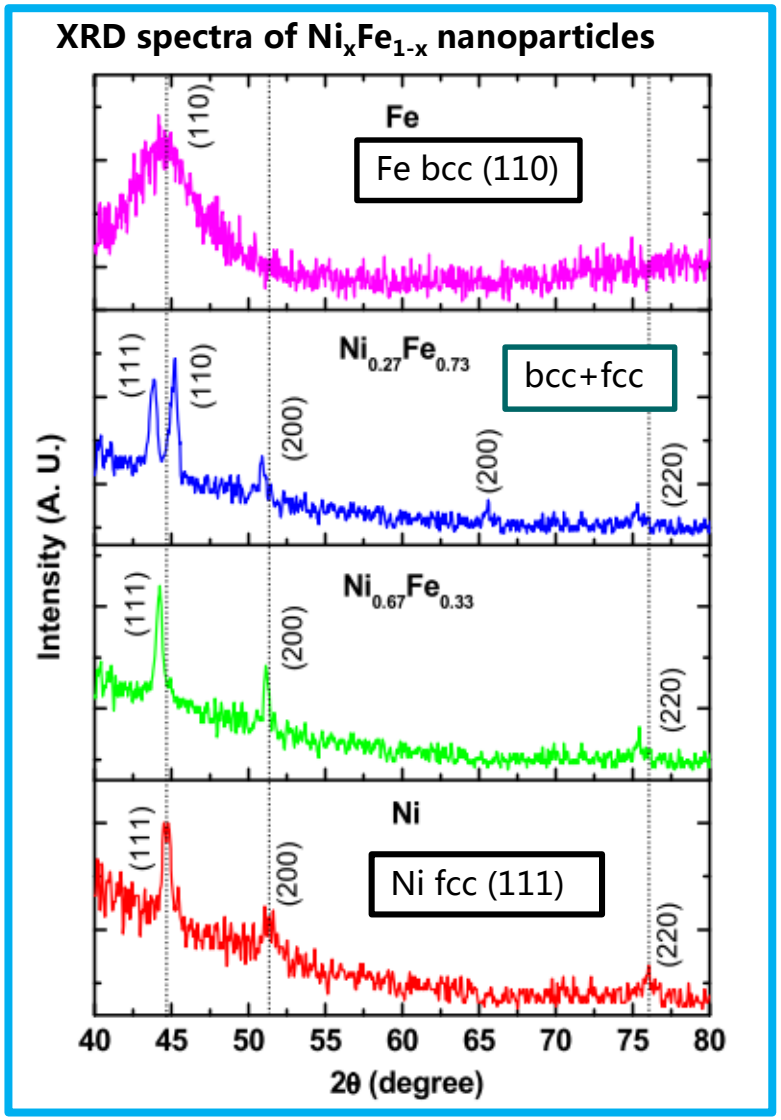

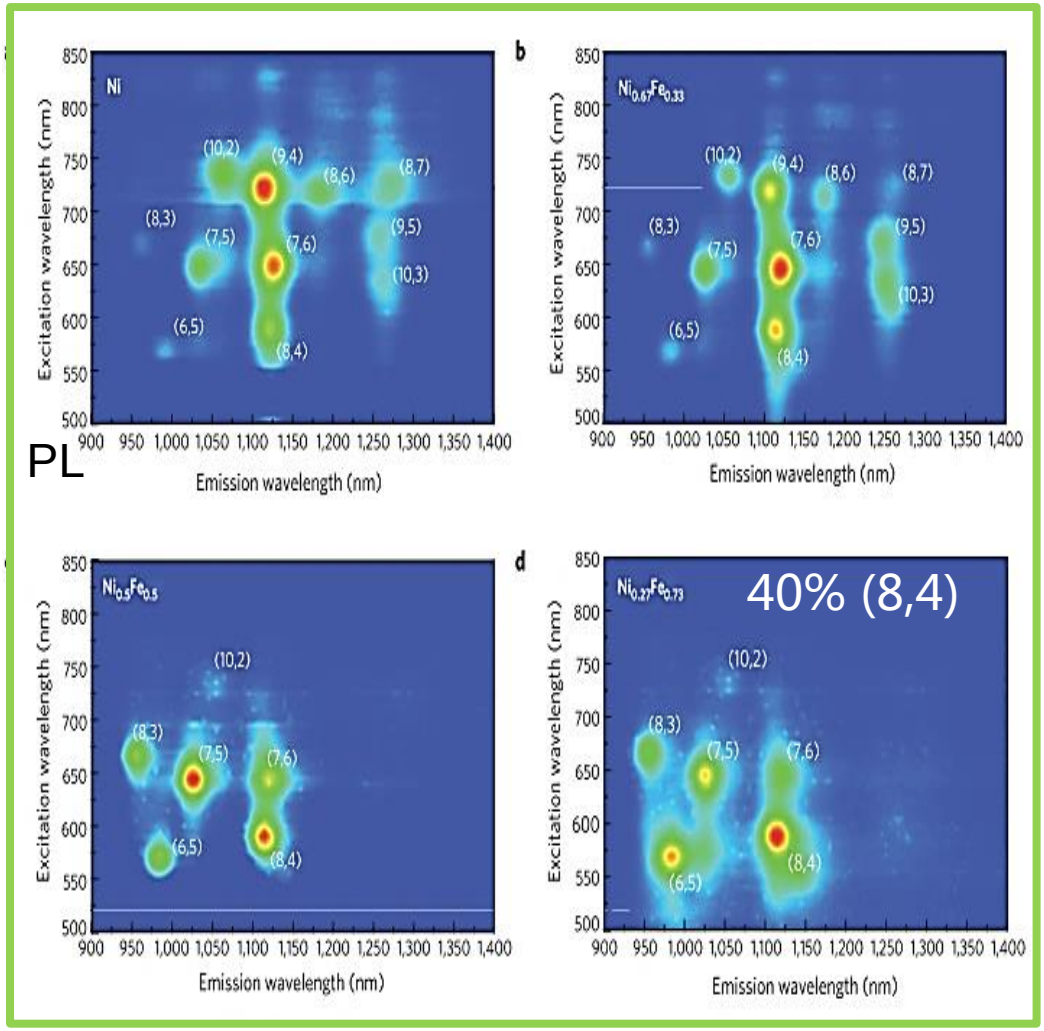

Sankaran*, *Nat. Mater.,* **2009**, 8 (11), 882
Sankaran, Bhethanabotla*, *Carbon*, **2012**, 50 (10), 3766

Growth of SWNTs on Lattice-Mismatched Epitaxial Cobalt NPs

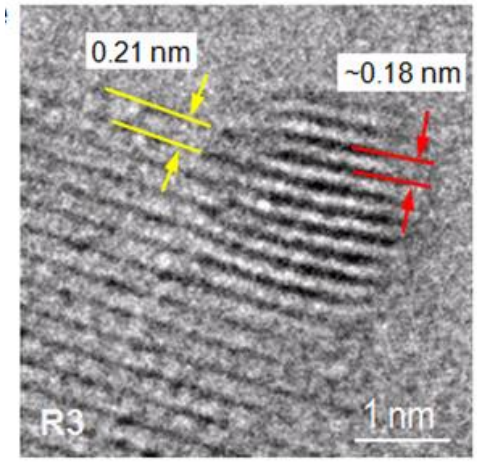

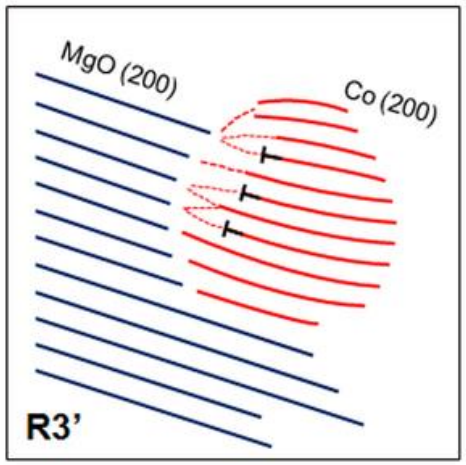

53% (6,5) tubes

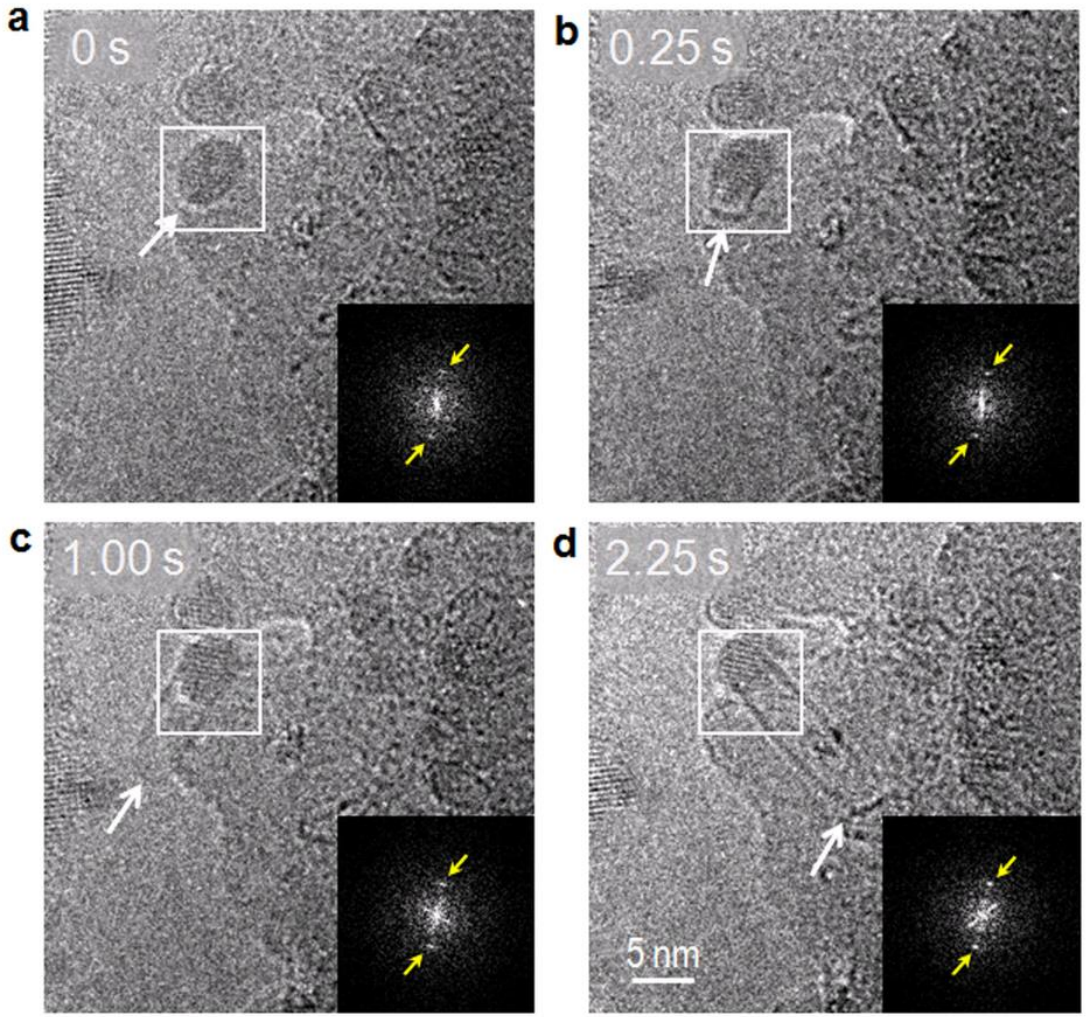

M. He, H. Jiang et al., *Scientific Reports* 2013, 3, 1460

Chirality selective growth of SWNTs with different catalysts

catalyst	(*n*,*m*)	selectivity	literature
Co-Mo	(6,5) (7,5)	28% (PL) 28% (PL)	*J. Am. Chem. Soc.* **2003**, 125, 11186.
	(6,5)	**55% (Abs)**	***J. Phys. Chem. B,* 2006, 110, 2108.**
Fe-Co	(6,5)	Unknown	*Chem. Phys. Lett.,* **2004**, 387, 198.
Fe-Ru	(6,5)	Unknown	*J. Am. Chem. Soc.,* **2007**, 129, 15770.
Fe-Ni	(8,4)	39.2% (PL)	*Nat. Mater.,* **2009**, 8, 882.
Co-Mn	(6,5)	47.4% (PL)	*J. Phys. Chem. C,* **2009**, 113, 21611.
Co-Cr	(6,5)	30.9% (PL)	*Appl. Catal. A,* **2009**, 368, 40.
Fe-Cu	(6,5)	Unknown	*J. Am. Chem. Soc.,* **2010**, 132, 13994.
	(6,5)	43% (ED)	*Chem. Mater.,* **2012,** 24, 1796.
Au	(6,5)	Unknown	*J. Am. Chem. Soc.,* **2010**, 132 , 9570.
Co-TUD-1	(9,8)	Unknown	J. Am. Chem. Soc., **2010**, 132, 16747.
Co-Pt	(6,5)	30% (PL)	*Chem. Commun.,* **2012**, 48, 2409.
Co-MgO	(6,5)	53% (ED)	*Sci. Rep.,* **2013**, 3, 1460.
Co-MCM-41	(7,5)	30.1% (PL)	*Carbon,* **2014**, 66, 134.

PL: Photoluminescence ED: Electron Diffraction Abs: Absorption

Our understanding on Crucial issues for catalysts in structure-controlled growth of SWNTs

- ✓ **Catalytic activity**
- ✓ **High meting point**
  ---- to maintain their crystal structure
- ✓ **Unique structure**
  ---- to ensure the high selectivity

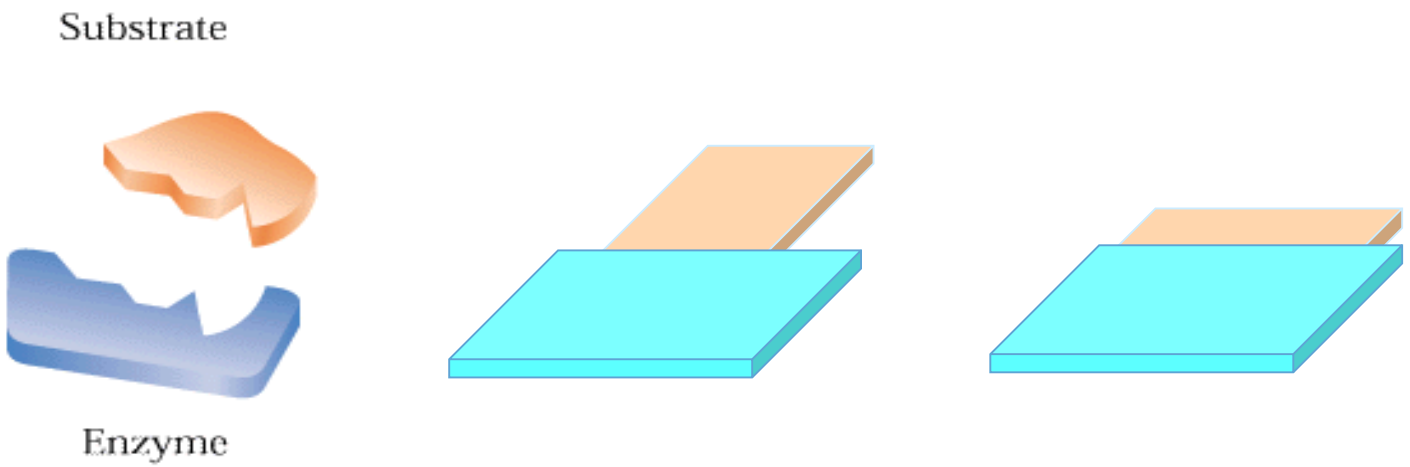

Our understanding on Cruc

catalysts in structure-controlled

s

- **Fixed composition**
- **Unique crystal structure**
- **Stable at high temperature**

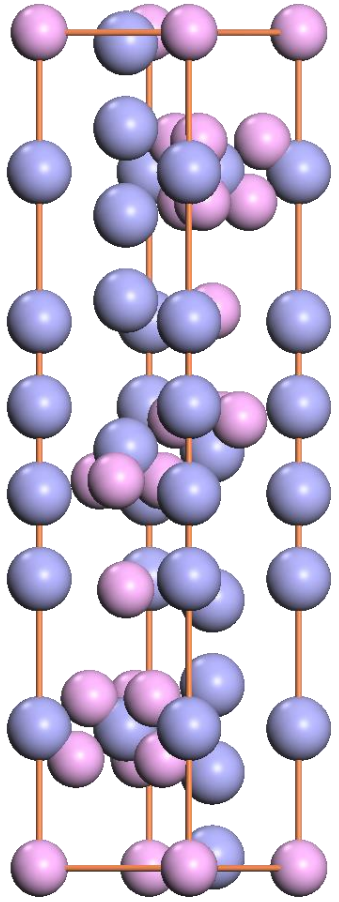

Trigonal W_6Co_7

hydrogen 1 H 1.0079																	helium 2 He 4.0026
lithium 3 Li 6.941	beryllium 4 Be 9.0122											boron 5 B 10.811	carbon 6 C 12.011	nitrogen 7 N 14.007	oxygen 8 O 15.999	fluorine 9 F 18.998	neon 10 Ne 20.180
sodium 11 Na 22.990	magnesium 12 Mg 24.305											aluminium 13 Al 26.982	silicon 14 Si 28.086	phosphorus 15 P 30.974	sulfur 16 S 32.065	chlorine 17 Cl 35.453	argon 18 Ar 39.948
potassium 19 K 39.098	calcium 20 Ca 40.078		scandium 21 Sc 44.956	titanium 22 Ti 47.867	vanadium 23 V 50.942	chromium 24 Cr 51.996	manganese 25 Mn 54.938	iron 26 Fe 55.845	cobalt 27 Co 58.933	nickel 28 Ni 58.693	copper 29 Cu 63.546	zinc 30 Zn 65.39	gallium 31 Ga 69.723	germanium 32 Ge 72.64	arsenic 33 As 74.922	selenium 34 Se 78.96	bromine 35 Br 79.904	krypton 36 Kr 83.80
rubidium 37 Rb 85.468	strontium 38 Sr 87.62		yttrium 39 Y 88.906	zirconium 40 Zr 91.224	niobium 41 Nb 92.906	molybdenum 42 Mo 95.94	technetium 43 Tc [98]	ruthenium 44 Ru 101.07	rhodium 45 Rh 102.91	palladium 46 Pd 106.42	silver 47 Ag 107.87	cadmium 48 Cd 112.41	indium 49 In 114.82	tin 50 Sn 118.71	antimony 51 Sb 121.76	tellurium 52 Te 127.60	iodine 53 I 126.90	xenon 54 Xe 131.29
caesium 55 Cs 132.91	barium 56 Ba 137.33	57-70 *	lutetium 71 Lu 174.97	hafnium 72 Hf 178.49	tantalum 73 Ta 180.95	tungsten 74 W 183.84	rhenium 75 Re 186.21	osmium 76 Os 190.23	iridium 77 Ir 192.22	platinum 78 Pt 195.08	gold 79 Au 196.97	mercury 80 Hg 200.59	thallium 81 Tl 204.38	lead 82 Pb 207.2	bismuth 83 Bi 208.98	polonium 84 Po [209]	radon 86 Rn [222]
francium 87 Fr [223]	radium 88 Ra [226]	89-102 **	lawrencium 103 Lr [262]	rutherfordium 104 Rf [261]	dubnium 105 Db [262]	seaborgium 106 Sg [266]	bohrium 107 Bh [264]	hassium 108 Hs [269]	meitnerium 109 Mt [268]	ununnilium 110 Uun [271]	unununium 111 Uuu [272]						

*	lanthanum 57 La 138.91	cerium 58 Ce 140.12	praseodymium 59 Pr 140.91	neodymium 60 Nd 144.24	promethium 61 Pm [145]	samarium 62 Sm 150.36	europium 63 Eu 151.96	gadolinium 64 Gd 157.25	terbium 65 Tb 158.93	dysprosium 66 Dy 162.50	holmium 67 Ho 164.93	erbium 68 Er 167.26	thulium 69 Tm 168.93	ytterbium 70 Yb 173.04
**	actinium 89 Ac [227]	thorium 90 Th 232.04	protactinium 91 Pa 231.04	uranium 92 U 238.03	neptunium 93 Np [237]	plutonium 94 Pu [244]	americium 95 Am [243]	curium 96 Cm [247]	berkelium 97 Bk [247]	californium 98 Cf [251]	einsteinium 99 Es [252]	fermium 100 Fm [257]	mendelevium 101 Md [258]	nobelium 102 No [259]

* Lanthanide series

** Actinide series

W-based intermetallic compounds !

Preparation of W-Co alloy nanocrystals at moderate conditions by using molecular clusters as precursors

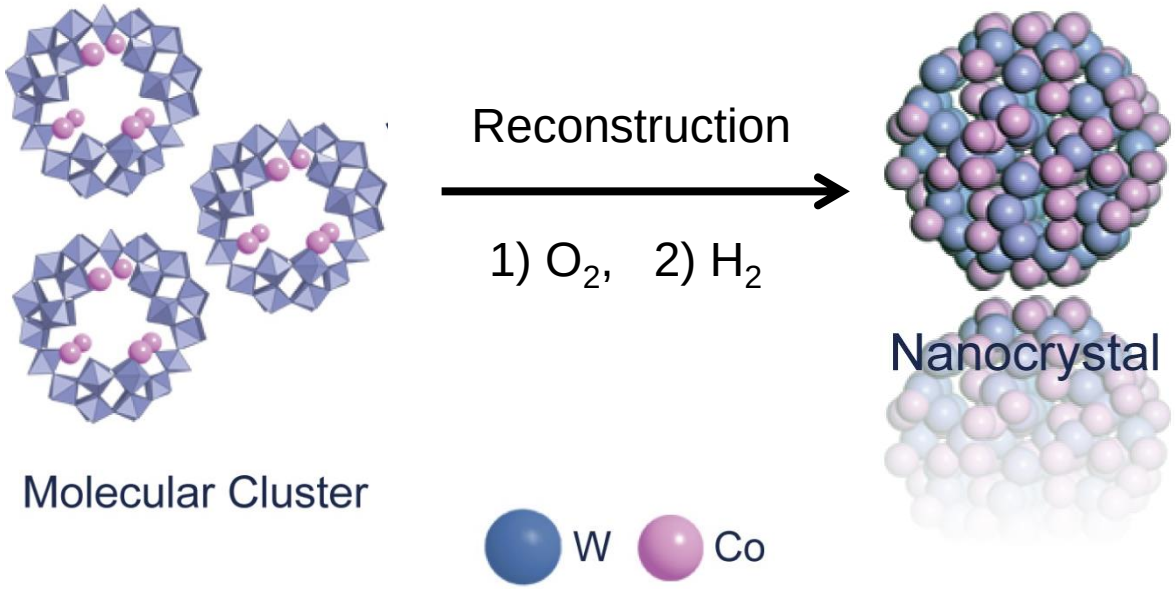

$Na_{15}[Na_3 \subset \{Co(H_2O)_4\}_6\{WO(H_2O)\}_3(P_2W_{12}O_{48})_3]\cdot nH_2O$
reported by E. Wang et al.

$\{W_{39}Co_6O_x\}$

- ✓ **Tungsten and cobalt atoms are already well mixed in the precursor**
- ✓ **Nano-scaled precursors**

Characterizations of the catalyst nanoparticles

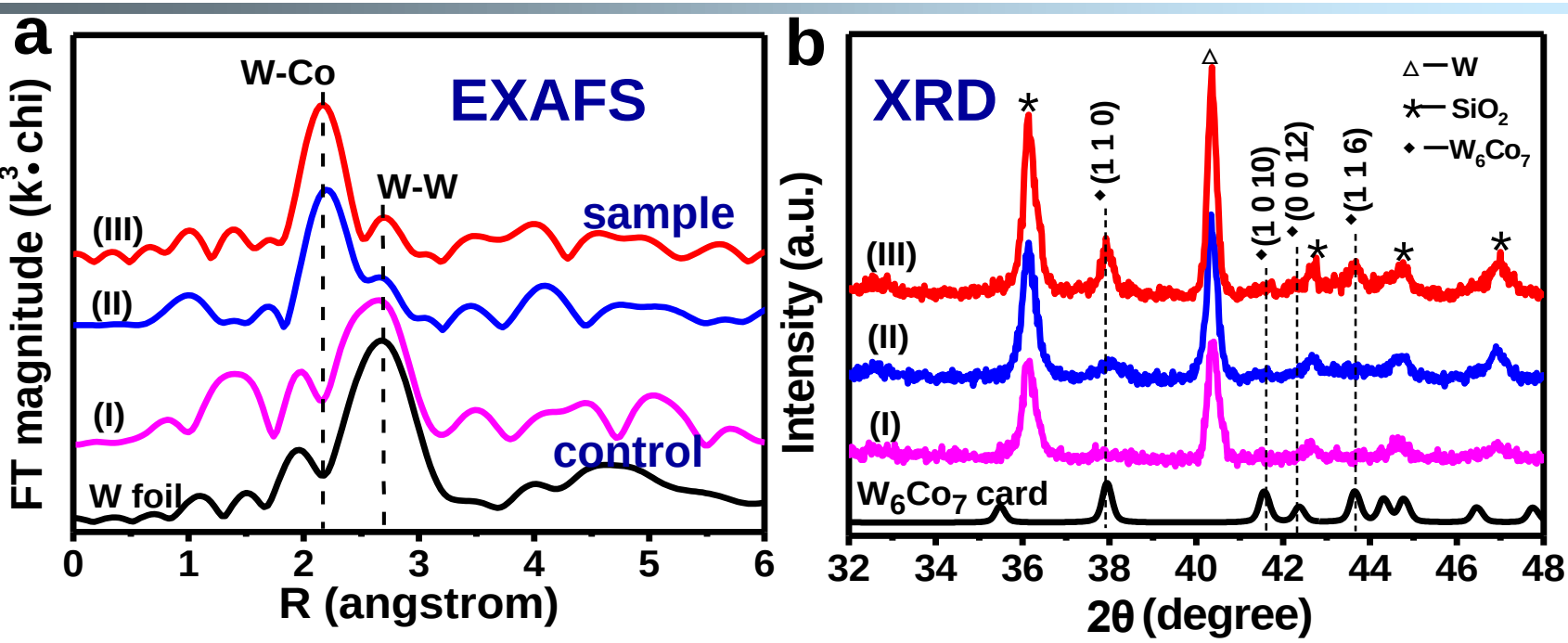

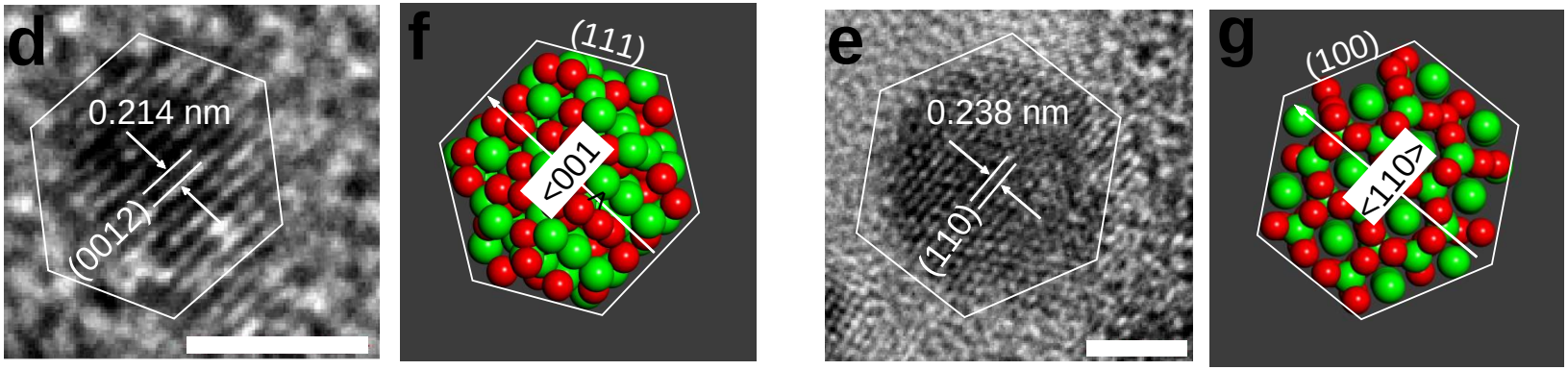

Scale bar: 2nm

Co_7W_6 m.p. ~2300 °C

In situ HRTEM at 1100°C

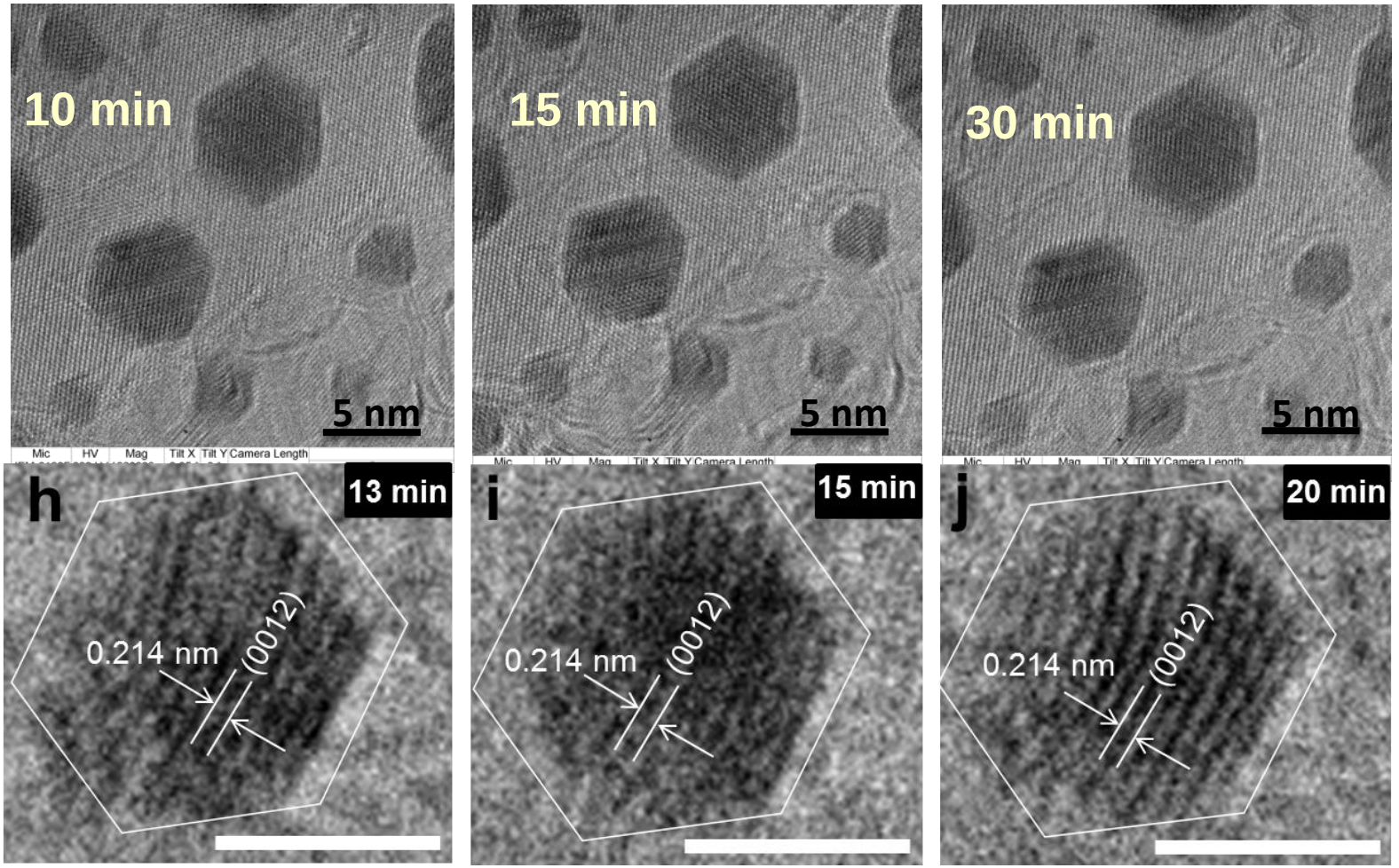

Si_3N_4

C

Scale bar: 2nm

Acknowledgement: Protochips Co., USA

Raman spectra of the control sample

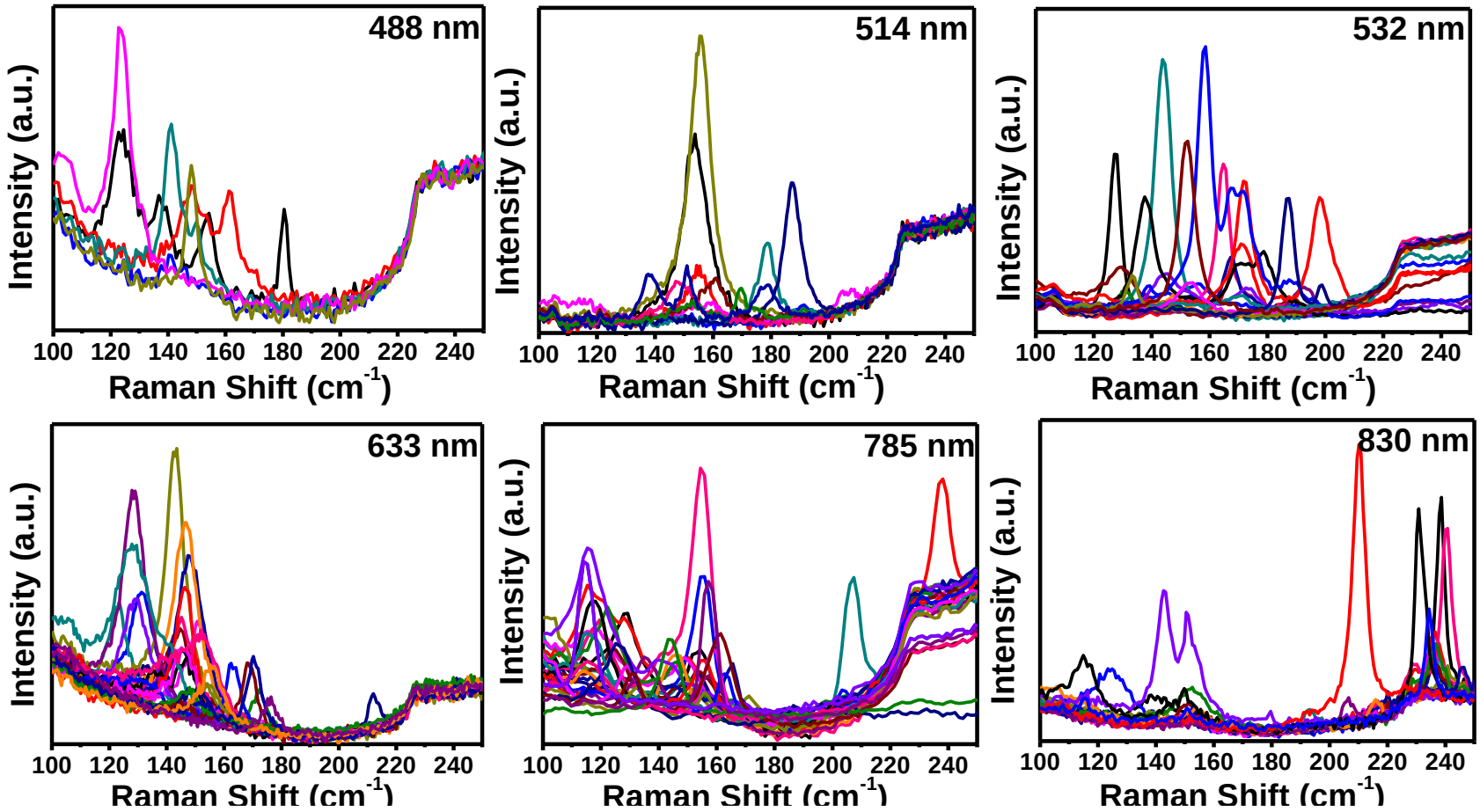

Raman spectra of our sample

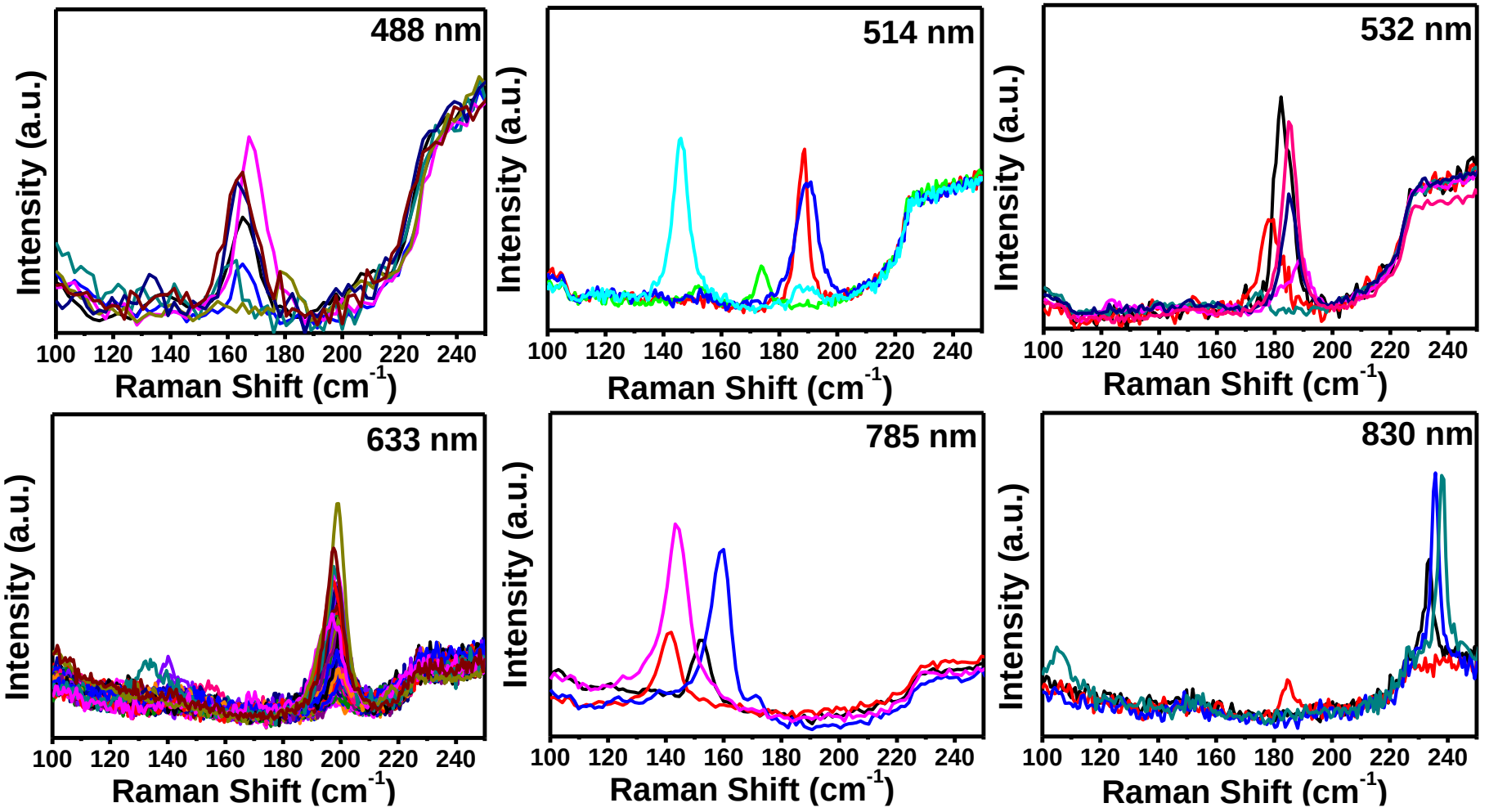

CVD temperature: 1030°C

Surface-enhanced Raman measurements

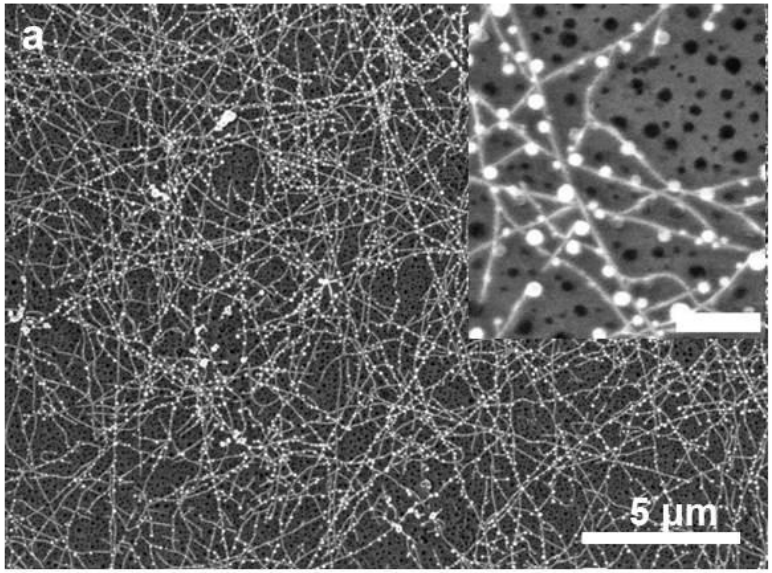

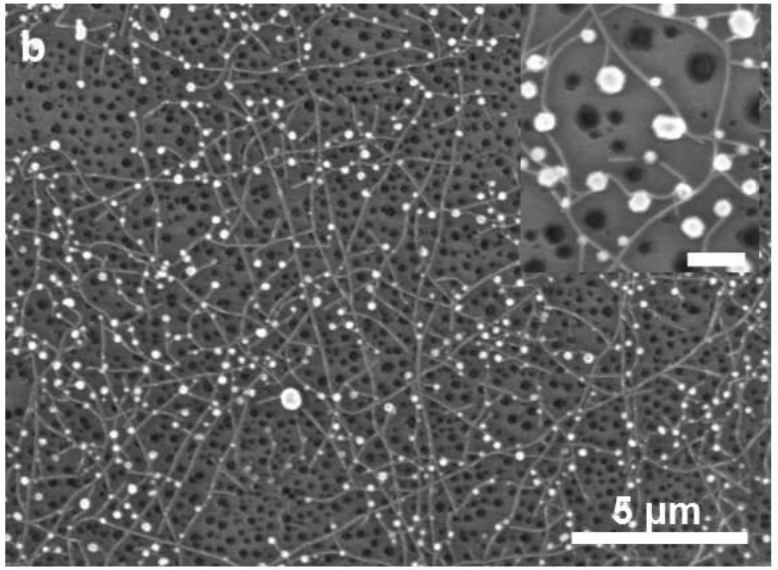

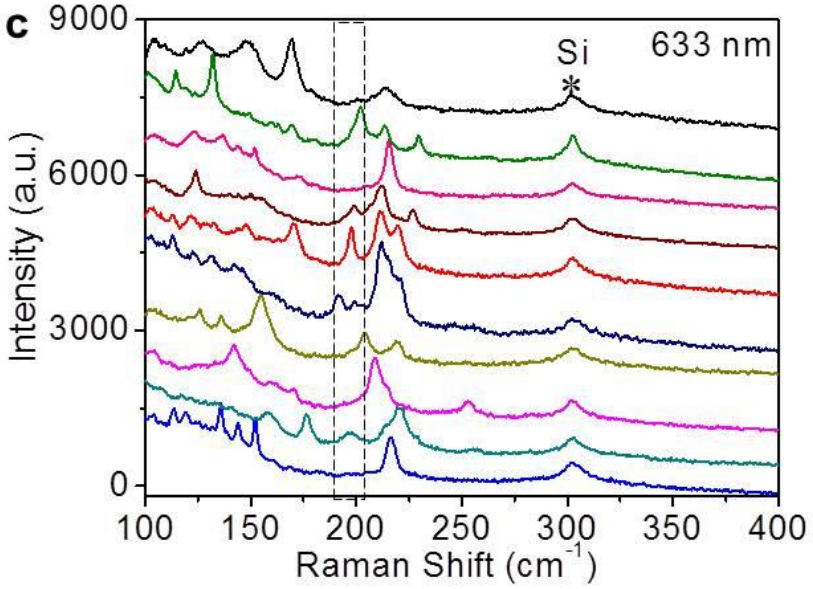

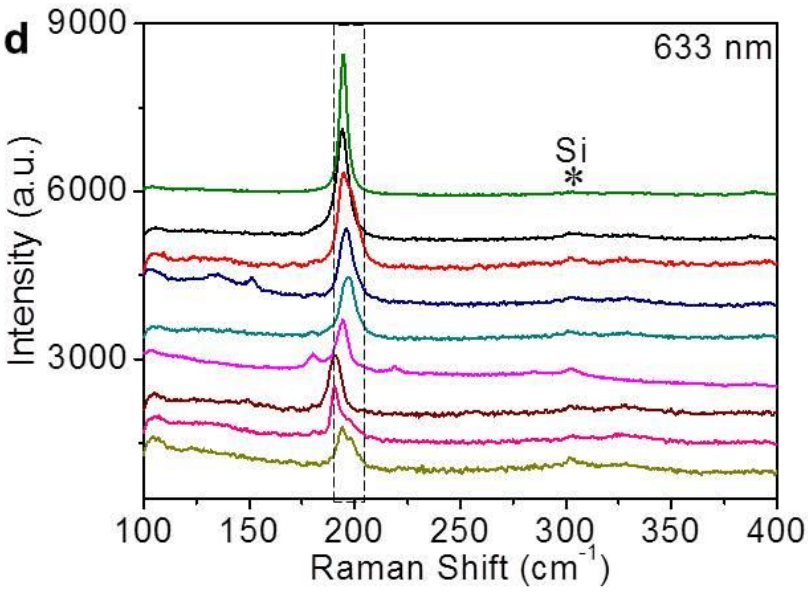

Chirality assignments

$d_t = 240.5/(\nu_{RBM} - 2.3)$

(12,6) tube
d= 1.24 nm

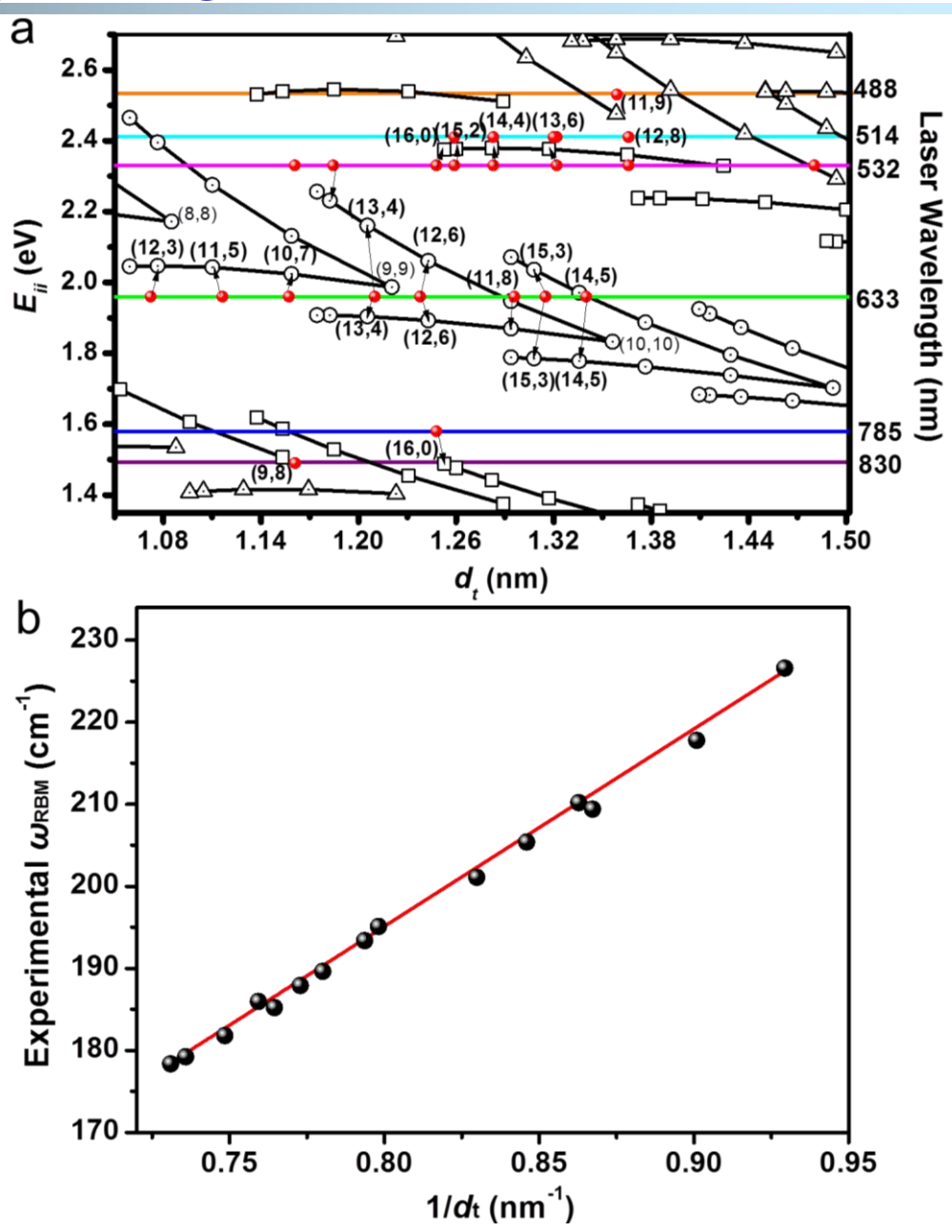

Chirality from electron diffraction and Raman

(12,6) tube

d= 1.24 nm

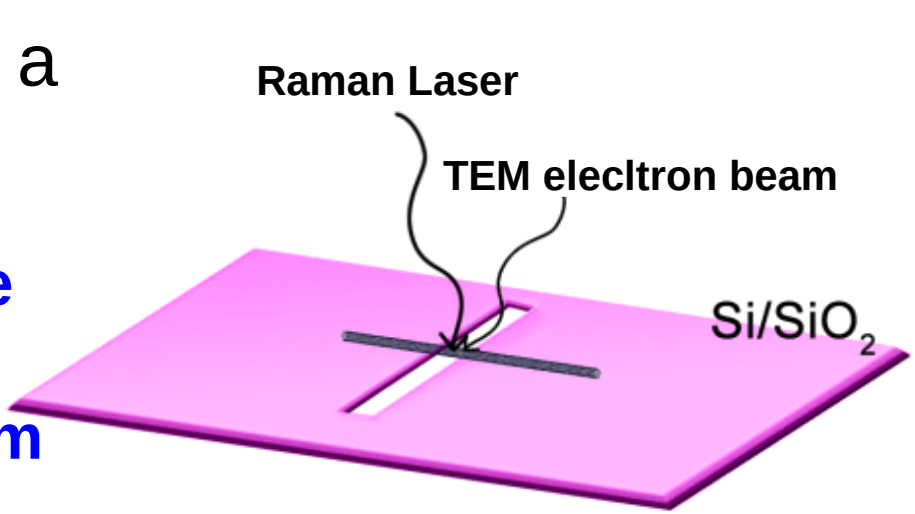

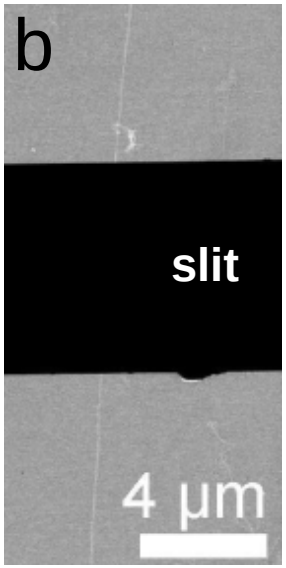

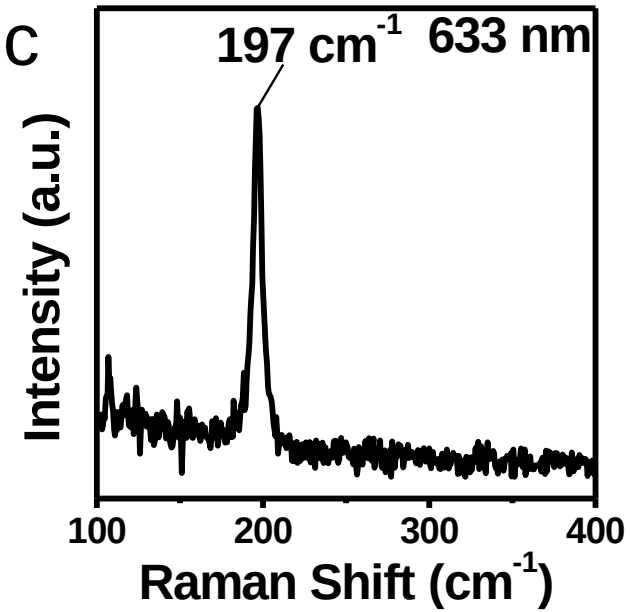

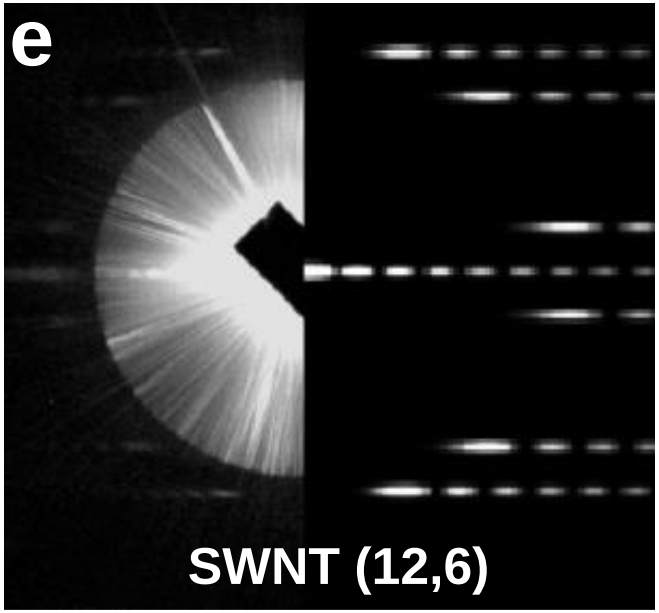

Quantification of the population for (12,6) SWNTs

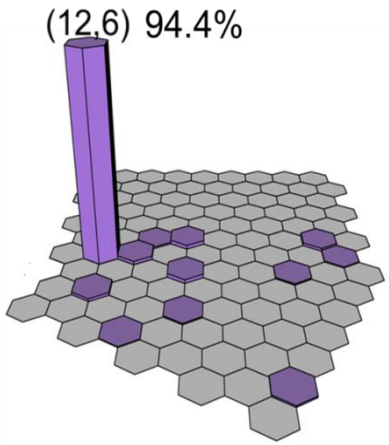

Raman RBM counting

7 SWNTs under the laser spot, lasers cover

~85% of all types of SWNTs ,

$$450 \cdot 7 \cdot x / [450 \cdot 7 \cdot x + 151/0.85] = x$$

(12,6) content X = 94.4%

Absorption

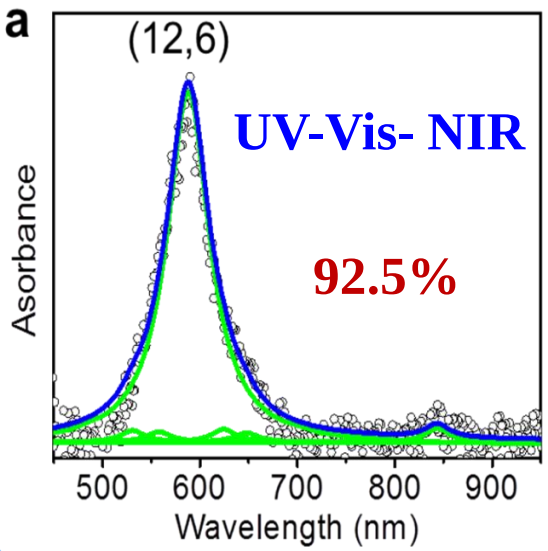

AFM-Raman

category	result
Total tube number by AFM	122
Total area AFM scanned	15550 μm²
Number of (12,6) SWNTs	214
Total area Raman mapped	28746μm²
(12,6) content	94.9%

The interface between (12,6) tube and Co_7W_6 nanocrystal

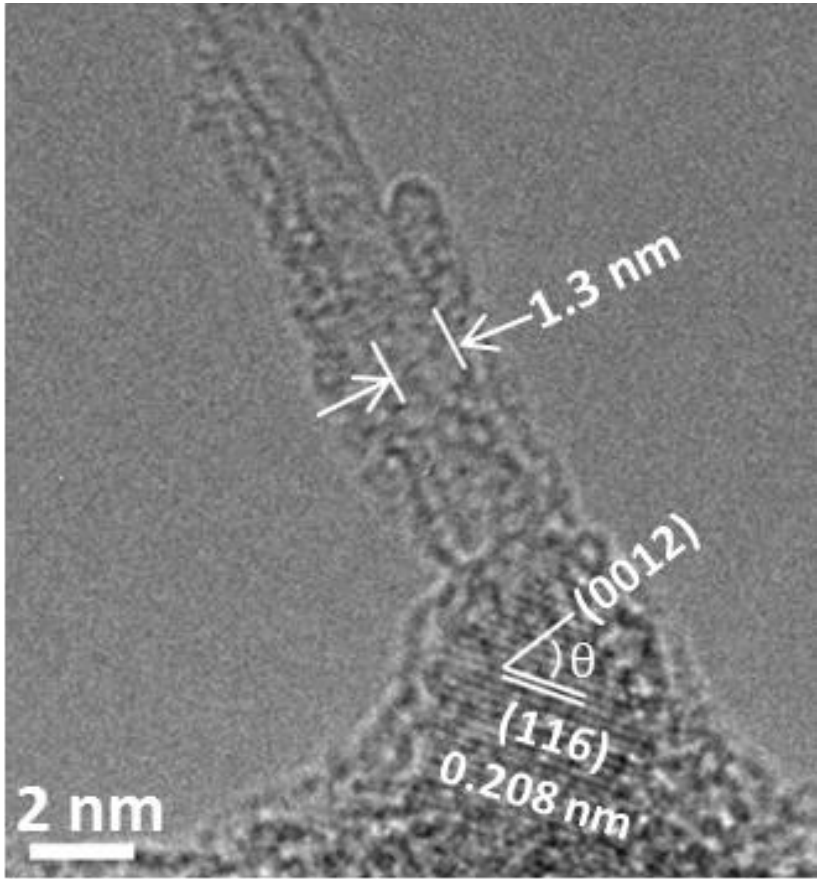

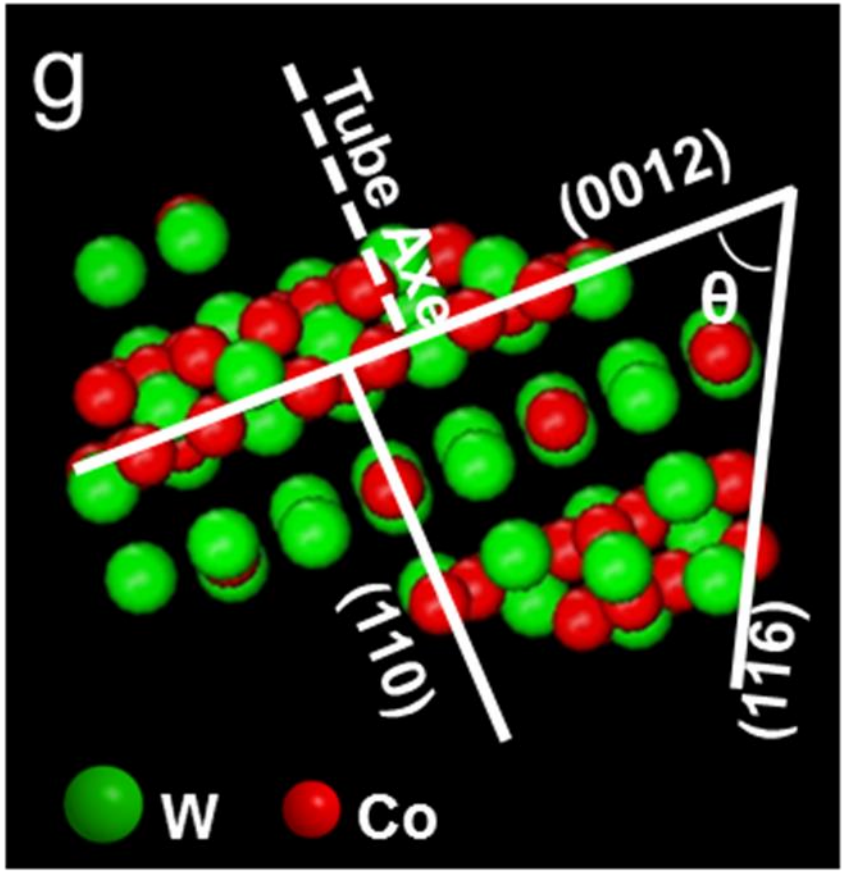

In situ TEM at 1100 º C in vacuum

On Carbon thin film

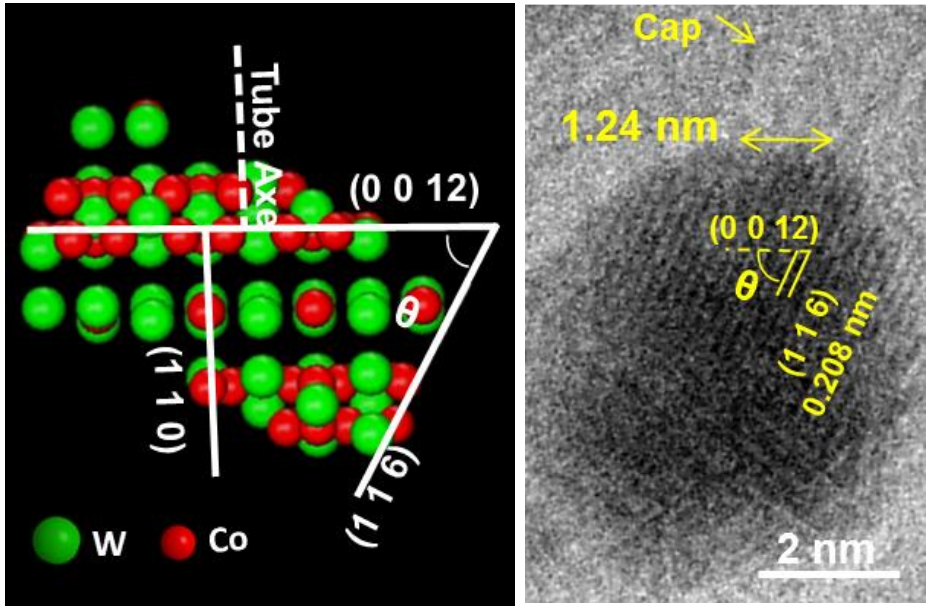

F. Yang/**Y. Li***, ***Acc. Chem. Res. 2016,*** 49, 606

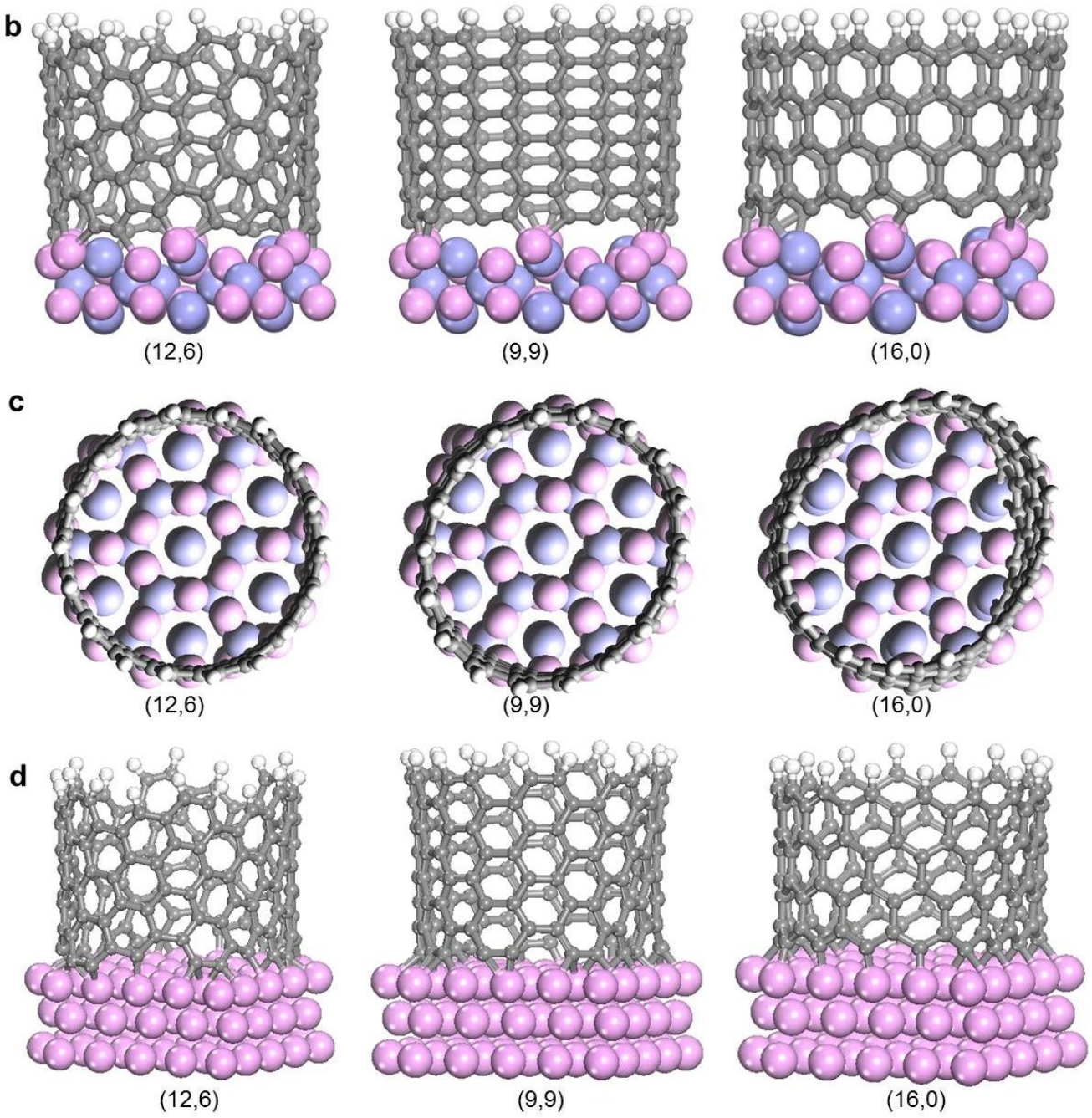
b
(12,6)
(9,9)
(16,0)
c
(12,6)
(9,9)
(16,0)
d
(12,6)
(9,9)
(16,0)
Co7W6
(0 0 12)
Co
(0 0 1)

Formation energy of SWNTs with around (0 0 12) plane of W_6Co_7 and (0 0 1) plane of *fcc*-Co.

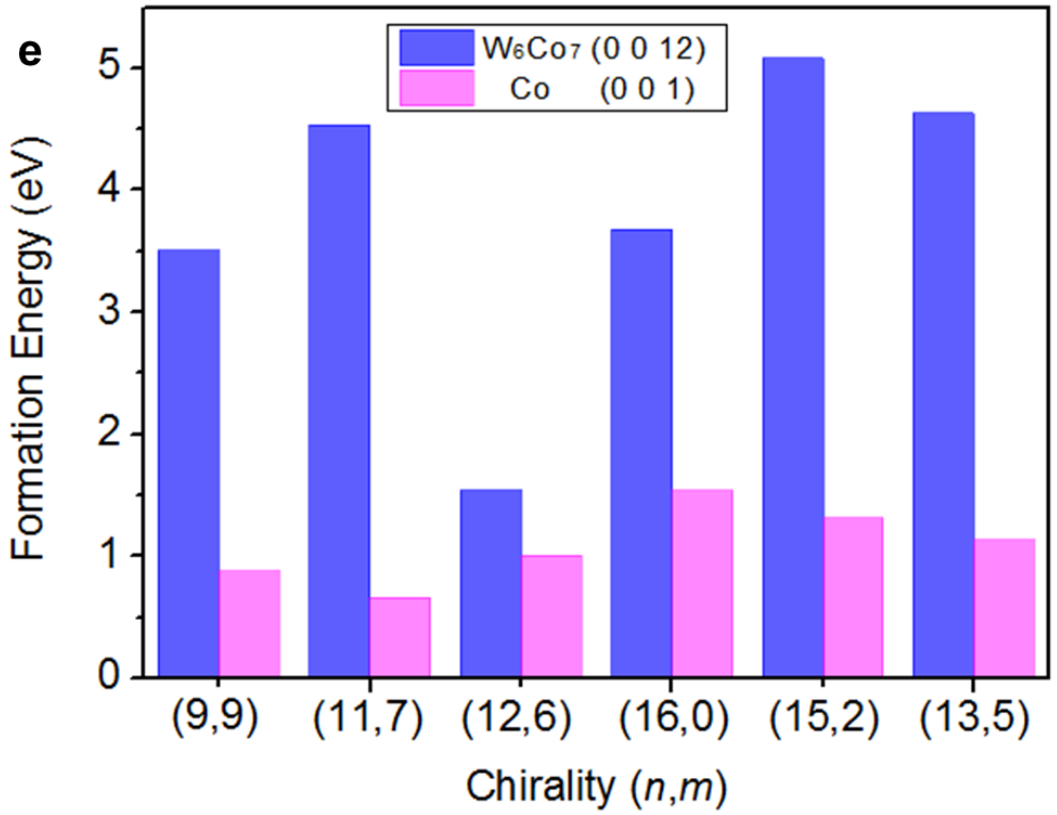

F. Yang/**Y. Li***, ***Acc. Chem. Res. 2016,*** 49, 606

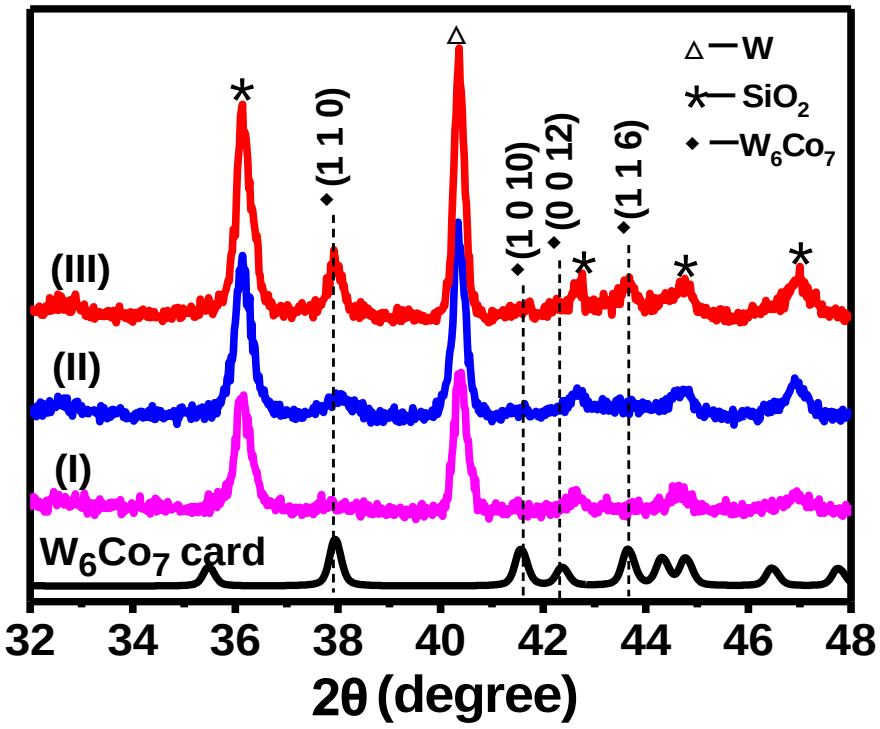

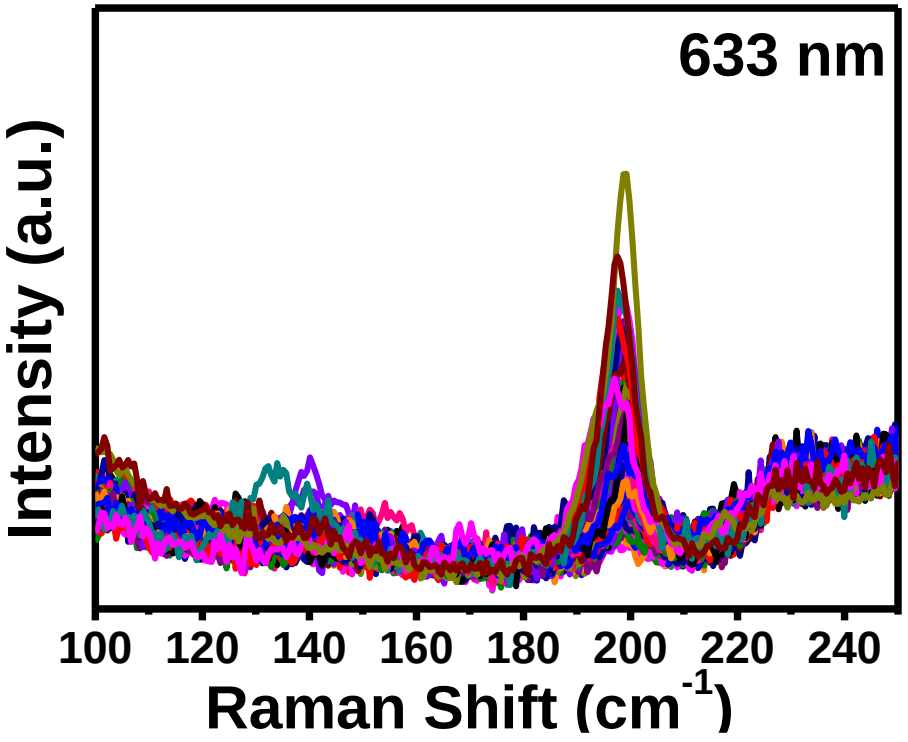

Catalyst preparation: 1030° SWNT growth: 1030°

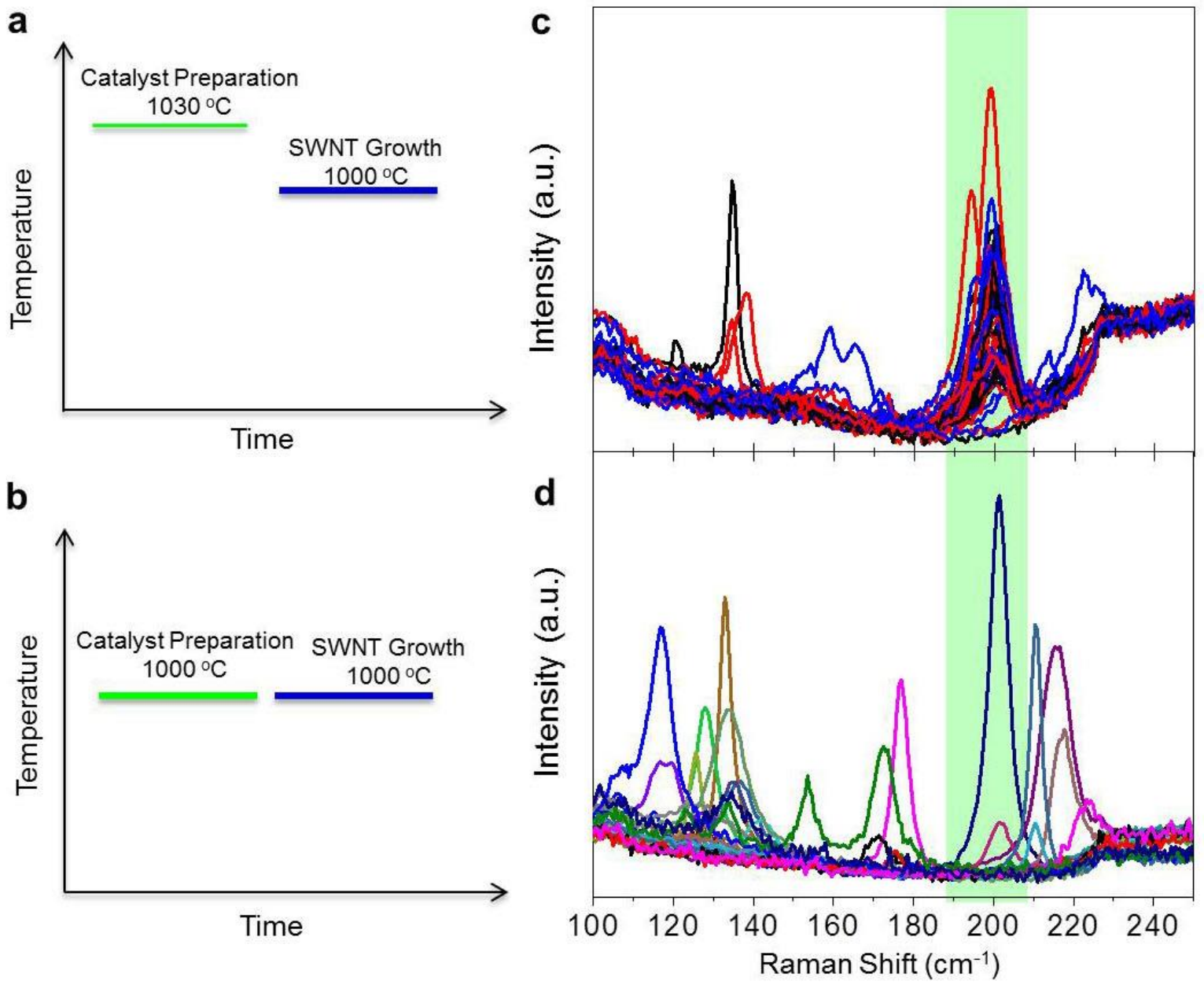
a
Catalyst Preparation
1030 °C
SWNT Growth
1000 °C
Temperature
Time
b
Catalyst Preparation
1000 °C
SWNT Growth
1000 °C
Temperature
Time
c
Intensity (a.u.)
d
Intensity (a.u.)
100 120 140 160 180 200 220 240
Raman Shift (cm-1)

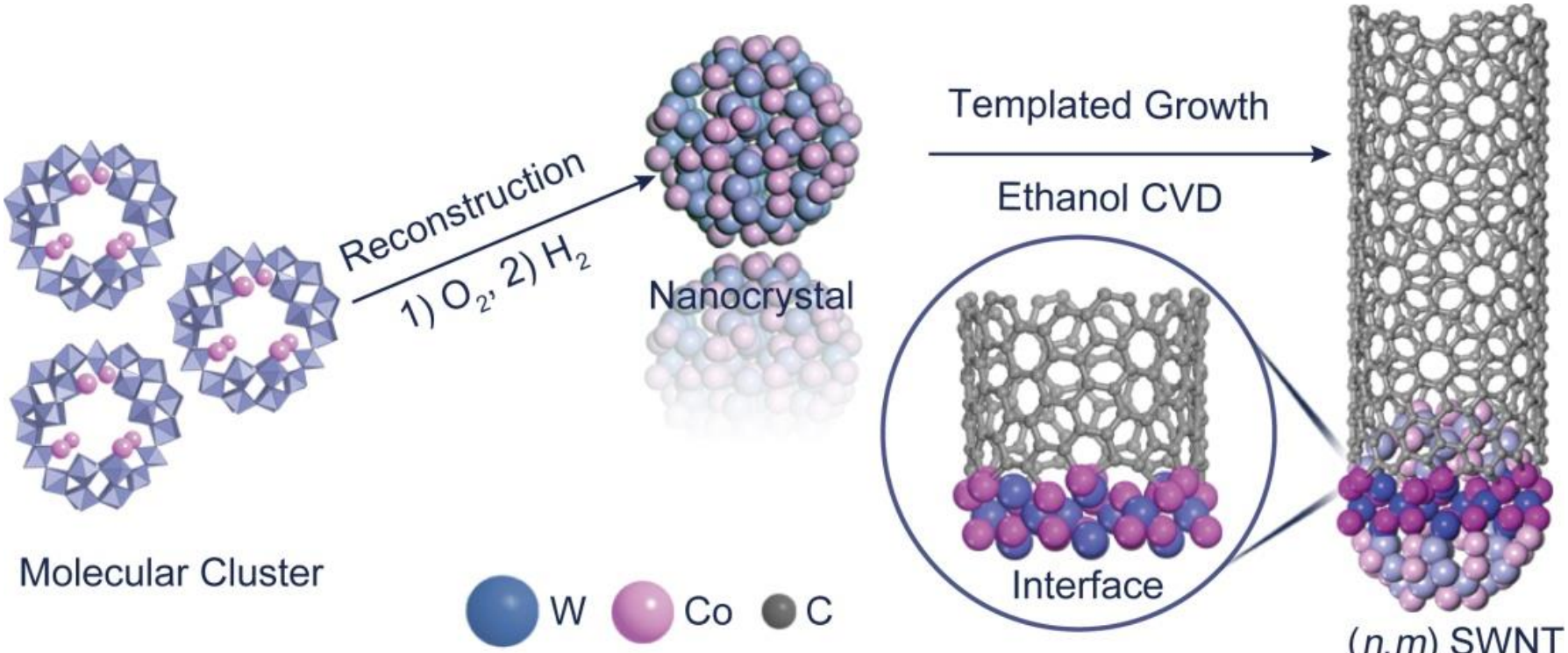

Is this strategy valid for other chiralities?

Besides catalyst, are there any other factors important for chirality specificity?

F. Yang/**Y. Li***, ***Nature 2014***, 510, 522-524

zig-zag tubes!

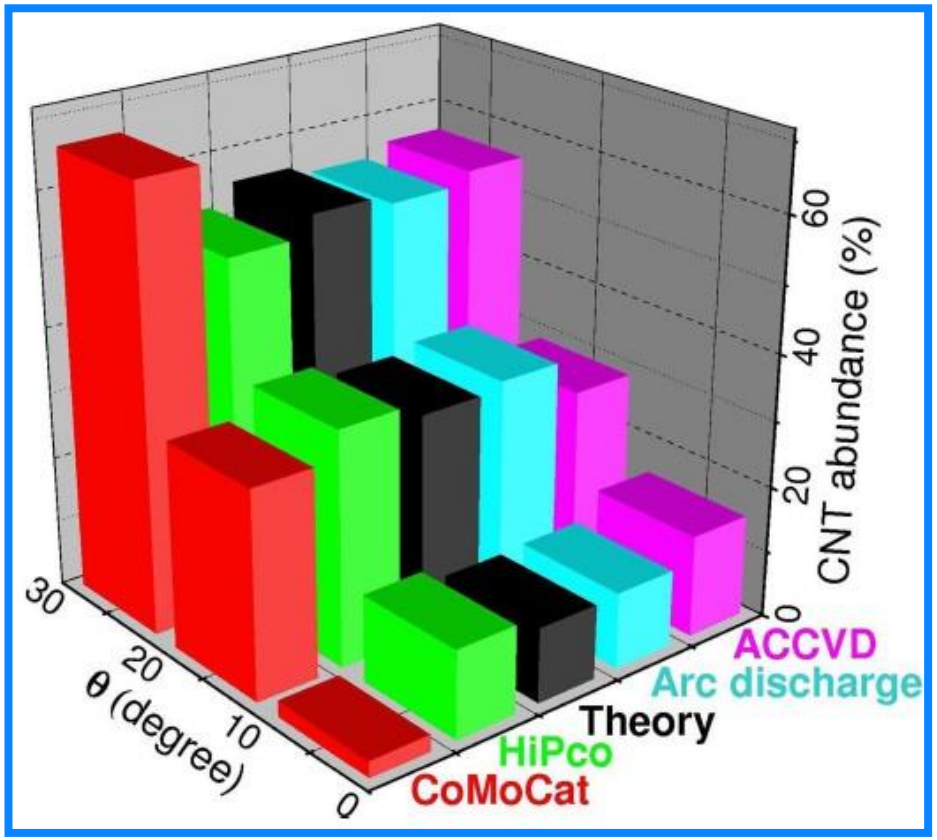

Population of SWNTs is approximately in direct proportion to chirality angel.

F. Ding, B. Yakobson, ***Proc. Natl Acad. Sci.* 2009**, 106, 2506

DFT simulation of tubes around (1 1 6) plane

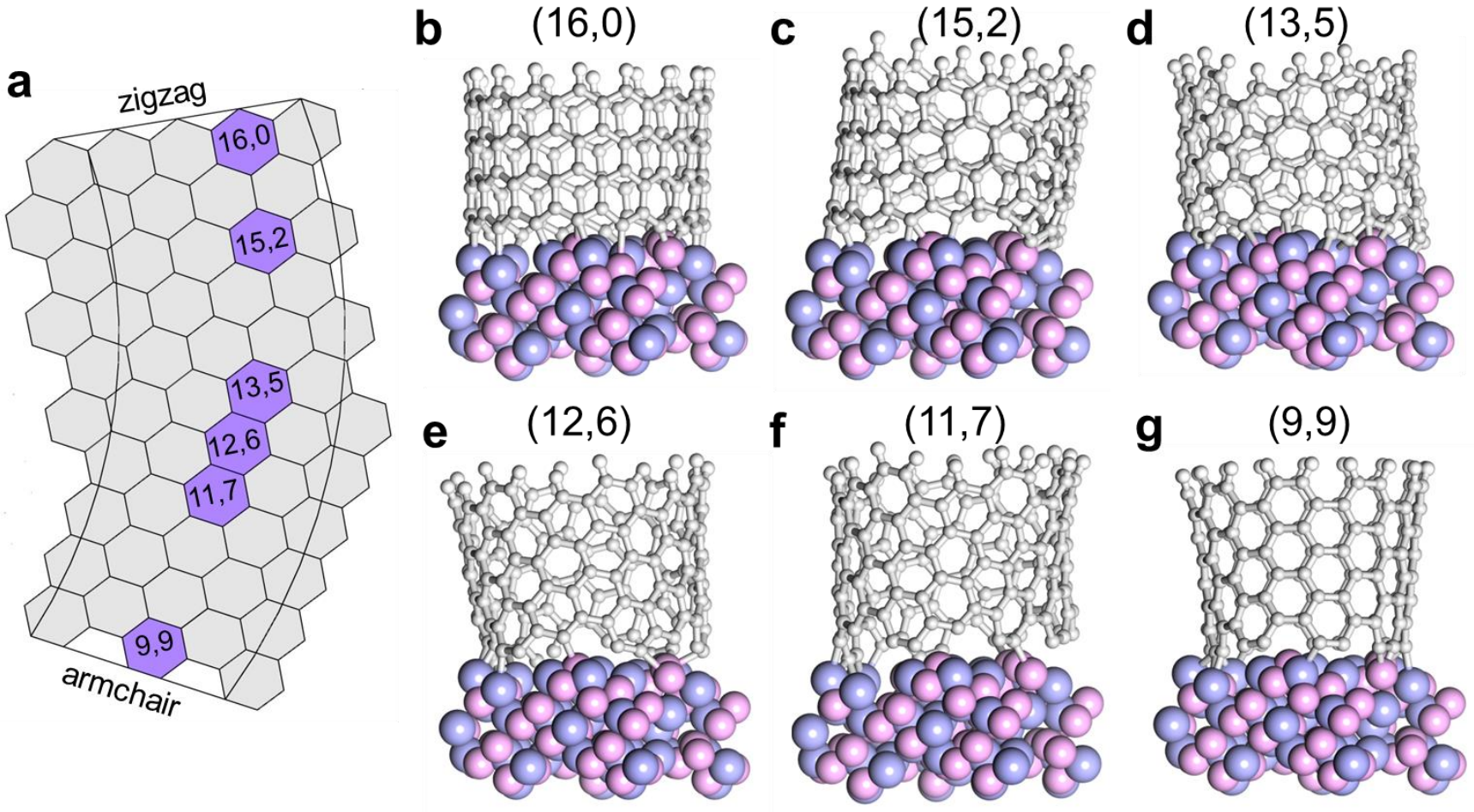

***JACS* 2015,** 137, 8688

XRD characterization of the catalyst

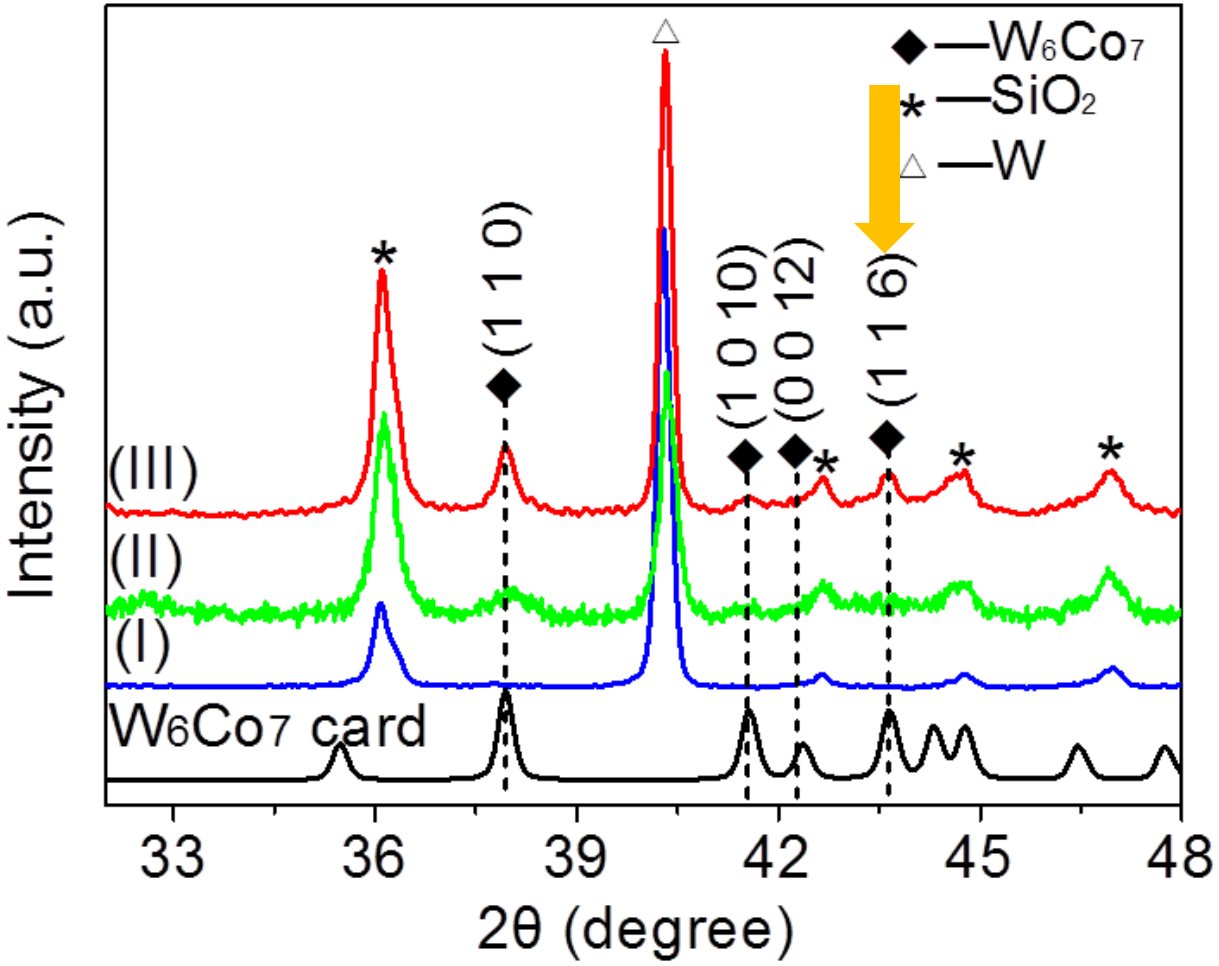

Abundance of (16,0) SWNTs

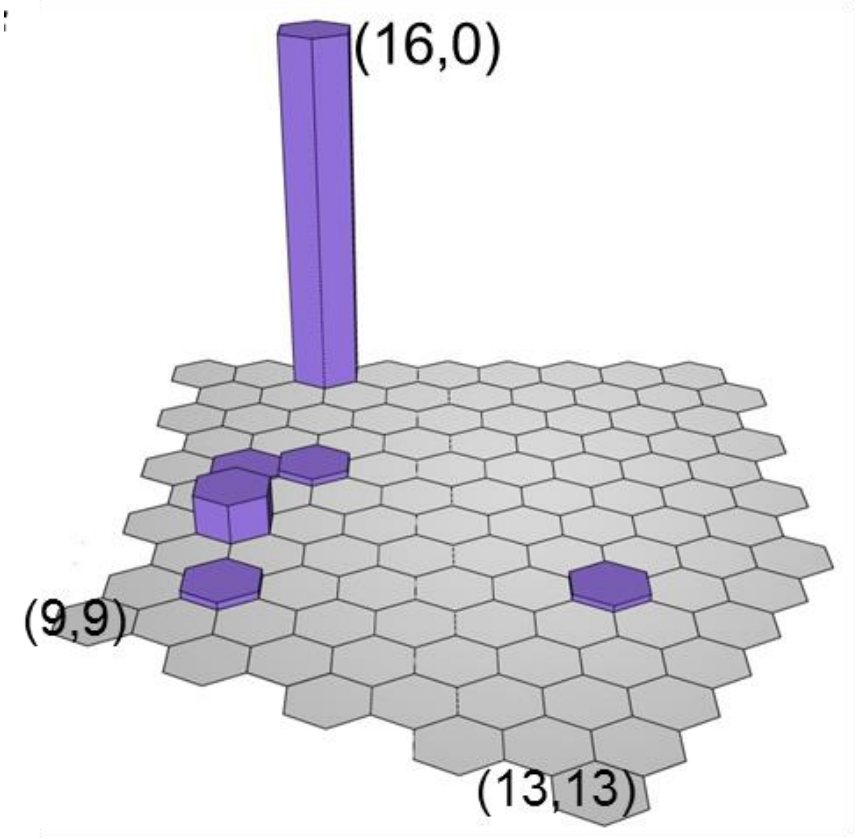

Relative abundances from 357 RBMs: 79.2%

***JACS* 2015,** 137, 8688

Content of (16,0) tubes at different conditions

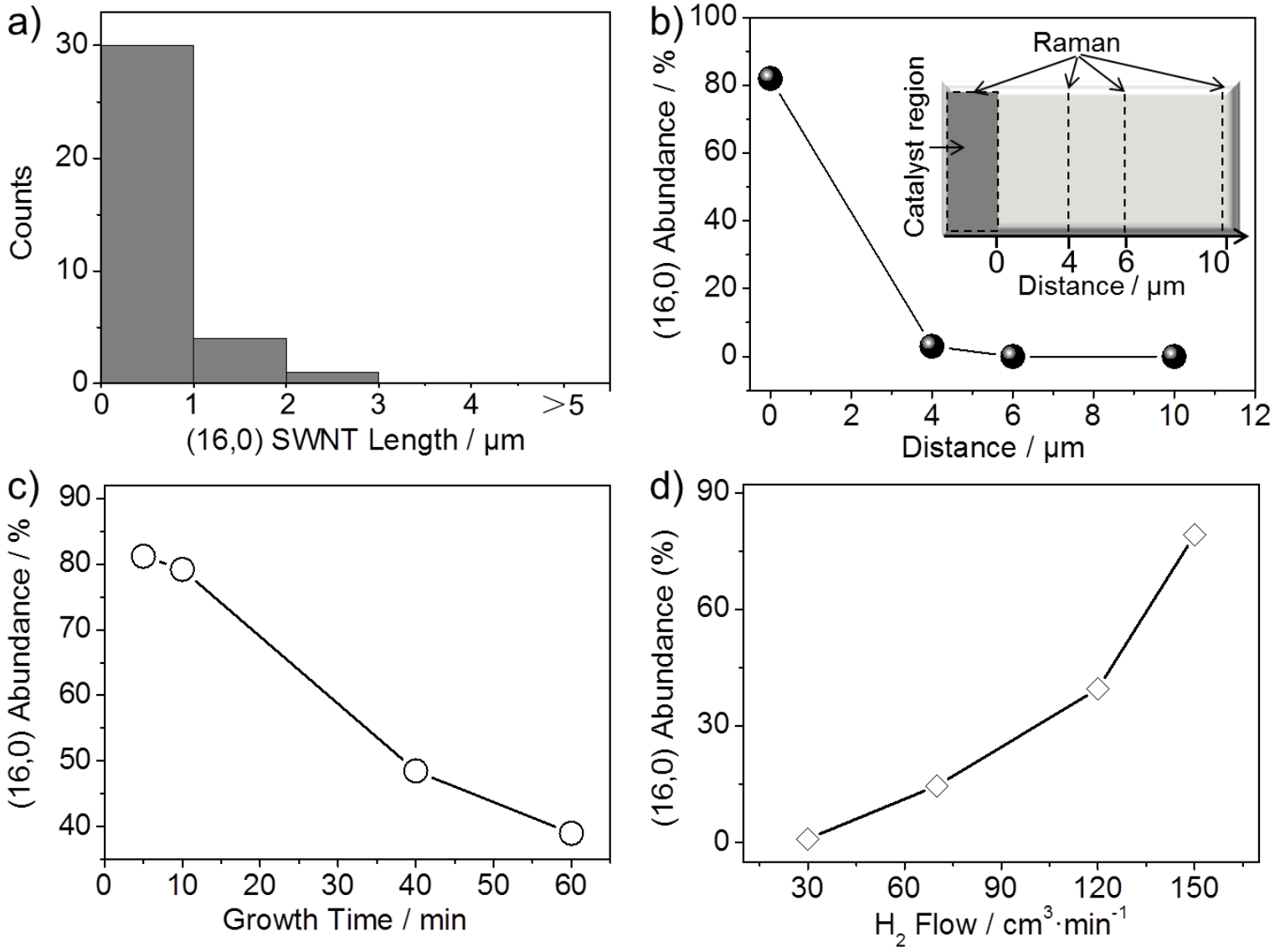

The growth of (16,0) tubes is kinetically unfavorable.

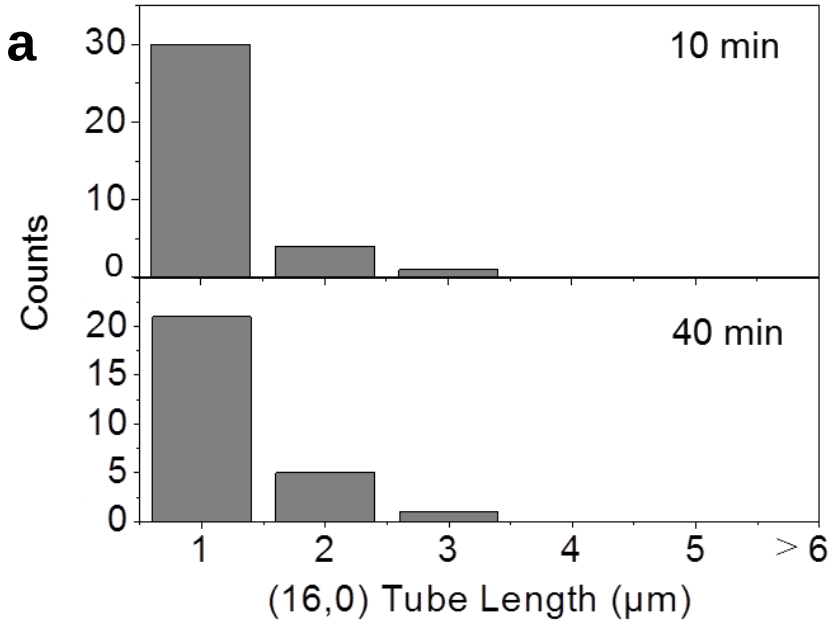
a
10 min
40 min
Counts
30
20
10
0
20
15
10
5
0
1
2
3
4
5
> 6
(16,0) Tube Length (μm)

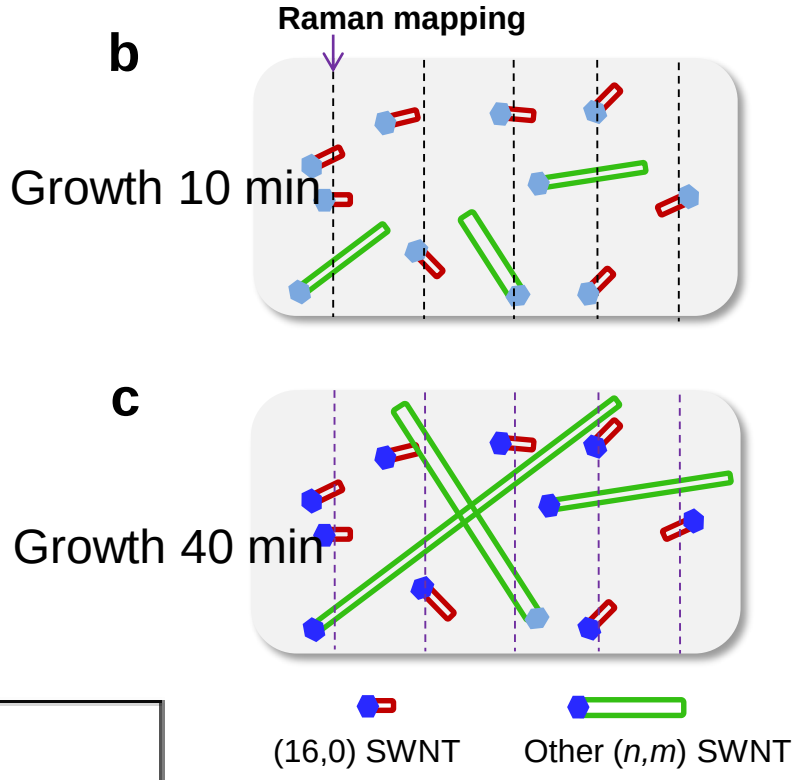
b
Raman mapping
Growth 10 min
c
Growth 40 min
(16,0) SWNT
Other (n,m) SWNT

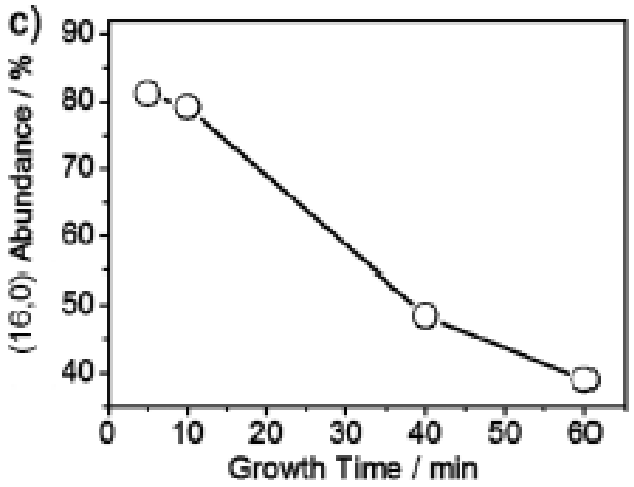
c)
(16,0) Abundance / %
90
80
70
60
50
40
0
10
20
30
40
50
60
Growth Time / min

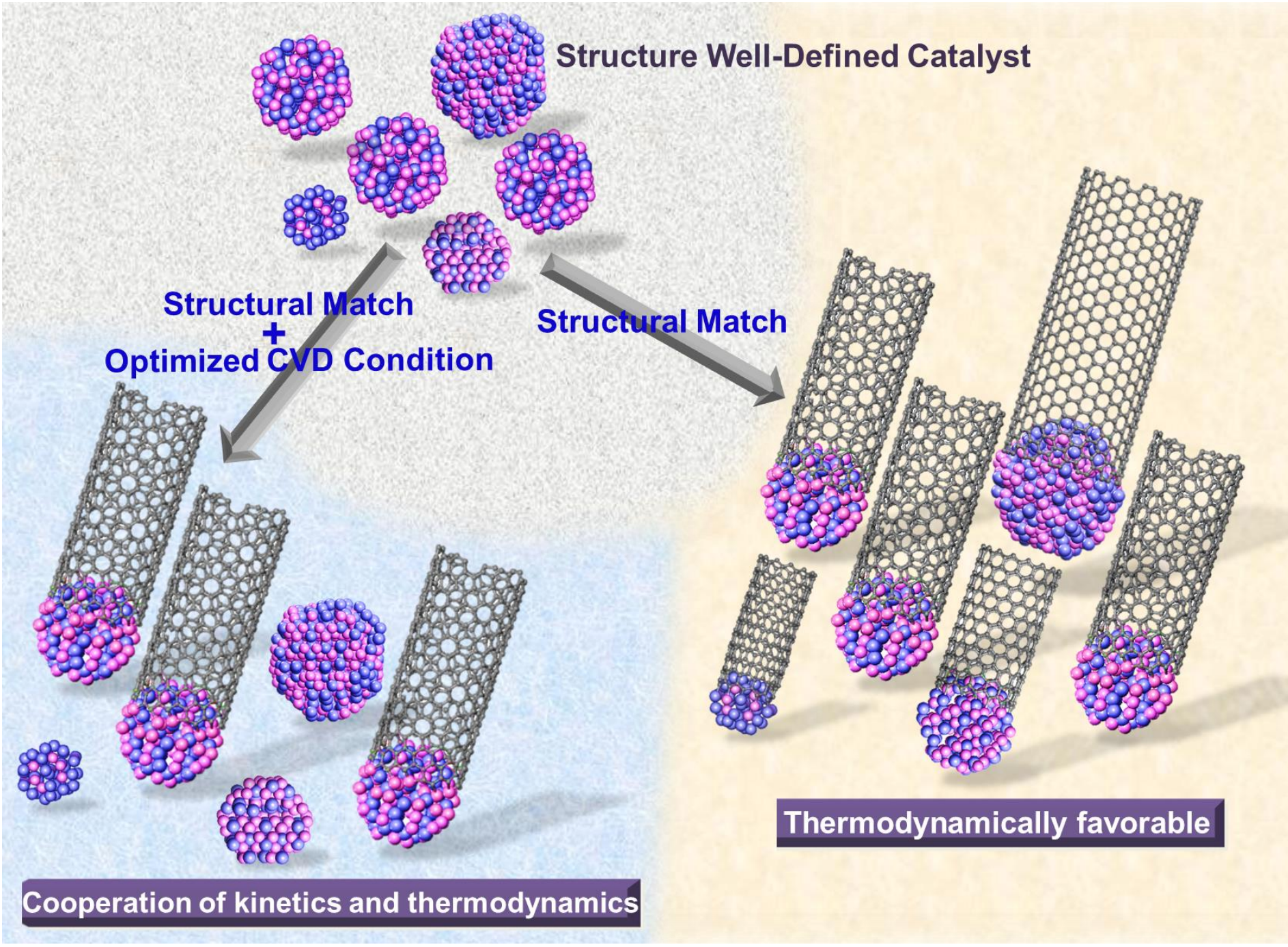
Structure Well-Defined Catalyst
Structural Match
+
Optimized CVD Condition
Structural Match
Cooperation of kinetics and thermodynamics
Thermodynamically favorable

Chemical & Engineering News, Cover Story, 8 June 2015

THE HYPE CYCLE

Hype is common to new technologies. The market analysis firm Gartner developed its so-called hype cycle to represent how hype and technology evolve together. C&EN has selected a handful of events to illustrate this cycle for nanotubes. Because nanotubes have potential in many applications, the events are not necessarily chronological.

VISIBILITY

MATURITY

TECHNOLOGY TRIGGER

1991
Sumio Iijima brings nanotubes to the attention of the scientific community (*Nature* 1991, DOI: 10.1038/354056a0).

Nanotube micrographs.

1995
Richard E. Smalley's team at Rice University develops a method to grow high-quality single-walled tubes (*Chem. Phys. Lett.* 1995, DOI: 10.1016/0009-2614(95)00825-O).

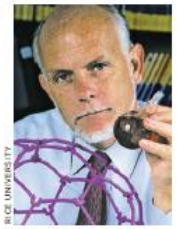

1998
Researchers create the first nanotube transistor that works at room temperature (*Appl. Phys. Lett.* 1998, DOI: 10.1063/1.122477).

PEAK OF INFLATED EXPECTATIONS

1999
Samsung researchers build a display using carbon nanotubes, leading some to speculate that nanotubes will be the next big thing in TV (*Appl. Phys. Lett.* 1999, DOI: 10.1063/1.125253).

Samsung's nanotube display.

Circa 2000
Researchers propose that carbon nanotubes could one day help build an elevator to space.

Artist's conception of a space elevator.

Circa 2005
Nanotubes' exciting physical properties have some people believing that nanotubes are destined to replace silicon in electronics.

Circa 2010
A nanotube surplus builds as manufacturers anticipate a demand that hasn't yet materialized.

TROUGH OF DISILLUSIONMENT

2004
With the isolation and characterization of graphene, researchers once invested in nanotubes start investigating new materials (*Science* 2004, DOI: 10.1126/science.1102896).

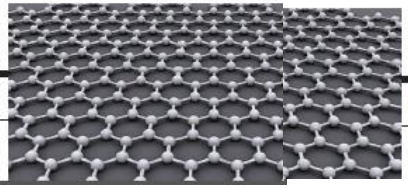

A sheet of graphene.

2013
Bayer MaterialScience shuts down its nanotube production operations.

Nanotubes separated in water.

2006
Scientists separate nanotubes by their electronic properties, an important step toward advanced nanotube electronics (*Nat. Nanotechnol.* 2006, DOI: 10.1038/nnano.2006.52).

SLOPE OF ENLIGHTENMENT

PLATEAU OF PRODUCTIVITY

stoked the public's curiosity, but it also brought out concerns. People began questioning what would happen if these nanoscopic tubes that were supposed to change their lives also entered their bodies. The nanotube community wasn't fully prepared for these questions.

"Multiwalled carbon nanotubes became the prototypical 'bad nano,'" says James M. Tour, a chemist at Rice and the Smalley Institute for Nanoscale Science & Technology. "Bad" here means toxic.

Large, rigid multiwalled tubes can act a lot like asbestos if inhaled, Tour explains. Small, flexible single-walled tubes, however, pose minimal risk, he states. "Nevertheless, everyone lumps them all together," Tour says.

"'Carbon nanotubes' is really a kind of a catchall term for a wide variety of different materials," says Philip G. Collins, a professor of physics who studies nanotube electronics at the University of California, Irvine. A truly nanoscopic single-walled tube differs greatly from a millimeter-long multiwalled structure, yet both are considered nanotubes.

This imprecise language is especially confounding when coupled with the volume of early publications submitted by researchers trying to carve out a place for themselves in a rapidly growing field, Collins says.

"Everything under the sun was published. Just about anything you can imagine, it's out there. 'You can make great peanut butter and jelly sandwiches out of nanotubes,'" he says, laughing.

Unfortunately, that also includes important results that appeared to contradict one another. Collins continues: "Nanotubes are toxic. Nanotubes aren't toxic. Nanotubes are perfect conductors. Oh, no they're not. Nanotubes are superstrong, except when they break."

The validity of each claim—and each can be valid—depends on the particular nanotubes, how they were processed, and how they were tested. Researchers now understand this well, and they have brought much needed clarity to the field, says Tour.

But early literature can still present challenges for new nanotube researchers, especially graduate students, who must suss out which claims are legit and under what conditions, Collins says.

Phaedon Avouris also worries about young scientists entering materials research. Avouris, who was Collins's postdoctoral adviser, performed some of the first experiments characterizing nanotubes at IBM. "It's very hard to tell young people to ignore the hype," he says. "We have too many people that follow fashion and patterns rather than their own passions."

Today, when scientists focus on studying a new material, there is a rush to characterize it, publish papers about its properties in prominent journals, and then move on to a different material, Avouris says. "We're left with a lot of unfinished work and unproven claims," he tells C&EN. Researchers develop a fundamental understanding of materials but not how to use them. "Few people are willing to work on the hard problems that will bring applications."

2014
Two separate groups report techniques for growing homogeneous nanotubes. (*Nature* 2014, DOI: 10.1038/nature13434 & DOI: 10.1038/nature13607).